Universität Stuttgart

Institute for Sanitary Engineering, Water Quality and Solid Waste Management

Master Thesis:

Phosphate recovery from wastewater with magnetic particles and enrichment of the reclaimed solution as a source for struvite precipitation

WS/SS 2015/2016

Student: Yamileth Milena Jiménez Gutiérrez

Matriculation number: 2845137

Master Study Program: WASTE

Supervisor: Dipl.-Ing. Asya Drenkova-Tuhtan, M.Sc.

Examiner: Dipl.-Ing. Carsten Meyer, RBM

Submission date: 30th of May, 2016

I would like to dedicate this Master Thesis to my husband Roberto, to my mother Yamileth, my father Warren and my brothers Marco and Alejandro, for their unconditional support during this period.

Confidentiality Agreement

The WASTE Office is not allowed to publish this Master Thesis as a pdf file on the WASTE website or to distribute the printed version, before the end of the project SuPaPhos.

_____

Yamileth Milena Jiménez Gutiérrez

Abstract

In this study phosphate was recovered from different wastewaters (WW) by using magnetic particles modified with layered double hydroxides (LDH). Afterwards, the enriched reclaimed solution was used for the precipitation of struvite. Adsorption and desorption cycles were performed in four types of raw wastewaters (LFKW (10 L), MBA, DSLF and UASB) by using the LDH-composite particles. After the different enriched reclaimed solutions were obtained, struvite precipitation kinetics were performed in order to find the optimum parameters of pH value and molar ratio of NH_4^+:Mg^{+2}:PO_4^{-3}, for further struvite precipitation. From the complete adsorption/desorption cycles, it was found that the LFKW (10 L) wastewater had the best adsorption total efficiency (96.6 %) and from this 85.4 % was desorbed, whereas the DSLF showed the lowest adsorption total efficiency (75.4 %) and from this 53.4 % was desorbed. In addition, it was found that the carbonate presence in the DSLF wastewater had a significant contribution to the low yield. Regarding the struvite precipitation kinetics and struvite precipitation measurements in synthetic WW and in the different reclaimed solutions, working at pH 8.5 revealed high phosphate uptakes in the kinetic reactions, regardless of the molar ratio of Mg^{+2}:NH_4^+:PO_4^{-3}. It was observed that at higher Mg^{+2}:NH_4^+:PO_4^{-3} molar ratio higher phosphate precipitation occurs, regardless the matrix type. Moreover, the color of the enriched reclaimed solutions revealed the color of the resulting struvite solid products, which can be attributed to the presence of the contaminants. Additionally, the experimental Mg^{+2}:NH_4^+:PO_4^{-3} molar ratios of the actual struvite precipitation were calculated and they were lower than the theoretical.

Keywords: Layered double hydroxides, phosphate recovery, adsorption/desorption cycles, magnetic particles, wastewater, struvite precipitation kinetics, struvite precipitation.

Acknowledgments

This master thesis was prepared from December 2015 until May 2016 during the fifth and sixth semesters of the Master Program ¨Air quality control, solid waste and wastewater process engineering¨ at the University of Stuttgart, Germany.

I would like to thank Dipl.-Ing. Asya Drenkova-Tuhtan, M.Sc for giving me the opportunity to perform this master thesis under her supervision and for her guidance during the work. Furthermore, I would like to thank to Dipl.-Ing. Carsten Meyer, RBM for the opportunity to complete this master thesis.

All the experiments, data calculations and the writing of this master thesis were performed by myself.

Table of content

List of Tables

List of Figures

List of Symbols and Abbreviation

ADP	Adenosine diphosphate
ATP	Adenosine triphosphate
CSTRs	Continuous Stirred Tank Reactors
DNA	Deoxyribonucleic acid
DOS	Dissolved organic substances
DS	Digested sludge
DSLF	Digested sludge liquor filtrate
EBRP	Enhanced biological removal of phosphorus
HS	Humic substances
IE	Ion exchange
IFDC	International fertilizer development center
IFIA	International fertilizer industry association
ISWA	Institut für Siedlungswasserbau, Wassergüte- und Abfallwirtschaft
LDH	Layered double hydroxides
MAP	Magnesium ammonium phosphate
MBA	Mechanical-biological waste treatment plant
PAOs	Polyphosphate accumulating organisms
PCS	Pollution Control Service
pK_{sp}	Solubility product
POPs	Persistent organic pollutants
RNA	Ribonucleic acid
LFKW	Lehr- und Forschungsklärwerk (Wastewater Treatment Plant forEducation and Research) at University of Stuttgart
SEM	Scanning electron microscopy
SST	Secondary settling tank
TSS	Total suspended solids
UASB	Upflow anaerobic sludge blanket
WW	Wastewater
WASSTRIP®	Waste Activated Sludge Stripping to Remove Internal Phosphorus
WWTP	Wastewater treatment plant

Chapter 1: Introduction

1.1 Motivation

There is a significant concern nowadays regarding how much phosphorus (P) reserves are globally available, motivating scientists and engineers to find alternatives to obtain phosphorus from secondary sources and to reduce dependency on the natural mineral reserves.

Phosphorus was discovered by the German alchemist Henning Brandt in the late 1600´s, when he distilled urine and observed that the product shined in darkness and was also flammable. Nevertheless, it was no until 1840 that the German chemist Liebig discovered that the soil used in agriculture had a deficiency of P as a nutrient; therefore, it was used for the production of fertilizers (Cordell and White, 2011).

Phosphorus is a non-metal and a very reactive element that exists as two main allotropes, white and red phosphorus, with the first one being the most common. However, it cannot be found as a free element in nature but bound in many minerals in the form of phosphates which exist in two forms, as sedimentary rocks and as igneous rocks. The first form also called apatites, where its chemical formula is $Ca_5(PO_4)_3(F,Cl,OH,Br)$ and exists as four types of calcium phosphate apatite: Hydroxyapatite, fluorapatite, chlorapatite, and bromapatite, where the second is the most common. Furthermore, these apatites contain impurities such as humic substances and heavy metals like cadmium, uranium and zinc. The P is present in the phosphate rocks between 30-40 % as a P_2O_5, which means that P is present between 5-13 % (Cordell and White, 2011 and Desmidt *et al*, 2015).

It is important to underline that the sedimentary rock sources of P have varieties of carbonate-fluorapatite, namely francolite, and are composed mainly of CO with > 1 % of fluorine and also contain Ca, Na and Mg. The igneous rock varieties contain carbonatites and alkali incrustations (Van Kauwenbergh, 2010).

P is a very import nutrient for all flora, fauna and human beings because it is present in DNA and RNA molecules, it is the second most common element in the animal skeleton, it has an

important role in biochemical reactions, it is part of the phosphorus cycle and moreover, contributes to the cellular energy transport as ADP and ATP (Cheng *et al* 2009 and Martin, 2010). In addition, phosphate products are predominantly used in agricultural but also in non-agricultural industries. In the former, it is used for the production of fertilizers, as pesticides and food additives in animal feed, where up to 90 % of all mined phosphates rocks are used. For the second sector, it is used in the human food industries, in the pharmaceutical industries, for the production of detergents and in chemical industries (Panasiuk, 2010 and Desmidt *et al*, 2015).

Phosphorus, along with nitrogen (N) and carbon (C), is important in nature for regulating the biological activity. However, unlike N and C, P cannot be obtained from atmospheric air as it cannot be readily circulated in the atmosphere. Therefore, it is a limiting nutrient in the crop soil and needs to be added as a fertilizer. Due to the steady increase in the world population (figure 1), there is more demand for the production and use of fertilizers, leading to increased demand for P, made worse by the limited supply of phosphate rock and it not being a renewable resource (Cordell *et al*, 2009).

Currently, there are two opinions regarding the supply of phosphate rock; some studies suggest that the reserves will be exhausted over the next 50 to 100 years but other studies say that they are sufficient for the next 400-1000 years. The IFIA (International Fertilizer Industry Association) recently disproved the ‘phosphate peak’ of 2009. However, they emphasized that the phosphate rocks is a nonrenewable resource. On the other hand, it is estimated that around the world, 180-190 million tons of phosphate rock are mined every year (Cooper *et al*, 2011, Desmidt *et al*, 2015, and Kalmykova *et al*, 2015).

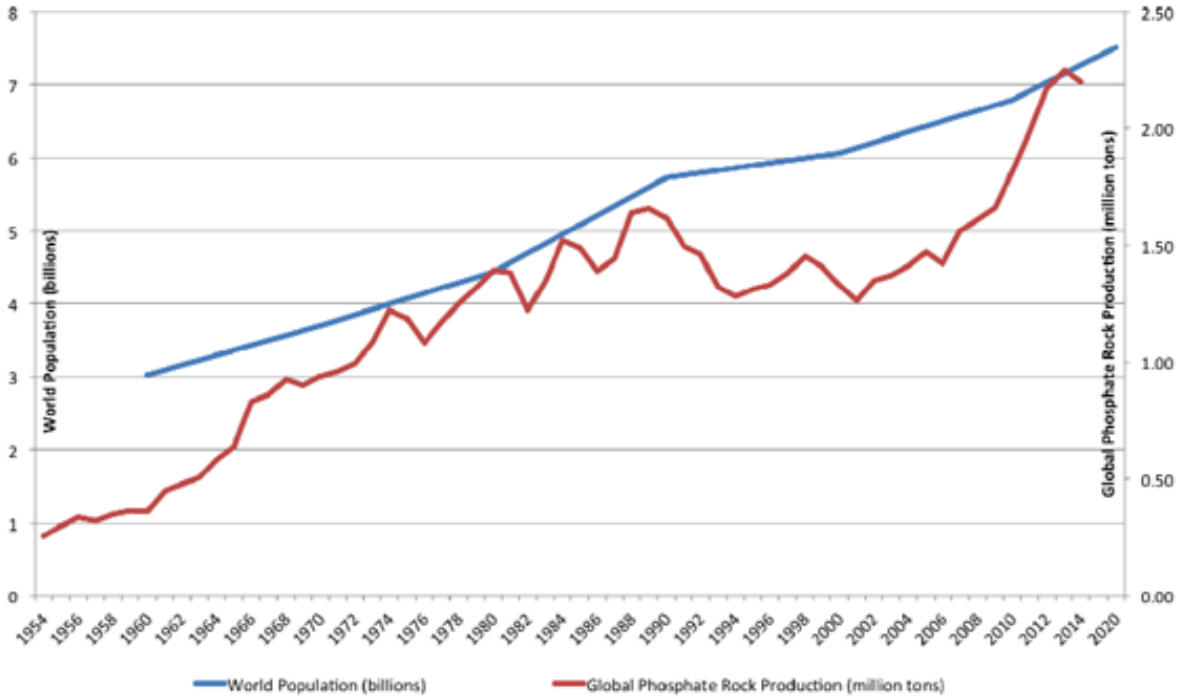

Figure 1. Global phosphate rock production vs world population increment (Bird, 2015).

As shown in figure 2, the four main producers of phosphate rocks are China, the United States, Morocco and Western Sahara (De Ridder *et al*, 2012).

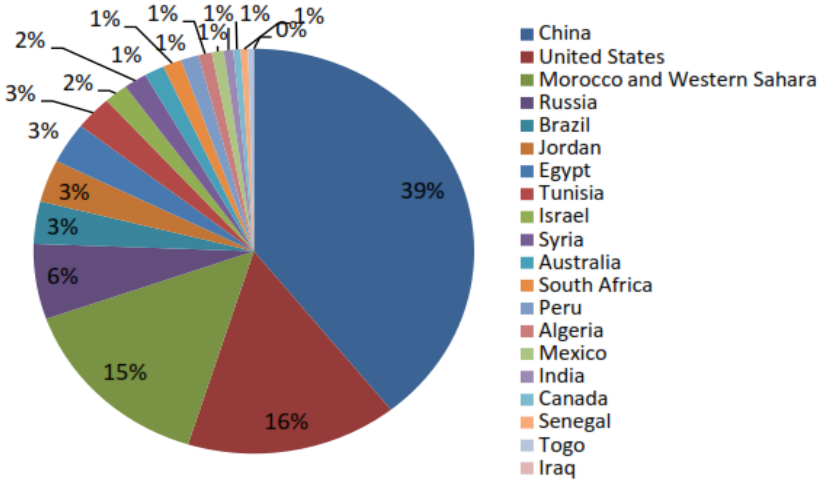

Figure 2. Main global producers of phosphate rock in 2011 (De Ridder *et al*, 2012).

Regarding the worldwide phosphate rock reserves, it can be observed in figure 3 that Morocco, China, Algeria, Syria and Jordan are the countries with the most reserves of phosphate rock, meaning around 95 % of it are present in those places, where Morocco and Western Sahara has

85 % of that total share. As there are no policies regarding the security of the P supplies, the high concentration of P in certain regions can lead to geopolitical concerns. Furthermore, Finland is the only country in the European Union that has deposits (Cordell and White, 2011 and Cooper *et al*, 2011).

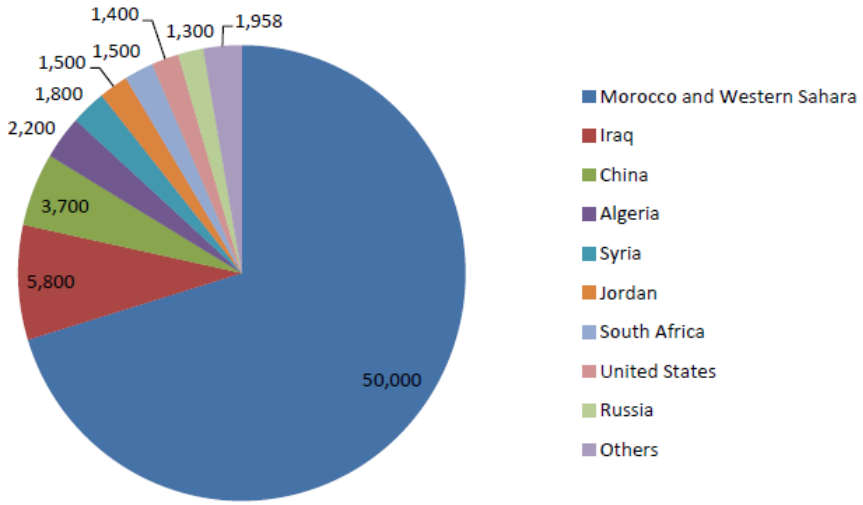

Figure 3. Global phosphate rock reserves (millions per ton) reported in 2012 (De Ridder *et al*, 2012).

Germany, which does not have any deposits of phosphate rocks, has to import unmilled P from other countries, such as Syria, Algeria and Egypt. In 2010, Germany imported approximately 118000 Mg and, from this amount, around 60 % was used for the production of fertilizers, 20 % for the development of feedstuffs and 6 % were used for the food industry (LAGA, 2010).

Another very significant issue is the losses occurring during every use of phosphorus/phosphate, which can be seen in figure 4.

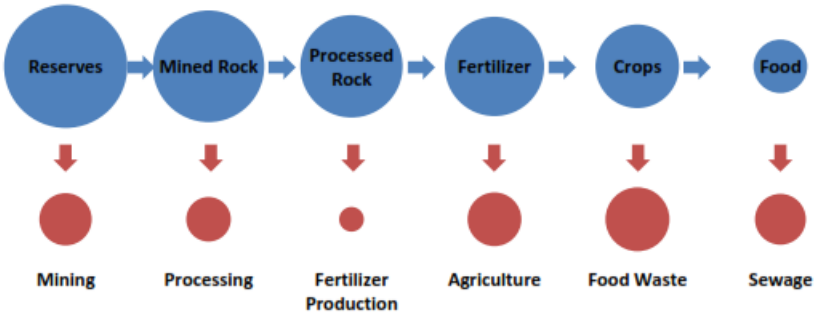

Figure 4. Major uses (blue circles) and sinks (red circles) of phosphate (De Ridder *et al*, 2012).

Concerning figure 4, it can be stated that the main sinks of phosphate are in food waste, agriculture, mining and sewage sludge. Therefore, the implementation of new technologies for the recycling of phosphate is of particular interest (De Ridder *et al,* 2012).

In addition to the limited supply, unmanaged loss of P into water bodies can have a negative effect due to uncontrolled and rapid growth of microorganisms, leading to eutrophication. The eutrophication causes a reduction of the biodiversity in the environment and in the water quality, an increase of undesirable organisms that can generate toxic substances, depletion of oxygen in the water and other consequences. Moreover, the eutrophication in the European Union water bodies is around 65 %. (Das *et al*, 2006, Panasiuk, 2010, and Ashekuzzaman and Jiang, 2014).

1.2 Phosphorus legislation in Europe and, specifically, in Germany

On May 21st, 1997 the European Union implemented a legal initiative to solve the problem of P and N discharge into water bodies in an effort prevent/limit eutrophication. They introduced the EC Urban Waste Water Treatment Directive 91/271/EC. Two main components emerged from this directive (Doyle and Parsons, 2002 and Pastor *et al*, 2008):

a- Sewage sludge discharge into the sea is forbidden.
b- It is necessary to eliminate or reduce N and P present in wastewaters before their final discharge into ¨sensitive areas¨. Specific limit values were set for these nutrients.

The typical concentration of P in a raw wastewater is 4 to 16 mg/L, where the orthophosphate (PO_4^{-3}) form is the main component. According to Directive (92/271/EEC), the effluent should have a P maximum concentration of 2 mg/L in an area between 10000 and 100000 inhabitants and 1 mg/L when the population is more than 100000 inhabitants (Mandel *et al,* 2013 and Ashekuzzaman and Jiang, 2014).

In Germany, the 91/271/EC Directive was incorporated into the German Law Water Resources Management Act, where the German Annex 1 of the Wastewater Ordinance controls the implementation of the EC Urban Waste Water Directive and the Water Resources Management Act (Wvgv, 2015).

1.3 Present solutions for the removal and recovery of phosphorus

To comply with the concentration limits, technologies have been developed to remove and recover P from wastewater. Those associated with this master thesis will be explained, but it should be noted that there are others that are not subject of interest in this work.

The P that enters a wastewater treatment plant (WWTP) comes predominantly from domestic, but also from agricultural/industrial sources. Once the P goes into the WWTP, it can be particle bound or dissolved in different forms, around 50 % of it is in the form of orthophosphate, which is a soluble inorganic compound, then 35 % as polyphosphate that comes principally from detergents and finally 15 % as organic phosphate. Municipal wastewater (WW) contains 6-8 mg/L of P (Parsons and Smith, 2008 and Nieminen, 2010).

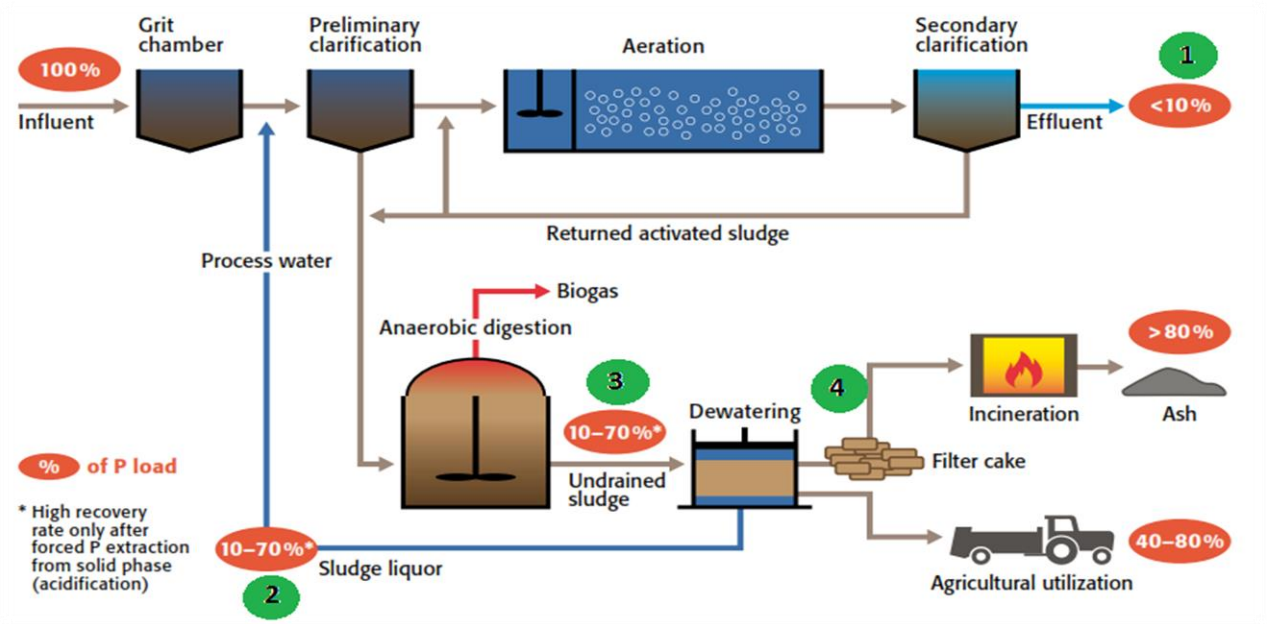

Figure 5. Possible points of phosphorus recovery within a WWTP scheme (Wollmann and Möller, 2015).

As shown in figure 5, the P can be recovered from four different stages of the wastewater or sludge treatment line within a WWTP. The **first stage** corresponds to the **effluent**, which contains less than 5 mg dissolved P/L, if no earlier targeted elimination takes place. The **second stage** is the **sludge liquor** that has 20-100 mg dissolved P/L, where the content of heavy metals and persistent organic pollutants (POPs) are low. The **third stage** consists of the **digested sludge** containing 30-40 g P/kg which is chemically/biologically bound; the P is bound in a

heterogeneous material that also contains, N, Ca, Mg, K, POPs and heavy metals. Finally, the **fourth stage** is the **sludge ashes** that has 60-80 g chemically bound P/kg. From each stage, the phosphorus recovery potential is 55, 50, 90 and 90 %, respectively (DWA Working Group CEC 1.1, 2013 and Egle *et al*, 2015).

Currently, two main processes are applied for P removal from WW; chemical precipitation and enhanced biological removal of phosphorus (EBRP). Chemical precipitation can remove around 90 % of the P of the total inflow. This procedure uses chemical salts of Fe^{+2}, Fe^{+3} and Al^{+3} bound to chloride or sulphate ions. Once the salt has been added, the metal phosphate solids precipitate and form a chemical sludge that is withdrawn together with the excess activated sludge. This chemical process exhibits two main disadvantages: the metal phosphates produced do not have any value as fertilizers and the sludge also contains metals (Parsons and Smith, 2008 and Drenkova-Tuhtan *et al*, 2016).

EBRP utilizes specific microorganisms called Polyphosphate Accumulating Organisms (PAOs) that take up excess phosphate from the WW, which can be achieved under anaerobic conditions. The EBRP transforms the diluted P into a more concentrated form that is stored inside the bacteria and results in a sludge with around 60-90 % of PAOs (Yuan *et al*, 2012).

For the recovery of P, there are three main processes that will be explained briefly in this work:

a) Precipitation and struvite crystallization from sludge liquor: Both processes transform the dissolved PO_4-P in the sludge liquors into a solid form. Precipitation involves the use of chemicals in order to obtain magnesium ammonium phosphate or struvite [$Mg(NH_4)PO_4 \cdot 6H_2O$] (Parsons and Smith, 2008, Nieminen, 2010; and Ewert *et al*, 2014). The struvite precipitation will be explained in detail in chapter 2.
b) Wet chemical technologies for P-recovery from sludge and sludge ash: Chemically and biologically bound P in sludge or sludge ash can be re-dissolved by utilization of a strong acid or base. Phosphate can then be recovered via precipitation (e.g. struvite), ion exchange, nanofiltration, etc. (Nieminen, 2010). The ion exchange method will be explained in chapter 2.

c) Thermal-chemical treatment: This can be used for the removal of heavy metals that are present in the sewage sludge. Phosphorus is concentrated in the sludge ashes, which contain around 17 % of P_2O_5, and the product can be used for fertilizers production (Nieminen, 2010).

1.4 Aim and specific objectives

The aim of this master thesis is to recover phosphate from wastewater using magnetic particles and enrich the reclaimed desorption solution with phosphate for the precipitation of struvite. It is important to mention that all the experiments were performed on a laboratory scale. The following specific objectives were formulated:

- ✓ Performance of adsorption and desorption cycles using ZnFeZr-LDH composite material at two different loadings of it, 15 and 32 wt %, in order to obtain enriched reclaimed solutions from different raw wastewaters for further MAP precipitation.
- ✓ Study the kinetics of phosphate removal due to struvite precipitation, at different molar ratio Mg^{+2}:NH_4^+:PO_4^{-3} and pH values in synthetic wastewater and enriched reclaimed solutions in order to find the optimum conditions.
- ✓ Maximize the struvite yield from the different matrices at optimum conditions (contact time, pH and Mg^{+2}:NH_4^+:PO_4^{-3} molar ratio) for further analysis.
- ✓ Comparison of the chemical composition (PO_4^{-3}, metals and anions) of the enriched reclaimed solutions before and after the struvite precipitation.

1.5 Master thesis structure

The first chapter explained the main issues concerning the global demand for P, as well as the current solutions for its removal and recovery. In addition, the directive legislations of the European Union and Germany were explained. The main aim and the specific objectives of this master thesis were then described.

The second chapter presents a literature review and explains what layered double hydroxides (LDH) are, as well as the principles of ion exchange and struvite precipitation. This chapter summarizes also some preliminary studies carried out at an earlier stage of the master thesis that served as a base for the design and performance of the current experiments.

The third chapter describes in detail the eighteen experiments that were performed in order to recover the phosphate from wastewater by using magnetic particles, followed by the phosphate enrichment of the reclaimed solution for the precipitation of struvite.

The fourth chapter includes a discussion of the results from the different experiments and a conclusion about the optimum conditions for the precipitation of struvite from the different enriched reclaimed solutions that were used.

The fifth chapter contains the main conclusions of this work as well as some recommendations for the development of further research.

Chapter 2: Ion exchange, layered double hydroxides and struvite

2.1 Ion Exchange

Ion exchange (IE) is a process in which ions present in a solution are exchanged using a highly polyelectrolyte insoluble solid (e.g. a resin) that is in contact with the solution ions. This ion exchanger contains ions that are to be interchanged with the targeted ions in a certain solution. Furthermore, IE is a reversible and stoichiometric process. This method is used mainly for water softening in the field of drinking water treatment (Jeffery *et al*, 1989 and Meyer, 2014).

It is important to mention that the exchange of ions has a strong dependency on the charge valence and the weight of the ions that are involved in the process. In the case of phosphate, due to its low concentration in the wastewater 4 to 16 mg/L (Rittmann *et al*, 2011 and Mandel *et al*, 2013), IE is very suitable for the recovery of P.

On the other hand, since ion exchange depends on the charge valence of an ion, phosphate can be found as different species at different pH values, i.e. as monovalent ($H_2PO_4^-$), as divalent (HPO_4^{-2}) and as trivalent (PO_4^{-3}), equation 1:

$$H_3PO_4 \xrightarrow{pK_{a_1}=2.15} H_2PO_4^- + H^+ \xrightarrow{pK_{a_2}=7.20} HPO_4^{2-} + 2H^+ \xrightarrow{pK_{a_3}=12.33} PO_4^{3-} + 3H^+ \quad (1)$$

This means that it can exist as the divalent anion HPO_4^{-2} and as the intermediate monovalent anion $H_2PO_4^-$ in WW streams where the pH is close to neutral. Additionally, the divalent anion presents two donor electrons whereas and the monovalent one, which means that both can act as ligands for the attraction and the formation of complexes with transition metals and, i.e. with the metals contained in the layer double hydroxides (LDH) structure, resulting in the removal of phosphate from WW streams (Chitrakar *et al*, 2007, Martin, 2010; and Yang *et al*, 2015).

In summary, some of the ion exchange processes that could be utilized in this work for the removal and the recovery of phosphate are capacitive deionization on oppositely charged electrodes, iron-based LDH compounds that contain cations and/or hydroxides and metal-loaded

chelating resin used to selectively remove phosphate (Rittmann *et al*, 2011). The LDH will be explained further in this work.

2.2 Layered double hydroxides (LDH)

The layered double hydroxides, known also as hydrocalcite-like compounds (HTlc), have been studied widely in the last three decades regarding their synthesis and applications. LDHs exist as minerals ($Mg_6Al_3(OH)_{16}CO_3 \cdot 4H_2O$) but they can also be economically synthetized in a relatively simple manner. The LDHs are anionic clays with a two-dimensional nanostructure, as shown in figure 6, where the brucite-like sheets ($Mg(OH)_2$), are positively charged, which are balanced by the intercalation of anions in the hydrated interlayered spaces, wherein CO_3^{-2} and Cl^- are the most frequently used. The layers can have monovalent, divalent, trivalent and, even, tetravalent cations and these results in a highly positive LDH materials. Since the LDHs have a weak interlayer bonding, they are perfect for the caption of organic and inorganic anions. On the other hand, those interlayer anions are linked by weak electrostatic forces that permit ion exchange. However, ion exchange is not the only mechanism contributing to the removal of phosphate - electrostatic attraction and formation of ligands can occur as well (Goh *et al*, 2008, Ashekuzzaman and Jiang, 2014 and Yan *et al*, 2015).

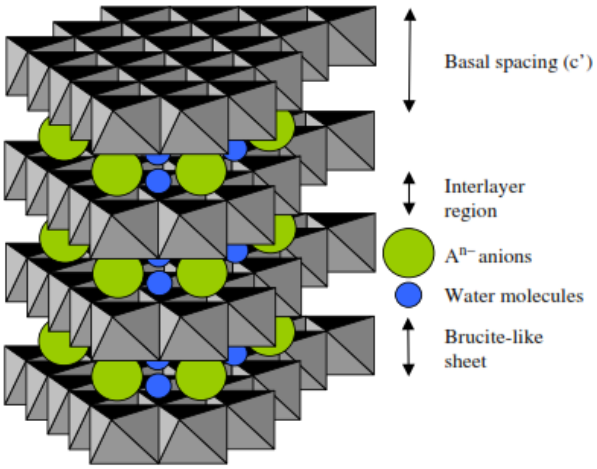

Figure 6. Structural representation of LDH materials (Goh *et al*, 2008).

The general formula of a LHD is given in equation 2, where M^{+2} and M^{+3} are the divalent and trivalent cations, respectively, A^{-n} is the interlayer anion with a valence *n* that can be organic, inorganic, carboxylate, oxyanion or a coordination compound, and *x* has values between 0.1 and

0.33. When this value is not in this range, impurities can be incorporated (Goh *et al*, 2008 and Koilraj and Kannan, 2010).

$$[M_{1-x}^{+2}M_x^{+3}(OH)_2]^{+x}(A^{-n})_{x/n}\cdot mH_2O \qquad (2)$$

LDH materials are widely used as adsorbents and ion exchangers because they have a high anion exchange capacity (3,0-4,8 meq/g), their surface area is large (20-120 m^2/g), they have a structure that is resistant to water and they have a high positively charged layer. The LDHs have special affinity to inorganic anions with small ionic radii and high valence charges. In the case of monovalent anions, the affinity decreases in the following order: $OH^- > F^- > Cl^- > Br^- > NO_3^- > I^-$ and, in the case of divalent ions, CO_3^{-2} is preferably adsorbed by LDHs as well as PO_4^{-3}. Several studies have shown their effectiveness as selective adsorbents for the removal of phosphate from municipal water, sea water, simple electrolytes, deionized water, sewage sludge filtrate and drain effluents (Koilraj and Kannan, 2010, Cheng *et al*, 2010, Cai *et al*, 2012 and Drenkova-Tuhtan *et al*, 2016).

However, the previous studies cannot be compared so easily due to the fact that the materials are synthetized under different conditions of co-precipitation and combinations of metals; and because of this the conditions for the adsorption of phosphate, such as pH, contact time, dose of the adsorber material, concentration of phosphate, temperature, etc., are different in every study (Drenkova-Tuhtan *et al*, 2016).

In this master thesis, all the adsorption and desorption cycles that were performed for the production of the different reclaimed solutions for further struvite precipitation used only one type of adsorber material (ZnFeZr-LDH). Moreover, this adsorber material (ZnFeZr-LDH) was chosen due to is high efficiency for adsorption and desorption of phosphate in synthetic water and wastewater effluents (Jiménez-Gutiérrez, 2015). The conditions for obtaining the different reclaimed solutions will be discussed in detail in chapter 3.

2.3 Struvite

In 1939, Rawn reported for the first time the observation of struvite when he was studying the sludge digestion in the digested sludge supernatant lines. He observed that the struvite was causing clogging in the pumps, pipes, screens and other aspects of the WWTP (Doyle and Parsons, 2008 and Bergmans, 2011). Considered an undesirable product then, currently struvite is sought after as a fertilizer, for a number of reasons that will be outlined below:

2.3.1 Struvite definition

Struvite is the name given to magnesium ammonium phosphate hexahydrate (MAP), a white-yellow-brownish crystal with an orthorhombic structure (figure 7). This crystal is formed of PO_4^{-3} and $Mg(H_2O)_6^{+2}$, both in octahedral arrangements with the ammonium groups, held together by hydrogen bonding. The crystals are obtained in different sizes (from 15 µm to 3,5 mm), shapes and transparencies, depending on the conditions that were used for their formation and the WW sources used (Dhakal, 2008, Bergmans, 2011 and Rahman *et al*, 2014).

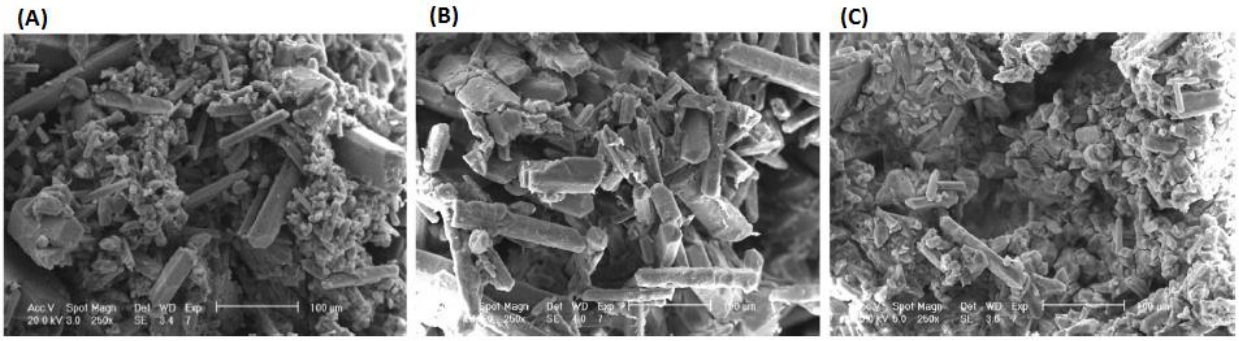

Figure 7. Struvite crystals obtained from sludge dewatered liquor at different total suspended solids solid concentrations: (A) 31 mg/L, (B) 116 mg/L and (C) 194 mg/L, images obtained by scanning electron microscopy (SEM) (Ping *et al*, 2016).

The percentage composition of the struvite is around 9.8% magnesium, 38.8% phosphate, 7.3% ammonium, and 44.1% water and organic compounds. It is important to mention that some side chemical compounds can be formed during the precipitation of struvite. Because of this, it is necessary to add an excess of Mg^{+2} and PO_4^{-3} ions in order to precipitate with the NH_4^+ ions (Türker and Çelen, 2010 and Bird, 2015).

2.3.2 Struvite precipitation

The precipitation of struvite can be divided into two processes: *Nucleation* and *crystal growth*. *Nucleation* is when the ions are combined with one another and form the first crystal cores with a defined size. *Crystal growth* is when the particles are in contact with the surface and are clustered around the structure of the crystal, where the reaction continues until equilibrium is achieved. A side process, agglomeration, can also occur, which consists of the formation of bigger crystals from the already existing particles; however, this process does not happen often. The main two processes are dependent on factors such as the thermodynamics of the equilibrium between the solid and the liquid, ionic strength, reaction kinetics and other physical-chemical parameters such as pH, temperature, supersaturation, Mg^{+2}:NH_4^+:PO_4^{-3} molar ratios, phosphate concentration, stirring, and interfering ions, including calcium, carbonate, chloride, sulphate, nitrates and others (Doyle and Parsons, 2002, Dhakal, 2008, Ezquerro, 2010, Desmidt *et al*, 2013 and Kozik *et al*, 2014).

2.3.2.1 Mg^{+2}:NH_4^+:PO_4^{-3} molar ratios

MAP precipitates when equimolar concentrations of magnesium, ammonium and phosphate are present in the solution and the thermodynamic solubility product (K_{sp}) is exceeded, where the struvite solubility product values are between 9.40 and 13.36 (Dhakal, 2008 and Kozik *et al*, 2014).

It has been observed that magnesium is the limiting element in the WW effluents and other sources for struvite precipitation. Therefore, its addition as $MgCl_2$ or MgO is required in order to achieve the desired molar ratio. If the magnesium content is increased, P removal will be higher on the struvite formation (Desmidt *et al*, 2013).

2.3.2.2 Phosphate concentration

Studies have shown that for struvite precipitation, the phosphate concentration (PO_4-P) of the wastewater source should be above 50 mg/L; below this concentration, it is better to use the WW source for calcium phosphate precipitation (Desmidt *et al*, 2013).

2.3.2.3 pH

Struvite precipitation has a strong dependency on the pH, due to the effect on struvite solubility and its thermodynamic properties. The struvite precipitation from synthetic WW has been studied extensively at different pH values in order to reach optimum conditions, which has been found to be between pH 8.0 and 10.7. It is important to note that the concentration of ammonium decreases when the pH increases to 9.0 (from 99 % to 64 %), therefore it is important to control this parameter during struvite precipitation. Keeping the pH around 8.5 does not cause significant drop on the ammonium content. To increase the pH of synthetic or real WW, different reagents are used: NaOH, $Mg(OH)_2$ or MgO, lime or caustic or CO_2 stripping (Ezquerro, 2010, Desmidt *et al*, 2013, Ariyanto *et al*, 2014 and Egle *et al*, 2015).

According to Abbona and Boistelle (1979), when the pH is above 8.0 struvite crystals are twinned dendritic, while when the pH is in the range between 7.0-8.0 the forms are tabular and if the pH is below 6.0, the crystals are elongated (Mehta and Batstone, 2013).

2.3.2.4 Kinetic reaction

The struvite precipitation starts when hydrogen ions are released, followed by the consumption of magnesium ions. The general reaction for the formation of struvite is the following (Le Corre *et al*, 2007):

$$Mg^{+2}_{(ac)} + NH_4^{+}_{(ac)} + H_2PO_4^{-}_{(ac)} + 6H_2O_{(l)} \rightarrow MgNH_4PO_4 \cdot 6H_2O_{(s)} + 2H^{+}_{(ac)} \quad (3)$$

According to the equation 3, the struvite formation rate could be presented as equation 4:

$$\frac{d[MgNH_4PO_4 \cdot 6H_2O]}{dt} = \frac{1}{2}\frac{d[H^+]}{dt} = -\frac{d[Mg^{+2}]}{dt} = -\frac{d[NH_4^+]}{dt} = -\frac{d[H_nP_4^{3-n}]}{dt} = K_r \quad (4)$$

where k is the reaction rate kinetics constant and r is the crystallization rate (mol/L·s).

The mechanism of struvite crystallization can be fitted by the first order and the second order. The first order kinetics model can be described according to equation 5 (Ariyanto *et al*, 2014):

$$\frac{-dC}{dt} = k(C_t - C_s)^n \quad (5)$$

where k is the constant rate, n is the order of the reaction, C_t is the concentration of the reactant at a certain time t, C_s is the concentration of the reactant at equilibrium and $-dC/dt$ is the consumption rate of the phosphate.

Equation 5 can be linearized with the following equation:

$$Ln(C_t - C_s) = -k_1 t + Ln(C_i - C_s) \quad (6)$$

where C_t is the reactant concentration at time t, C_s is the equilibrium concentration, k is the first order kinetics term/constant, and C_i is the initial concentration (Quintana *et al*, 2005).

Regarding the second order kinetics model, equation 5 can be linearized to give equation 7 (Ariyanto *et al*, 2014):

$$\frac{1}{(C_t - C_s)} = \frac{1}{(C_i - C_s)} + k_2 t \quad (7)$$

where the k_2 is the second order rate constant.

According to Nelson *et al*, 2003 regarding the effect of the pH on struvite precipitation in anaerobic swine lagoon wastewater systems, the phosphate removal rate increased when the pH was increased from 8.4 to 9.0 and the reaction rate followed a first order reaction model.

2.3.2.5 Influence of ions

The WW effluents generally are hard waters due to the high calcium and magnesium ions concentration. The presence, specifically, of calcium might inhibit the struvite precipitation because it blocks the active sites and leads to a competition for orthophosphate ions to produce calcium phosphate (equation 8) instead of MAP. On the other hand, if an excess of magnesium is present, the purity of the struvite is affected (Doyle and Parsons, 2002, Le Corre *et al*, 2005 and Pastor *et al*, 2008).

$$5Ca^{+2} + 3PO_4^{-3} + H_2O \rightarrow Ca_5(PO_4)_3OH + H^+ \quad (8)$$

In the work of Song *et al*, 2007, a P concentration of 80 mg/L was used for the struvite precipitation, where they studied the effect of magnesium in different Mg/P molar ratios (1.0; 1.2; 1.4; 1.6 and 2.0). They found that by increasing the Mg/P molar ratio, an increase in the P removal efficiency (85 to 97 %) is achieved for the whole pH range.

Some studies suggest that a molar ratio of Ca^{+2}:PO_4^{-3}=1.25 affects the struvite formation when the concentration of PO_4-P is 100 mg/L in the influent. Moreover, molar ratio of Ca^{+2}:PO_4^{-3} =2.0, with an influent concentration of PO_4-P=80 mg/L, leads to calcium phosphate precipitation but no struvite. The presence of some other ions in the WW solution leads to an influence of the ionic strength, producing an increase in the electrostatic interactions between the ions that causes a decrease in their activities. Due to this, the availability of orthophosphate ions decreases and the struvite formation is affected (Desmidt *et al*, 2013).

Other ions that affect the struvite formation are carbonate and bicarbonate, as they can form complexes with calcium (equation 9) present in the WW, leading to a decrease of the P precipitated as MAP. Both carbonate and phosphate compete with each other for the active sites on the crystals, limiting the nucleation and growth (Ferguson and McCarty, 1971 and Le Corre *et al*, 2005).

$$Ca^{+2} + CO_3^{-2} \rightarrow CaCO_3 \quad (9)$$

2.3.2.6 Dissolved organic substances (DOS)

The main components of the dissolved organic substances (DOS) are humic substances (HS) that are composed of carboxylic, phenolic, alcoholic, quinone, amino and amido groups. These organic groups can undergo ion exchange, complex formation, redox reactions and adsorption, reducing the formation of the struvite (Zhou *et al*, 2015).

In the study of Bouropoulos *et al*, 2000 the precipitated struvite crystals had high negative charges, which had an influence on the agglomeration of the crystals. The sludge contains microbial cells that are negatively charged and this could have an effect on the struvite formation due to electrostatic repulsion between them and the highly negatively charged struvite (Bouropoulos and Koutsoukos, 2000 and Desmidt *et al*, 2013).

2.3.3 Struvite characteristics and applications

The solubility of struvite in water is low, 160 mg/L at room temperature and at pH 7.0. Its solubility product has a range value between 10^{-10} and $10^{-13.3}$. Due to this, it has a slow activity that makes it ideal to add it to the soil as a fertilizer. Moreover, it has a low content of heavy metals, in contrast to the fertilizers that are manufactured from phosphate rocks that have a

considerable quantity of heavy metals (Doyle and Parsons, 2002, Pastor *et al* 2008 and Harrison *et al*, 2011).

When used as a fertilizer, struvite has the following benefits; it is pure, has no odor, is easy to transport and to handle, and can be found as granular or in concentrated form. The P content of struvite is around 11 to 26 % and its concentration depends on the method and source used for its production (Kataki *et al*, 2016).

Struvite is already used as a fertilizer in rice crops in Japan. The cost of the production of 1 Mg of struvite varies in cost depending on location; from 140 $ in Australia to 460 $ in Japan. In contrast, it costs 40 to 50 $ to manufacture from phosphate rocks (Doyle and Parsons, 2002 and Ezquerro, 2010).

Other advantages to recover struvite from waste streams are: It is possible to extract nutrients from waste which are in excess before its final disposal; the volume of sludge can be reduced up to 49 % when the P is recovered as calcium phosphate from sewage sludge (Kataki *et al*, 2016).

2.4 State of the Art

2.4.1 Layered double hydroxide ion exchangers on superparamagnetic microparticles for recovery of phosphate from wastewater

Several studies have been done for the recovery of phosphate from WW by using superparamagnetic microparticles modified with ion exchanger materials. Mandel *et al*, 2013, used MgAl-LDH and MgFe-LDH doped with Zr ions in order to increase the selectivity. Those LDHs were precipitated in a NaOH solution (pH 10) and then ultrasonically deposited on multicore Fe_3O_4 integrated into a matrix of SiO_2. They performed this under batch and continuous processes, as observed in figure 8. The LDH materials are charged positively while the superparamagnetic particles bear a negative charge, which form a composite material that has a strong attraction between the LDHs and the superparamagnetic particles.

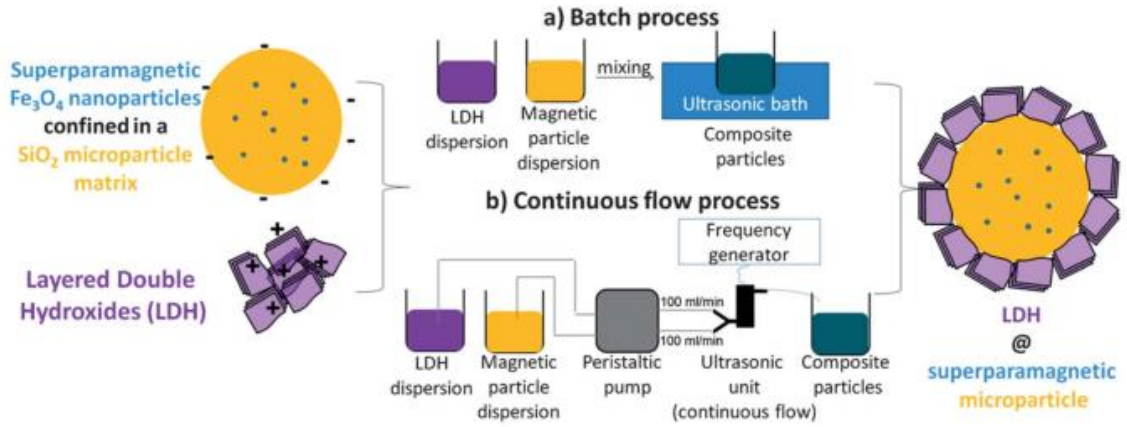

Figure 8. Composite formation by ultrasonic treatment in batch and continuous processes (Mandel *et al*, 2013).

Once obtained, the composite materials were used for the recovery of phosphate from distilled water and wastewater, where the initial concentration of PO_4^{-3} was adjusted to 10 mg/L PO_4-P with H_3PO_4. Both water and WW had a neutral pH and the corresponding volume of composite particles was added to each of them in order to achieve LDH concentration of 200 mg/L in 100 mL of those water solutions. The contact times were 1 h and 24 h, at 20 °C with stirring. At the end, a magnet was used for the separation of the particles and the supernatant liquid was collected for analysis. The concentration of phosphate was measured photometrically. Additionally, the composite materials were regenerated with 100 mL of two desorption solutions: 0.1 M NaOH and 2.0 M NaCl with a contact time of 24 h.

It was observed that after the first two desorption cycles, the MgFeZr-LDH had the highest efficiency. Regarding the phosphate uptake, the best composite material was MgFeZr-LDH with 30 mg PO_4-P/g LDH.

2.4.2 Phosphate recovery from wastewater using engineered superparamagnetic particles modified with layered double hydroxide ion exchangers

Drenkova-Tuhtan *et al*, 2013 screened several LDH materials and MgFeZr-LDH material was chosen for the development of phosphate adsorption kinetics under different contact time, pH, concentration of particles and adsorption isotherms. Desorption studies were also performed to understand the recovery of phosphate and the regeneration of the particles within 15 cycles. It

was observed, that phosphate adsorption in each cycle was in the range of 75 to 97 % with a contact time of 1 h.

Mandel *et al*, 2013 used LDH concentration of 200 mg/L LDH in the experiments. In contrast, in the research of Drenkova-Tuhtan *et al*, 2013, the concentration was increased up to 400 mg/L LDH in 1.0 L of wastewater spiked with phosphate. Adsorption kinetics was carried out in three pH ranges: 4.5-5.0; 5.5-6.0 and 7.0-8.0 at 20 °C with a contact time of 24 h. Phosphate concentration was analyzed photometrically. The results can be seen in figure 13. The adsorption isotherm experiment was done at 20 °C, pH 4.5 and contact time 24 h. The pH effect in the range from 3.0 to 9.0 was also studied after regulation with 1 M HCl and 1 M NaOH. Afterwards, they investigated the phosphate adsorption with different particles concentration from 40 to 1500 mg/L at pH 4.5.

For the desorption experiments, several desorption solutions of 1.0 L each were used: NaCl, NaOH, $NaHSO_4$, $NaHCO_3$ and NaOH + NaCl at different concentrations and pH values and contact time 1 h (30 min for the last desorption solution). Finally, 15 cycles of adsorption/desorption were run.

The best adsorption kinetics was observed at pH 4.5-5.0, adsorbing 90 % of the phosphate after 45 min with a maximum phosphate uptake of 23 mg P/g LDH, as shown in figure 9. The adsorption isotherms showed maximum phosphate uptake of 35 mg PO_4-P/g LDH. Concerning the different particle concentrations, at 1000 mg/L almost 100 % of the phosphate was removed. From all the tested desorption solutions, the best desorption efficiency (98.2 %) was observed with the 1 M NaOH+4 M NaCl. Finally, within the 15 cycles, the maximum efficiency was observed after 3 cycles, reaching a 99 % adsorption, as can be seen in figure 10.

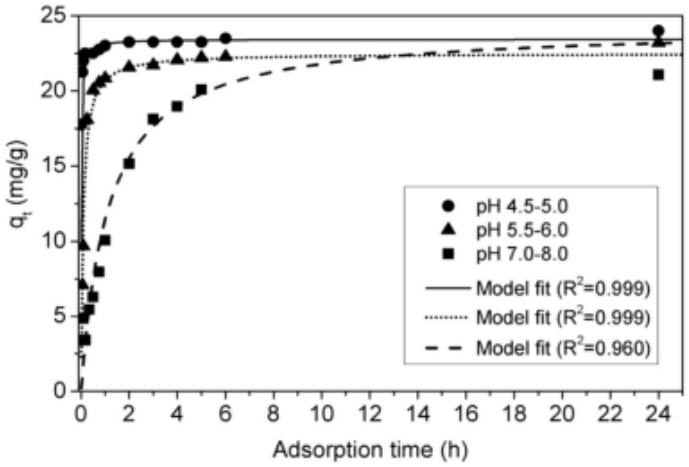

Figure 9. Phosphate adsorption kinetics on 400 mg/L of MgFeZr-LDH in three different pH ranges (Drenkova-Tuhtan *et al*, 2013).

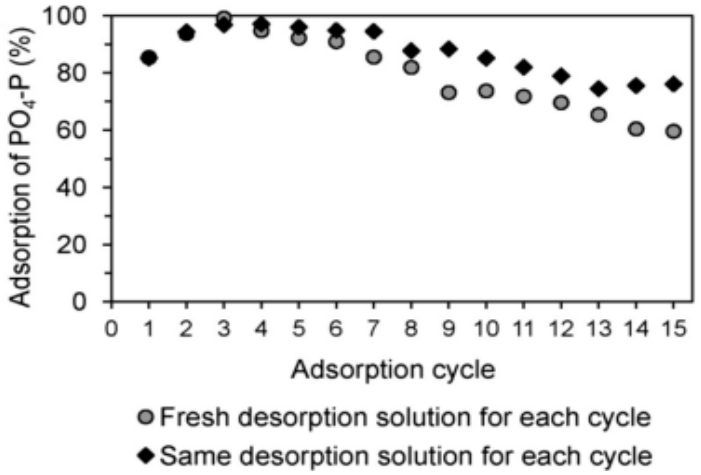

Figure 10. Adsorption efficiency throughout 15 cycles using 400 mg/L MgFeZr-LDH at pH 4.5 and 1 h contact time (Drenkova-Tuhtan *et al*, 2013).

2.4.3 Study on the sorption-desorption-regeneration performance of Ca-, Mg- and CaMg-based layered double hydroxides for removing phosphate from water

Ashekuzzaman and Jiang, 2014, synthetized and combined different divalent and trivalent metals for their incorporation in LDH materials (MgAl-, CaAl-, MgFe-, CaFe-, CaMgAl- and CaMgFe-LDH). Those LDHs were precipitated in a 2.0 mol/L NaOH solution (pH=12.6-13.5) and then stirred for 130-150 min at room temperature.

Once obtained, the composite materials were used for the recovery of phosphate from deionized water (P concentration: 50 mg/L) and real effluent from the Shieldhall WWTP in Glasgow, Scotland (soluble P concentration: 3.6; 1.4 and 5.6 mg/L at three different sampling times). Both synthetic water and real effluent had neutral pH and were used for the different experiments. For the screening of LDH materials, both synthetic water and real effluent had 10 mg/L P concentration. An adsorbent dose of 0.3 g/L was used with a contact time 2 h at room temperature and pH 7.0 with stirring. The best adsorption efficiency (85-90 %) was observed with the Ca-based LDHs. Different adsorbent dose ranges (0.05 to 0.45 g/L, figure 11) of the various LDH materials were used in order to find the best dose. The best performance was with the 0.3 g/L dose after 20 h mixing and the Ca-Al-60 LDH material had the highest maximum adsorption capacity (71 mg P/g).

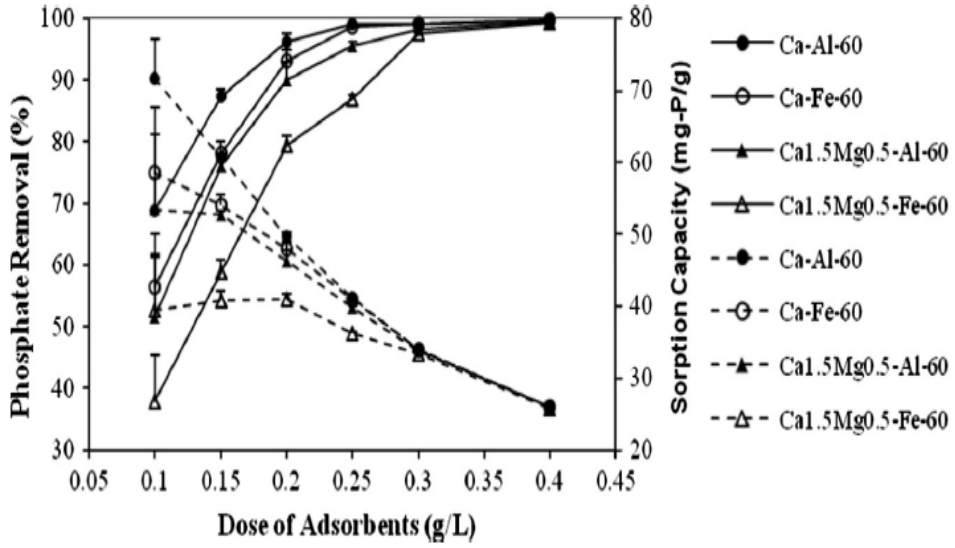

Figure 11. Phosphate adsorption efficiency vs. different adsorbent doses of various LDH materials at pH 7.0 and 20 h contact time. Solid and doted lines respectively indicate the percentage of removal and sorption capacity (Ashekuzzaman and Jiang, 2014).

Adsorption kinetics was carried out with the four different LDH materials at maximum contact time 4.5 h (figure 12). Equilibrium was achieved after 2 h with phosphate adsorption efficiency 98-99 %. Experimental data were fitted with pseudo-first and second order kinetics models, and the second one had higher correlation coefficients (R^2).

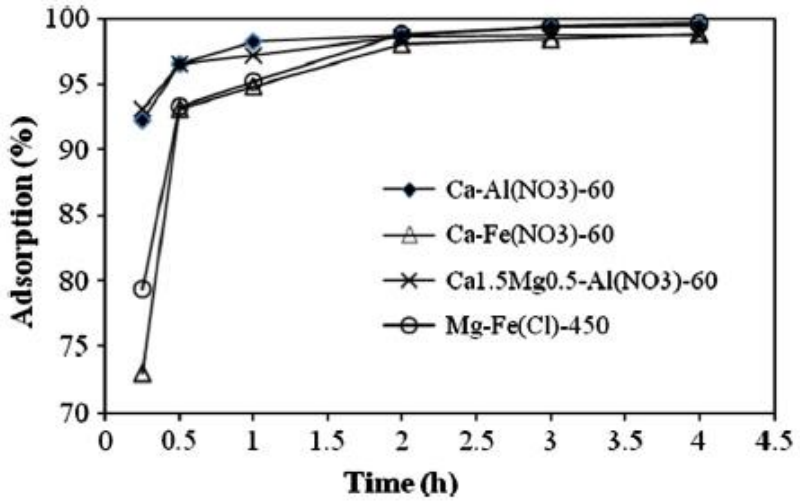

Figure 12. Phosphate adsorption kinetics with different LDH materials at [$P_{initial}$]=10 mg/L, pH 7.0 and 0.3 g/l for Ca-based LDHs and 2 g/L for Mg-Fe(Cl)-450 (Ashekuzzaman and Jiang, 2014).

In a further experiment the effect of pH in the range 3.0 to 12.0 was studied on the selected LDH materials. They observed that the Ca- and CaMg-based LDHs had a constant adsorption efficiency (98 %) in the pH range 3.5 to 10.5; meanwhile on the Mg-based LDH performed best between pH 3.0 and 7.5.

For the real effluent spiked up to 10 mg P/L only two LDH materials were used (Ca-Al(NO_3)-60 and Mg-Fe(Cl)-450). A 90 % adsorption removal was achieved with the first LDH material and adsorbent dose of 1.5 g/L, whereas 98 % efficiency was accomplished with the second LDH and adsorbent dose of 4.0 g/L.

For the regeneration of the different LDH materials, two NaOH solutions with different concentrations were used for the desorption of phosphate, 20 % and 4 % for the Ca-Mg-Fe(Cl)(NO_3)-450 and Mg-Fe(Cl)-450, respectively. It was found that desorption had negative impact on the Ca-based LDH due to loss of layered structure of the LDH material in the first cycle and the desorption efficiency decreased approximately down to 30 %. Nevertheless, the Mg-based LDH had a very good regeneration and reuse and its structure was stable.

2.4.4 Determination of the process variables for adsorption and desorption of phosphate from wastewater by selective ion exchangers on magnetic particles

In the study of Jiménez-Gutiérrez, 2015, experiments were performed with synthetic and real WW, where the initial concentration of PO_4-P was adjusted to 10 mg/L with H_3PO_4. A LDH material concentration of 200 mg/L was used. Adsorption and desorption kinetics for pure CaZnFeZr-LDH and composite particle material with 7.6 wt% CaZnFeZr-LDH were performed. The best phosphate adsorption efficiency (above 90 %) was achieved with the pure material after 1 h and 24 h, whereas for the composite material efficiency was 85.4 % and 92.1 % after 1 h and 24 h, respectively. Ten adsorption/desorption cycles were performed by using three different desorption solutions (1 M $NaHCO_3$, 1 M NaOH + 1M Na_2CO_3 and 3 M NaOH), where the last one showed best performance.

The effect of pH was studied by using CaZnFeZr-LDH with concentrations 80 mg/L and 48 mg/L LDH, in a pH range 3.0 to 12.0 and contact time of 24 h. On the other hand, ZnFeZr-LDH was used as well with 64 mg/L and 345 mg/L LDH concentration, in a pH range of 2.0 to 13.0 and .contact times 30 min, 1 h and 24 h. The CaZnFeZr-LDH achieved higher phosphate uptake (99.5 %) at pH 3.0 with the 80 mg/L LDH concentration, whereas the ZnFerZr-LDH achieved its maximum uptake (99.1 %) at pH 5.0 with the 345 mg/L LDH concentration.

The effect of adsorbent dosage was investigated (figure 13) in filtered and unfiltered WW (10 mg/L PO_4-P) using the ZnFerZr-LDH composite material. Best phosphate uptake of 99.2 % was achieved in the filtered WW after 24 h using a dosage of 259 mg/L LDH.

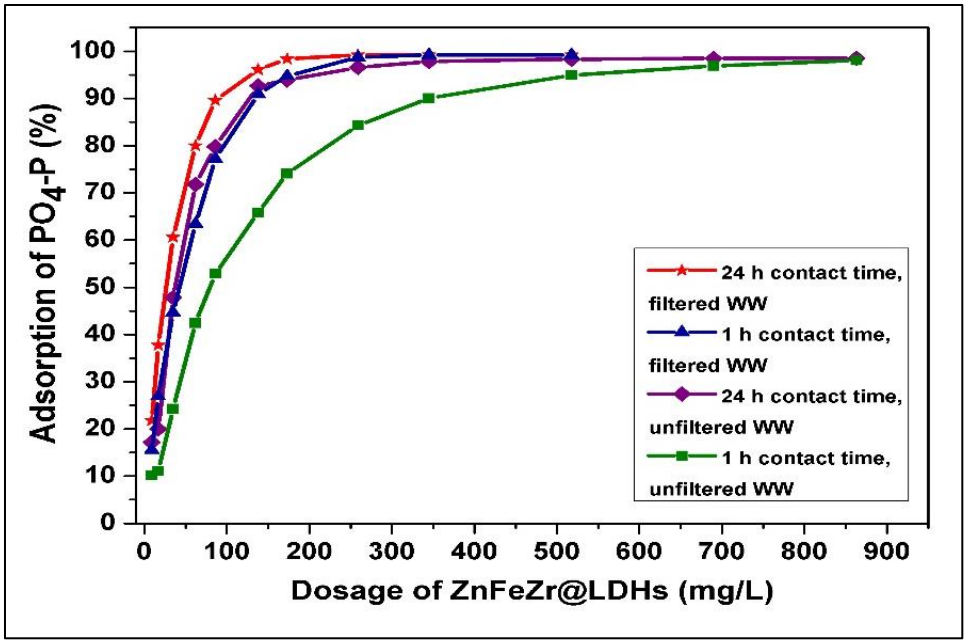

Figure 13. Adsorption of phosphate onto ZnFeZr-LDH as a function of adsorbent dosage. Reaction conditions: T= 22-23 °C; $[PO_4\text{-}P]_{in}$= 10 mg/L, pH=7.0-8.0 (Jiménez-Gutiérrez, 2015).

On the other hand, adsorption isotherms were developed for the filtered and unfiltered WW-PO_4-P solutions and fitted with two different adsorption models, Freundlich and Langmuir, equations 10 and 11, respectively:

$$logq_e = logk_{f+}\frac{lgC_e}{n} \qquad (10)$$

$$\frac{C_e}{q_e} = \frac{1}{K_L q_m} + \frac{C_e}{q_m} \qquad (11)$$

where C_e (mg/L) and q_e (mg/g) correspond to the equilibrium adsorbate concentration in the aqueous and solid phase. n is the constant that indicates the Freundlich isotherm curvature and K_f ((mg/g)/(mg/L)^n) is the Freundlich equilibrium constant, q_m (mg/m) is the maximum adsorption capacity and K_L (L/mg) is the Langmuir adsorption equilibrium constant (Yan *et al*, 2015). From these two isotherms, Freundlich model fitted better with correlation coefficients above 0.90.

Adsorption kinetics experiment was performed (figure 14) by using filtered and unfiltered WW with 10 mg/L PO_4-P each. The filtered WW reached equilibrium at about 4 h with a phosphate uptake of 99.0 %.

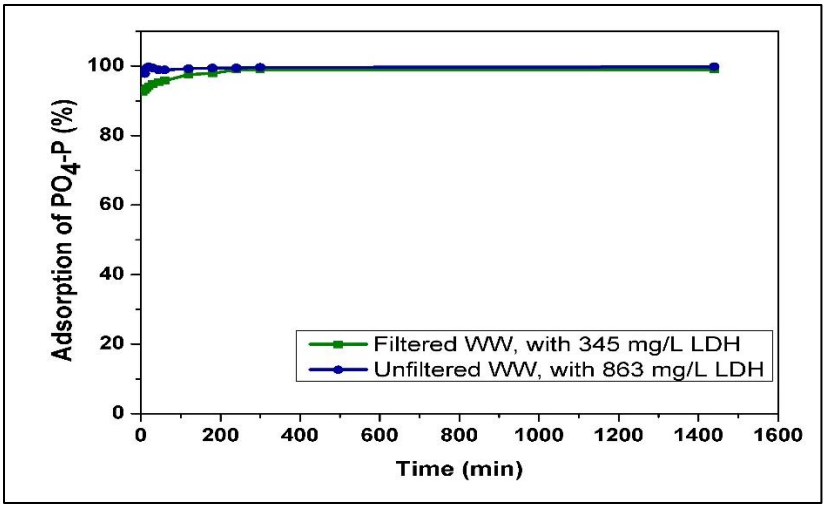

Figure 14. Adsorption of phosphate onto ZnFeZr-LDH as a function of the contact time in filtered and unfiltered WW. Reaction conditions: pH=7.0; $[PO_4\text{-}P]_{in}$= 10 mg/L, T=22-24 °C (Jiménez-Gutiérrez, 2015).

The pseudo-first order of Lagergren and pseudo-second order of Ho (equations 12 and 13, respectively) were calculated in order to conclude which one fitted the data better.

$$\log(q_e - q_t) = log q_e - \frac{k_1}{2.303} t \qquad (12)$$

$$\frac{t}{q_t} = \frac{1}{k_2 q_e^2} + \frac{t}{q_e} \qquad (13)$$

where q_e and q_t (mg/g) are the phosphate amount adsorbed on the adsorbents at equilibrium and at time *t*, respectively; *t* (min) is the contact time, k_1 (1/min) and k_2 (g/(mg·min)) are the rate constant of pseudo-first and pseudo-second order kinetic models (Yan *et al*, 2015).

It was found that the correlation coefficients were higher for the pseudo-second order than for the pseudo-first order model.

Chapter 3: Experimental description

3.1 Equipment and materials

For the measurements in this master thesis, equipment and materials from different laboratories at the Institute for Sanitary Engineering, Water Quality and Solid Waste Management (ISWA), the University of Stuttgart, Germany, were used.

3.2 Chemical reagents

All chemical reagents used in the different experiments are listed in table 1.

Table 1. Chemical reagents used in the different experiments.

Name	Chemical formula	Concentration	Manufacturer
Sodium hydroxide	NaOH	0.1; 1.0; 3.0 (mol/L)	Merck
Sulphuric acid	H_2SO_4	0.1; 1.0; 3.0; 9.17 (mol/L)	
Phosphoric acid	H_3PO_4	1000 (mg/L)	
Magnesium chloride hexahydrate	$MgCl_2 \cdot 6H_2O$	50; 150; 169; 195; 543; 935; 6000 (mg/L)	
Ammonium chloride	NH_4Cl	50; 150; 169; 195; 630; 6000 (mg/L)	

3.3 Experimental methodology

3.3.1 Adsorption and desorption cycles with different wastewater matrices: Using composite particle with 32 wt % ZnFeZr-LDH (sample MS-55-3)

The different raw wastewaters (RWW) and their origin which were used to perform the adsorption and desorption cycles are listed in table 6. In addition, their physicochemical characteristics are summarized in appendix A3-1.

Table 2. Raw wastewater matrices used in the adsorption and desorption cycles.

Nr	Raw wastewater matrices	Origin	Abbreviation
1*	SST effluent + H_3PO_4 10 mgPO_4-P/L spiked (unfiltered)	LFKW WWTP at ISWA	LFKW 10 L
2	MBA Process Water	Mechanical-Biological Waste Treatment Plant Landfill Kahlenberg	MBA
3	Digested sludge liquor filtrate	WWTP Offenburg	DSLF
4	Upflow anaerobic sludge blanket, centrifuged and filtered	Research Project TWIST++, ISWA	UASB

*1 RWW will be called LFKW 10 L experiment from now on to facilitate the understanding. The rest of the matrices remain as MBA, DSLF and UASB.

For the performance of the experiments, three vessels were filled with 1.0 L of the RWW, listed as 2, 3 and 4 in table 2. Regarding the 1st RWW, a larger vessel was used in order to use 10.1 L of RWW. For every adsorption cycle, 101 mL of RWW was taken out and then spiked with 1.01 mL of phosphoric acid (1000 mg/L) in order to reach a concentration of 10 mg/L PO_4-P in the solution. In every experiment 100 mL of blind sample was taken out for analysis and the rest was used for the adsorption cycles.

In the first adsorption cycle of each RWW, the corresponding volume of 15 wt % or 32 wt % ZnFeZr-LDH composite particles were dosed, as shown in table 3.

Table 3. Dose of ZnFeZr-LDH composite particles in the first adsorption cycle.

Raw wastewater	Composite particles used	Total suspended solids (mg/L)	ZnFeZr-LDH concentration (g/L)	Initial PO_4-P concentration (mg/L)
LFKW 10 L	15 wt % ZnFeZr-LDH	<1	1.0	9.7
MBA	32 wt % ZnFeZr-LDH	<1	0.32; 0.64, 0.80 and 1.00	4.7
DSLF	32 wt % ZnFeZr-LDH	110	1.2 and 2.0	49.8
UASB	32 wt % ZnFeZr-LDH	260	1.0	10.3

Note: For the MBA, from cycle 1-5 LDH dosage=0.32 g/l, from cycle 6-10 LDH dosage=0.64, from cycle 11-19 LDH dosage=0.80 g/L and from cycle 20-28 LDH dosage=1.00 g/L. For the DSLF, from cycle 1-4 LDH dosage=1.20 g/L and from 5-27 LDH dosage=2.00 g/L.

The reaction started once the composite particles were added to the vessels. The experiments were carried out at room temperature and the solutions were mixed with a magnetic stirrer. The

pH was regulated using 1 M H_2SO_4 or 1 M NaOH in order to maintain the pH in the range of 7.0-8.0. There was an exception for the DSLF RWW in which the pH was maintained at 5.0 after the 9th cycle in order to degas the WW, due to the considerable amount of carbonate concentration.

The contact time for each adsorption cycle was 20 min. The pH and the temperature were measured at the beginning and at the end of the experiment. The particles were separated using a strong hand magnet (figure 15). After approx. 30 minutes of particle settling, the supernatant liquid was removed and collected in another vessel, where it was homogenized before taking a sample for analysis. In the case of the LFKW 10 L experiment 1.0 L sample was taken every time, while for the MBA, DSLF and UASB tests, 200 mL, 250 mL and 250 mL were taken, respectively. It is important to note that in the case of the LFKW 10 L experiment it was necessary to pump out the supernatant liquid as shown in figure 16. The supernatant liquids were filtered with a 0.45 μm membrane filter before analysis. The pH, temperature and conductivity of the filtered supernatant liquids were measured and afterwards the phosphate concentration was analyzed photometrically according to DIN EN ISO 6678:2004.

Figure 15. Separation of the magnetic particles before and after using a strong hand magnet.

Figure 16. Pump system used for the supernatant liquid collection of the LFKW 10 L experiment.

The first desorption cycle was performed by addition of 1 M NaOH desorption solution (prepared in distilled water) into the respective reactors that contained the composite particles. 10 L of desorption solution were used in the LFKW 10 L experiment and 1.0 L in all the rest. The pH and temperature were measured at the beginning and end of the 20 minute contact time, without any pH regulation during desorption. After that, the particles were separated with the magnet and only 10 to 50 mL of supernatant liquid was sampled and then filtered with a 0.45 μm membrane filter. The remaining supernatant liquid was stored in order to be reused in the next cycles. At the end of each desorption cycle pH, temperature and conductivity of the filtered supernatant liquid were measured and afterwards the phosphate concentration was analyzed photometrically.

The procedures of the adsorption and desorption cycles were repeated 19, 28, 27 and 25 times for the LFKW 10 L, MBA, DSLF and UASB experiments, respectively. In the case of the DSLF measurements, two reclaimed solutions were obtained because at cycle 14 the NaOH desorption solution was exhausted, so it was decided to start the 15^{th} cycle with a fresh 1 M NaOH desorption solution. However, due to the fact that some minimal volume of desorption solution can remain at the bottom of the vessels and raise the pH of the next adsorption cycle, it was

necessary to wash the particles, which was performed from cycle 7 onwards for the DSLF and from the 16th cycle on for the UASB experiments.

3.3.2 Kinetics of PO_4-P removal during MAP precipitation at different pH values and at different molar ratios of Mg^{+2}:NH_4^+:PO_4^{-3} from synthetic wastewater

Two experiments were performed in order to study the adsorption kinetics of the struvite from synthetic WW. A synthetic liquor was prepared using H_3PO_4, NH_4Cl and $MgCl_2 \cdot 6H_2O$ analytical grade.

A- First experiment:

300 mL of a stock solution of H_3PO_4 1000 mg PO_4-P/L (prepared in distilled water) was added into a vessel of 1.0 L. In a separate vessel, 300 mL of precipitant solution of $NH_4Cl/MgCl_2 \cdot 6H_2O$ was prepared with a concentration of 100 mg/L in both salts (prepared in distilled water). The pH, temperature and conductivity parameters of each solution were measured. The molar ratio used in this experiment was 1.3:1.8:1.0 of Mg^{+2}:NH_4^+:PO_4^{-3}.

Once the solutions were prepared, the precipitant solution was added into the 1.0 L vessel that contained the phosphate solution at room temperature, which counts as the time 0 for the kinetics. The solution was mixed with a magnetic stirrer and the pH was regulated with solutions of 1 M H_2SO_4 or 1 M NaOH in order to maintain the pH at 8,5. After 5, 10, 15, 20, 30, 45, 60, 90 and 120 minutes, respective samples were taken. The supernatant liquids were filtered through a 0.45 µm membrane filter and afterwards, the conductivity as well as the phosphate concentrations of the filtered solutions were measured photometrically.

B- Second experiment (repetition)

The procedure was the same as described in A, with the following exceptions:

- Molar ratio of Mg^{+2}:NH_4^+:PO_4^{-3}: 2.7:2.0:1.0.
- Precipitant solution concentration: 300 mg/L both salts.
- Two more times were taking into account (150 and 180 minutes).
- pH: 9.0.

3.3.3 Kinetics of PO_4-P removal due to MAP precipitation from the obtained enriched reclaimed solutions at certain pH and molar ratio of Mg^{+2}:NH_4^+:PO_4^{-3}

Nine experiments were performed with the obtained enriched reclaimed solutions that were prepared in section 3.3.1. It is important to indicate that apart from the mentioned solutions, a fifth (not prepared by myself during this master thesis) reclaimed solution was provided and also tested. This reclaimed solution was obtained after completing 60 adsorption / desorption cycles using the SST effluent of the LFKW plant at ISWA and a 1 M NaOH as a desorption solution. The main physico-chemical characteristics of the enriched reclaimed solutions are summarized in table 4 and the complete characteristics can be found in the table A3-1 in the appendix.

Table 4. Main physicochemical characteristics of the enriched reclaimed solutions.

Enriched reclaimed solutions	P_{total} (mg/L)	$[PO_4\text{-}P]_{element}$ (mg/L)	PO_4^{-3} (mg/L)	pH	T° (°C)	CO_3^{-2} (mg/L)	NH_4^+ (mg/L)	Mg^{+2} (mg/L)	Cl^- (mg/L)	Na^+ (mg/L)	Ca^{+2} (mg/L)	K^+ (mg/L)
60th cycle LFKW	260.0	260.0	796.8	12.7	25.8	571.0	-	0.04	75.0	8.90	0.43	19.8
19th cycle LFKW 10 L experiment	170.0	169.0	511.8	12.8	20.0	5.0	18.6	0.25	170.0	7.28	0.43	23.5
28th cycle MBA	131.0	118.0	376.9	12.9	23.9	0.0	17.7	0.32	2300.0	14365.0	0.26	1137.0
14th cycle DSLF	185.0	179.0	548.6	10.0	17.9	1457.0	934.7	2.38	150.0	5401.0	2.13	213.0
25th cycle UASB	168.0	137.0	419.8	12.7	22.6	35900	86.5	774	280.0	5510.0	18.2	40.2

A- Kinetics with the 60th cycle reclaimed solution:

The concentrations of Mg^{+2} and NH_4^+ were not taken into account for the struvite kinetic measurements due to their low concentrations. A 1.0 L stock solution of NH_4Cl-$MgCl_2 \cdot 6H2O$ (390 mg/L of each salt) was prepared in distilled water. In the second experiment, 866 mL of the stock solution was taken and diluted to 1.0 L with distilled water in order to achieve a concentration of 338 mg/L. From both solutions, 100 mL was used in the adsorption kinetics test. The pH, temperature and conductivity parameters were measured. The molar ratios of Mg^{+2}:NH_4^+:PO_4^{-3} were 1.9:2.5:1.0 and 1.7:2.2:1.0 in the first and second experiments, respectively.

Precipitant solutions of 100 mL (390 and 338 mg/L) were added into two 250 mL vessels which contained 100 mL of the 60th cycle reclaimed solution each. The reclaimed solution was neutralized in advance to pH 7.8 with HCl_{conc}. The reactors were mixed with a magnetic stirrer

and pH was regulated as explained above in order to maintain the pH 9.0 during the struvite precipitation reaction. Samples were taken at predetermined times of 5, 10, 15, 30, 60 and 120 minutes. The supernatant liquids were treated and analyzed as was explained in the last section.

B- Kinetics with the 19th cycle LFKW 10 L experiment reclaimed solution

The concentrations of Mg^{+2} and NH_4^+ were not considered for the struvite adsorption kinetics because they were very low, as in the previous section, and Mg and NH4 were added completely through external source. Two experiments were performed with this reclaimed solution. The P-removal kinetics measurement procedure was the same as in a), with the following variations:

- Molar ratio of Mg^{+2}:NH_4^+:PO_4^{-3}= 2.0:2.5:1.0 and 4.0:5.2:1.0.
- Precipitant solution concentration: 6000 mg/L both salts.
- Samples at two additional contact times (180 and 240 minutes) were taken.
- The pH during struvite precipitation was maintained at pH 8.5.

C- Kinetics with the 28th cycle MBA reclaimed solution

The concentrations of Mg^{+2} and NH_4^+ were not considered for the struvite kinetics due to their low concentrations and they were added externally. Three experiments were performed with this reclaimed solution. The same procedures for measuring the adsorption kinetics were applied as in a), with the following exceptions:

- Molar ratio of Mg^{+2}:NH_4^+:PO_4^{-3}: 2.0:2.5:1.0; 2.6:3.4:1.0 and 6.0:8.0:1.0.
- Precipitant solution concentration: 6000 mg/L both salts. From this solution, 3.075 mL, 4.000 mL and 27.125 mL were taken and added to 100 mL, 100 mL and 300 mL of the 28th MBA reclaimed solution, respectively.
- In addition to the times mentioned above, samples at 180 minutes for the second experiment, and 180 and 240 minutes for the third, were also measured.
- Reaction pH was 8.5.

D- Kinetics with the 14th cycle DSLF reclaimed solution

The NH_4^+ concentration of this reclaimed solution was sufficiently high (934.7 mg/L), therefore only 0.8672 g of $MgCl_2 \cdot 6H_2O$ was added directly into 110 mL of DSLF reclaimed solution in order to reach a molar ratio Mg:PO_4 of 1.7. The same procedures for measuring the adsorption kinetics were applied as in a), with the following exceptions:

- Molar ratio was Mg^{+2}:NH_4^+:PO_4^{-3}= 6.7:9.0:1.0.
- Additional sampling at 3 h and 4 h.
- The reaction pH was 8.5.

E- Kinetics with the 25th cycle UASB reclaimed solution

The UASB reclaimed solution contained a NH_4^+ concentration of 86.5 mg/L, therefore, in order to achieve a molar ratio 6.0:8.0:1.0 of Mg^{+2}:NH_4^+:PO_4^{-3}, it was necessary to add NH_4Cl and $MgCl_2 \cdot 6H_2O$ directly into 110 mL of UASB reclaimed solution. The same procedures for measuring the adsorption kinetics were applied as in a), with the following exceptions:

- Additional sampling at 3 h and 4 h.
- The reaction pH was 8.5.

3.3.4 Maximize the struvite yield from synthetic wastewater and the obtained enriched reclaimed solutions at optimal pH, contact time and Mg^{+2}:NH_4^+:PO_4^{-3} molar ratio

Once the contact time, pH value and Mg^{+2}:NH_4^+:PO_4^{-3} molar ratios were defined for the struvite adsorption kinetics measurements in each reclaimed solution, the next step was maximize the MAP yield. Table 5 shows the optimal conditions at which each struvite precipitation was performed. All the experiments were performed at room temperature and mixed with a magnetic stirrer at 500 rpm.

The pH of the reclaimed solutions was adjusted with HCl_{conc} as was explained in section 3.3.3 and conductivity was also measured. The respective precipitant solutions of NH_4^+ and Mg^{+2} were then added to each reactor vessel, containing the enriched reclaimed solutions and reaction started immediately. Temperature and pH were recorded at the beginning and at the end of the struvite precipitation. Samples were taken at predefined contact times and the solutions were filtered using filter paper. The supernatant liquid was collected in vessels in order to measure its pH, temperature, conductivity and phosphate concentration. The filter papers with the retained struvite were dried at room temperature and weighed.

Table 5. Conditions of the struvite precipitation from synthetic WW and different enriched reclaimed solutions.

Number	**Matrix type**	**Contact time (h)**	**pH**	**Molar ratio Mg^{+2}:NH_4^+:PO_4^{-3}**	**Total matrix volume (mL)**
1	Synthetic WW	3.0	8.5	2.7:2.0:1.0	320
2	60^{th} cycle LFKW	2.0	9.0	1.0:2.5:1.0	100
3	60^{th} cycle LFKW	2.0	9.0	1.7:2.2:1.0	100
4	19^{th} cycle LFKW 10 L	2.0	8.5	2.0:2.5:1.0	300
5	19^{th} cycle LFKW 10 L	3.0	8.5	4.0:5.2:1.0	680
6	28^{th} cycle MBA	4.0	8.5	6.0:8.0:1.0	190
7	14^{th} cycle DSLF	2.0	8.5	6.7:9.0:1.0	600
8	25^{th} cycle UASB	2.0	8.5	6.0:8.0:1.0	600

Chapter 4: Results and discussion

4.1 Adsorption and desorption cycles with the different raw wastewater matrices by using the composite particle with 32 wt % ZnFeZr-LDH (sample MS-55-3)

Based on previous results (Jiménez-Gutiérrez, 2015) and as mentioned in section 2.4.4, the ZnFeZr-LDH composite material showed the best performance under optimized experiment conditions. Therefore, the ZnFeZr-LDH modified particles were used as the composite material to perform the adsorption/desorption cycles on the RWWs of the LFKW 10 L experiment, MBA, DSLF and UASB tests, which had the following numbers of complete cycles: 19, 28, 27 and 25, respectively.

4.1.1 LFKW 10 L experiment adsorption/desorption cycles

According to figure 17, in each adsorption cycle, more than 80 % (from the 100 mg PO_4-P initial mass per cycle) of the phosphate was adsorbed onto the ZnFeZr-LDH composite material. This good performance of the phosphate adsorption was observed for each cycle, meaning that in total 96.6 % of the dosed phosphate was adsorbed after 19 cycles. Furthermore, the results indicate that the phosphate uptake was not affected by the presence of other anions such as CO_3^{-2}, Cl^-, NO_3^- and SO_4^{-2}, which their concentrations were: 39, 149, 40.7 and 76 mg/L, respectively, which were all higher than the phosphate concentration of 10 mg/L and this result was expected.

The desorption cycles also demonstrated satisfactory performance, reaching efficiencies higher than 75 %. However, cycles 4, 8 and 9 showed low desorption of PO_4-P: 42, 53 and 31 mg, respectively. In these cycles, it was observed that, during the settlement of the particles, the supernatant liquid was turbid and yellow. This yellowish color could be attributed to the composite material releasing iron due to the high pH value. In contrast, cycles 6, 7, 13 and 19 had desorption concentrations higher than 100 % and this could be due to some non-adsorbed phosphate residues that desorbed later.

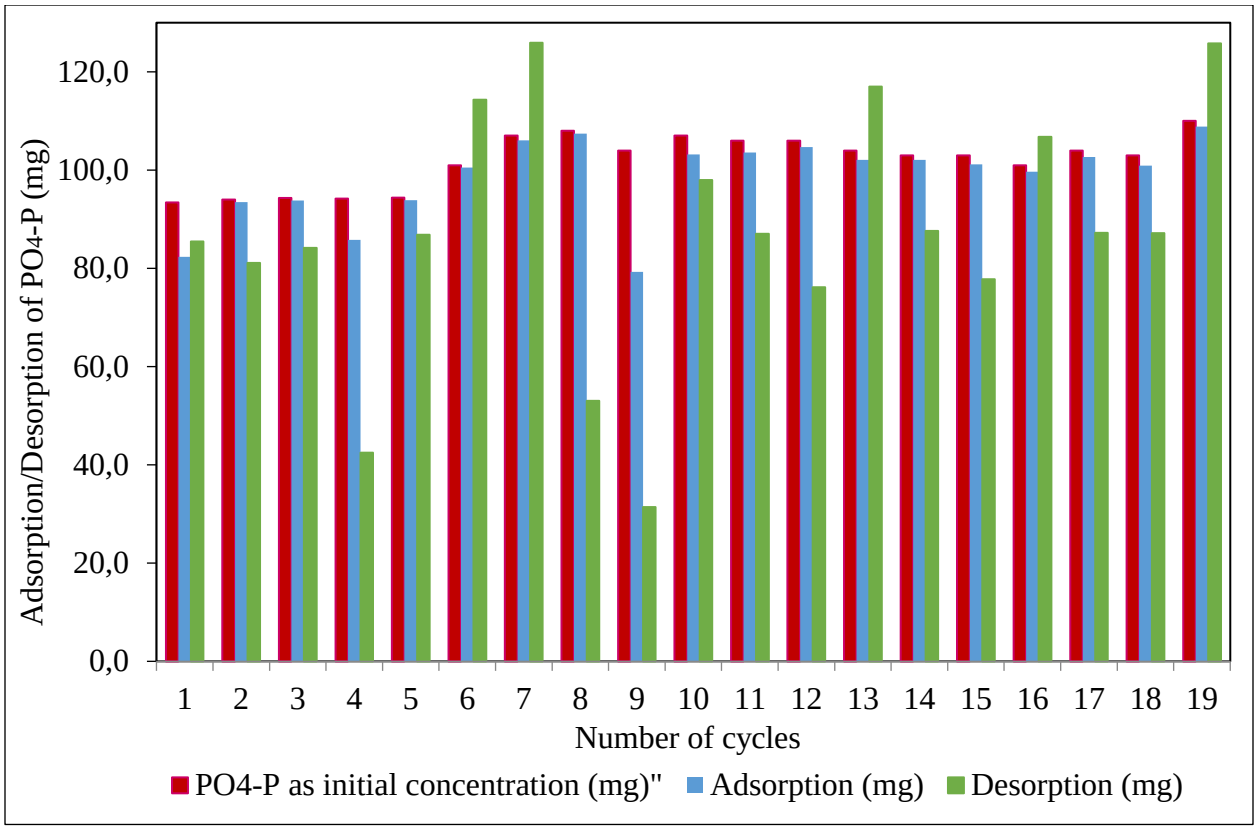

Figure 17. Adsorption/desorption of phosphate from LFKW 10 L with 15 wt% ZnFeZr-LDH. Reaction conditions: 1 M NaOH desorption solution. Contact time=20 min ads/des. Adsorption pH=7.0-7.5 and desorption pH=12.0-13.6. [LDH]=1 g/L, T=17-25 °C. $[PO_4\text{-}P]_{in}$= 93-100 mg per cycle.

Figure 18 shows the adsorption and desorption efficiency of phosphate with the ZnFeZr-LDH composite material. As mentioned before, a total of 96.6 % of the dosed phosphate was adsorbed and from this, 85.4 % was desorbed afterwards.

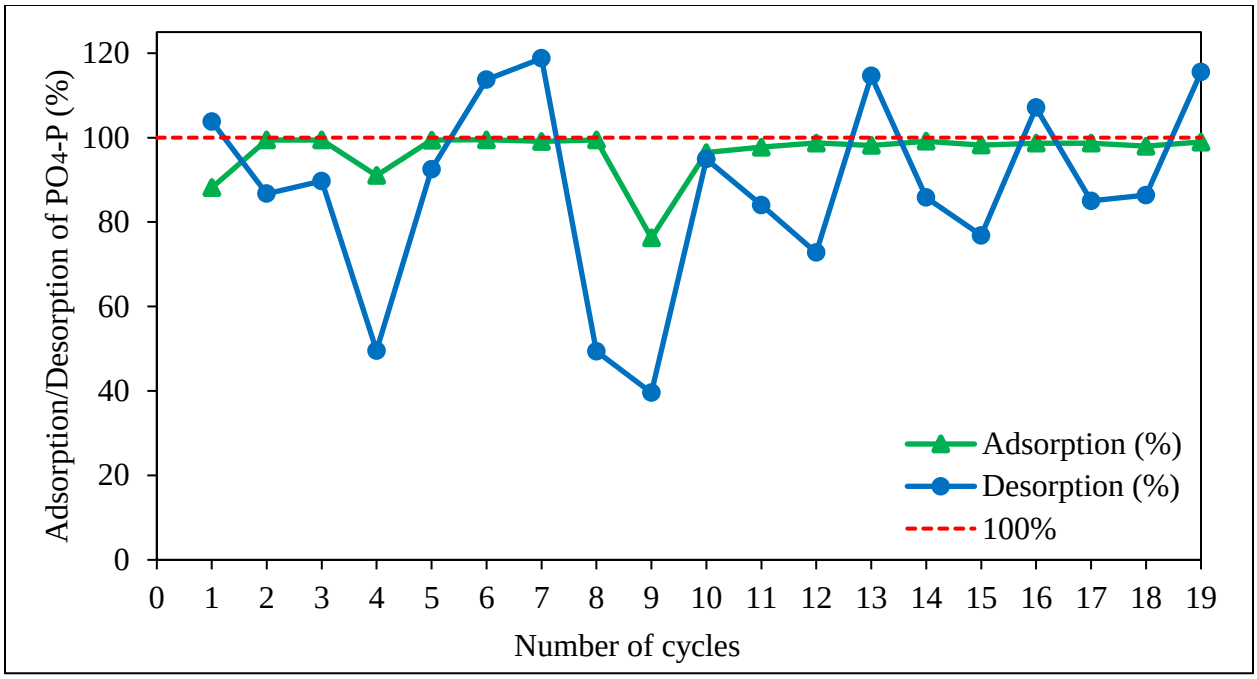

Figure 18. Adsorption/desorption efficiency of phosphate from LFKW 10 L with 15 wt% ZnFeZr-LDH composite particles throughout 19 cycles.

Figure 19 illustrates the enrichment with phosphate in the reclaimed solution after each desorption cycle. At the end of the 19th cycle, the concentration was 169 mg PO_4-P/L which is sufficient for further struvite precipitation.

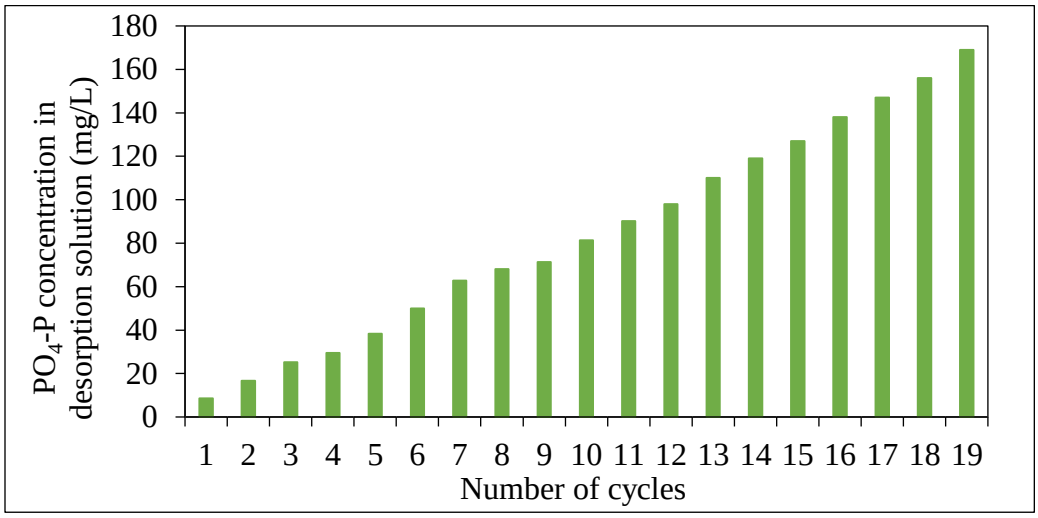

Figure 19. Enrichment of phosphate in LFKW 10 L desorption solution after every desorption cycle.

4.1.2 MBA adsorption/desorption cycles

In figures 20 and 21, it can be observed that the first five adsorption cycles had low efficiencies (below 60 %), in comparison with the 90 % adsorption goal. This was a result of the low concentration of ZnFeZr-LDH composite material that was added, namely 0.32 g/L. In the next five cycles, double LDH concentration of 0.64 mg/L was used, which improved the phosphate adsorption. Nevertheless, the efficiency was still insufficient and the LDH concentration was increased two more times, to 0.80 g/L and then to 1.00 g/L. This last concentration is the one that demonstrated in previous studies (Jiménez-Gutiérrez, 2015) to be the optimum concentration for the removal of phosphate; this conclusion is also valid for WWs (from the SST effluent at LFKW, ISWA) spiked with phosphoric acid in order to reach PO_4-P concentrations of 100 and 300 mg/L. As observe, after cycle 6 the adsorption performance remained constant, whereby a total of 82 % of the dosed phosphate was adsorbed.

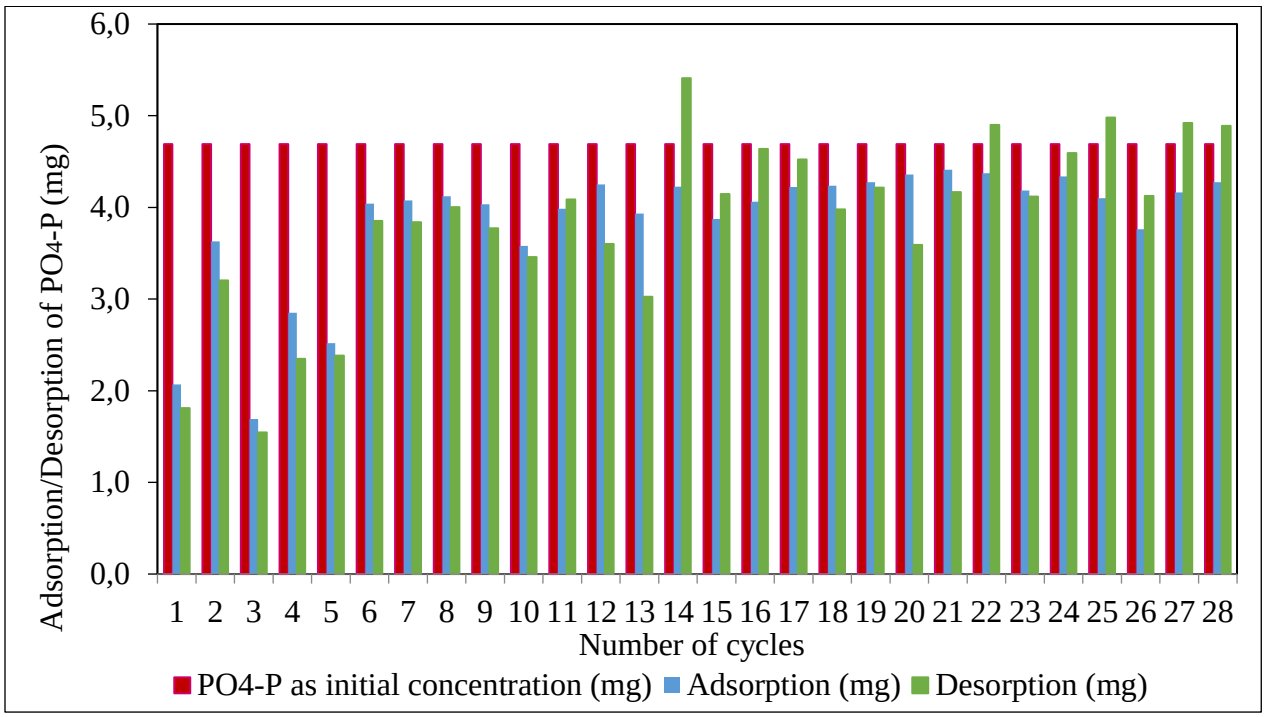

Figure 20. Adsorption/desorption of phosphate from MBA wastewater with 32 wt% ZnFeZr-LDH. Reaction conditions: 1 M NaOH desorption solution. Contact time= 20 min ads/des. Adsorption pH=7.5-7.8 and desorption pH=12.2-13.0. [LDH]=0.32; 0.64; 0.8 and 1 g/L, T=21-25 °C. $[PO_4\text{-}P]_{in}$= 4.69 mg per cycle.

The MBA had a considerable concentration of CO_3^{-2}, Cl^-, NO_3^- and SO_4^{-2} (442, 5400, 753 and 100 mg/L, respectively). These anions might compete with phosphate during adsorption. In the studies of Goh *et al*, 2008, the competition between anions follows the order $HPO_4^{-2} > SO_4^{-2} > CO_3^{-2} > NO_3^-$. This competition, due to the high concentration of these anions comparable to the PO_4-P concentration (4.7 mg/L), could be part of the explanation or the low obtained yield over the first five cycles.

Regarding the desorption cycles, despite the low performance in the first five adsorption cycles, these cycles reached desorption rates higher than 1.5 mg, out of the 2.5 mg phosphate that were adsorbed. Additionally, from cycle 14 to 28 the desorption of phosphate increased and could be due to some non-adsorbed phosphate residues that also desorbed in this period.

Figure 21 shows the total adsorption and desorption efficiency of phosphate with the ZnFeZr-LDH composite material. A total of 82 % of the dosed phosphate was adsorbed and, from this, 82.3 % was desorbed afterwards.

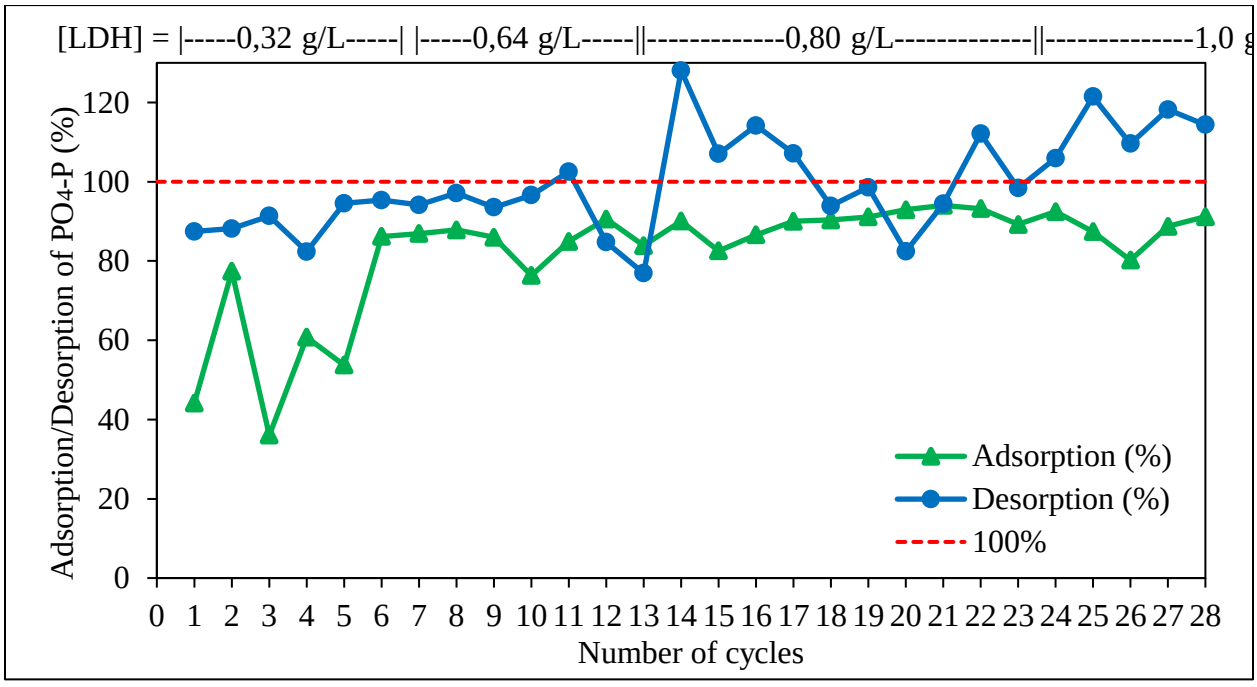

Figure 21. Adsorption/desorption efficiency of phosphate from MBA wastewater with 32 wt% ZnFeZr-LDH composite particles throughout 28 cycles.

Figure 22 demonstrates the enrichment with phosphate in the reclaimed solution after each desorption cycle, with a final concentration of 123 mg PO_4-P/L.

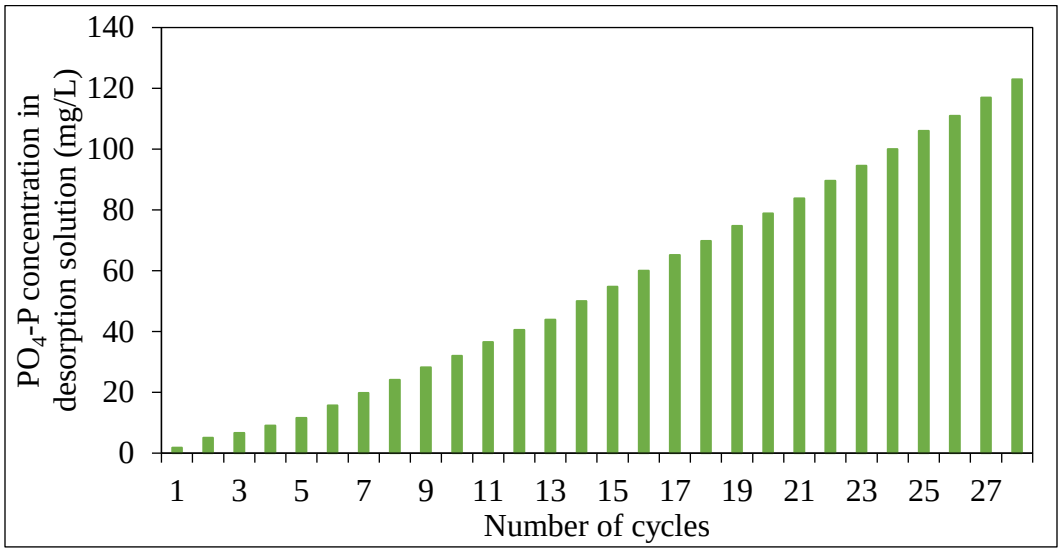

Figure 22. Enrichment of phosphate in MBA desorption solution after every desorption cycle.

4.1.3 DSLF adsorption/desorption cycles

As can be seen in figures 23 and 24, the total amount of phosphate adsorbed fluctuated with each cycle throughout the experiment. The first 10 adsorption cycles had a pH between 7.5 and 9.5 because the concentration of carbonate in the RWW was still unknown during the cycles. Once it was realized that the carbonate concentration was high (1060 mg/L), it was decided to work at pH 5.0 in order to improve the adsorption performance; due to the carbonate buffer capacity, working at this pH allows $CO_{2(g)}$ to be released into the atmosphere. In fact, bubbles formation were observed during the experiment in the solution, indicating the release of gas (figure 25). This issue is important because the carbonate inhibits the phosphate adsorption, as it competes for the adsorption sites on the LDH-particles, which resulted in the reduction of the total adsorbed phosphate (only 75.4 %), in comparison with the LFKW 10 L experiment and the MBA wastewater. In contrary, the anions Cl^-, NO_3^- and SO_4^{-2} in the DSLF RWW had low concentrations, thus not affecting the total adsorption performance. In addition, the DSLF contained a high concentration of total suspended solids (110 mg/L), which could clog the pores of the LDH-particles leading to a reduction of the contact surface area on the LDH available for the adsorption of phosphate.

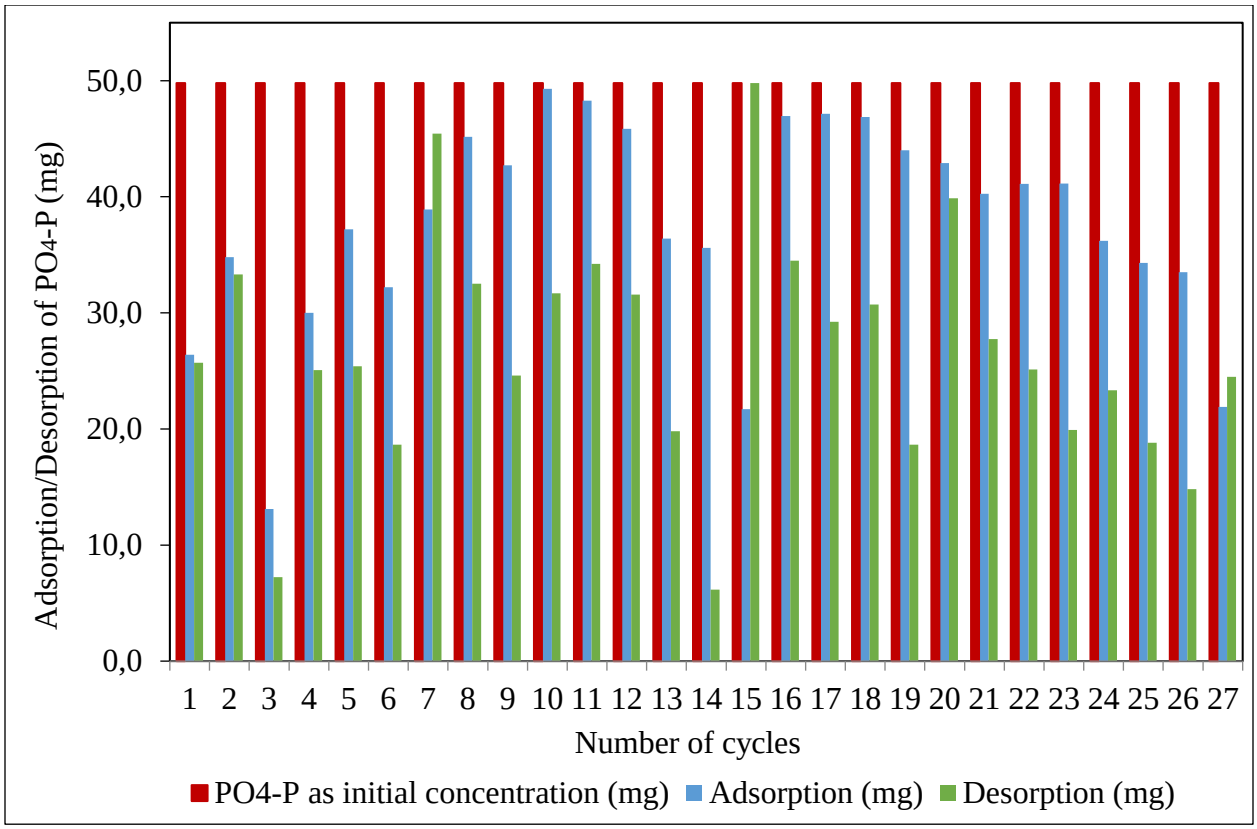

Figure 23.Adsorption/desorption of phosphate from DSLF wastewater with 32 wt% ZnFeZr-LDH. Reaction conditions: 1 M NaOH desorption solution. Contact time= 20 min ads/des. Adsorption pH=7.0-9.5 from cycle 1-10 and 5.0 from cycle 11-27. Desorption pH=10.3-13.2. [LDH]=1.2 and 2 g/L. T=18-24.5 °C. $[PO_4\text{-}P]_{in}$= 49.8 mg per cycle.

In the case of the desorption cycles, the total amount desorbed across the measurement fluctuated with each cycle. However, in this experiment two 1 M NaOH desorption solutions were necessary for the enrichment of the phosphate. In cycle 12 (figure 4-8), it can be observed that the phosphate desorption dropped, whilst cycle 14 had the lowest desorption efficiency (17.3 %), due to the desorption solution which was already exhausted of OH^- anions, resulting in a decrease in the regeneration of the LDH-particles that reduced the ion exchange between OH^- and phosphate anions. This hypothesis can be supported by the rapid decrease in the conductivity of the desorption solution (table A1-3 in the appendix A1). For this reason a second, 1 M NaOH, desorption solution was added from cycle 15 onwards. A significant rise in the phosphate desorption (229 % desorption efficiency) as a result of the excess concentration of OH^- anions in the media was observed. During this desorption, the solution was also exhausted, as can be

inferred from the rapid decrease of the conductivity from cycles 20 to 26 (table A1-3 in the appendix A1). From the total 75.4 % of the dosed phosphate was adsorbed, 53.4 % was desorbed, resulting in a reclaimed solution with the lowest enrichment compared to the LFKW 10 L experiment and MBA enriched reclaimed solutions above.

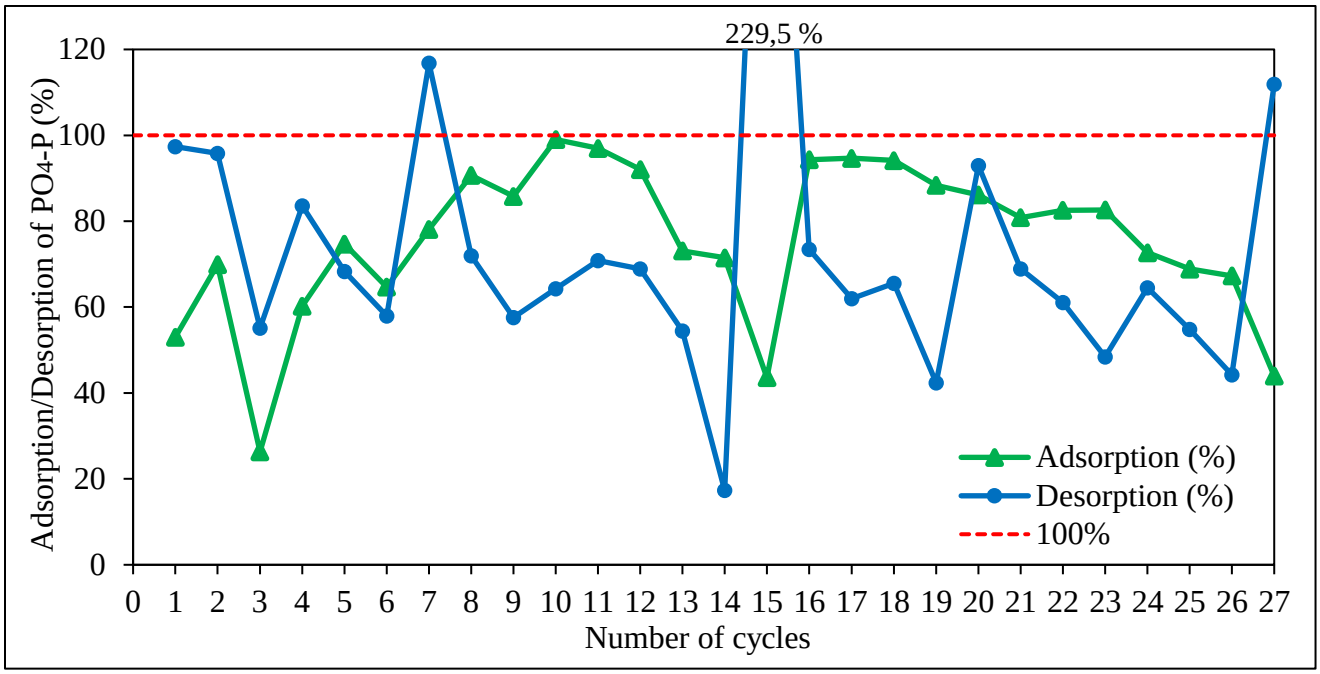

Figure 24. Adsorption/desorption efficiency of phosphate from DSLF wastewater with 32 wt% ZnFeZr-LDH composite particles throughout 27 cycles.

Figure 25. Production of $CO_{2(g)}$ during phosphate adsorption cycles with DSLF RWW.

Figure 26 shows the phosphate enrichment in both desorption solutions, which at the end was 179.0 mg PO_4-P/L. It can be suggested that, at a certain point, this desorption solution cannot be enriched further than 180-190 mgPO_4-P/L due to the enrichment remaining nearly constant in the last desorption cycles.

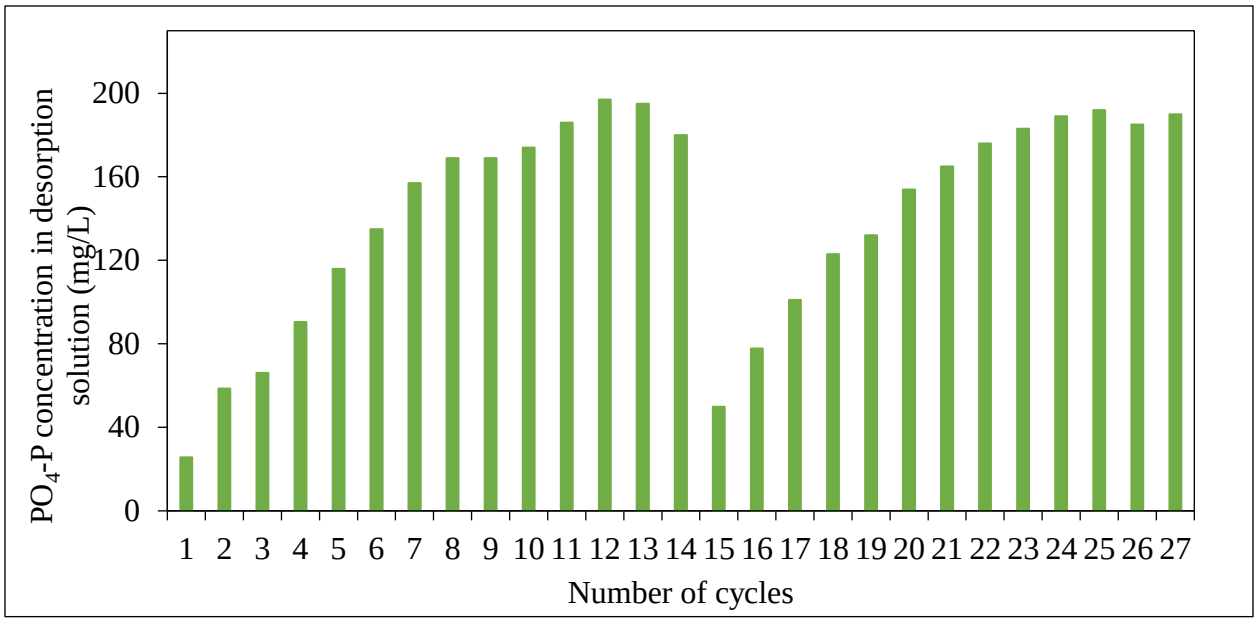

Figure 26. Total enrichment of phosphate in DSLF desorption solution after every desorption cycle.

4.1.4 <u>UASB adsorption/desorption cycles</u>

The UASB had the highest concentration of total suspended solids (260 mg/L) out of all four RWWs that were tested for adsorption and desorption cycles, which may cause clogging of the LDH-particles and reduction of the contact surface area available for the adsorption of phosphate.

According to figure 27, the adsorption and desorption cycles performance from 1 to 8 was satisfactory. From cycle 1 to 3 the working pH was 7.0 in contrast to cycle 4 to 7 where the pH was 5.0 to degas the detected carbonate with concentration of 84 mg/L after cycle 3. It was observed that changing the pH to 5.0, did not enhance the phosphate adsorption, meaning that the carbonate presence did not affect the phosphate removal for this kind of RWW. Based on this result, it was decided to continue the adsorption cycles working with pH 7.0-7.5. However, from

cycle 9 phosphate removal decreased, likely because of the high concentration of TSS, which affected the phosphate elimination. The concentration of the anions NO_3^- and SO_4^{-2} in the UASB were low (4.4 and 52 mg/L, respectively), but the Cl^- anion concentration was high (330 mg/L), affecting the total adsorption performance. Based on this observation, decision was made to start washing the particles from cycle 16 until the end, as even a minimal volume of desorption solution remaining at the bottom of the vessel could raise the phosphate concentration and pH in the next adsorption cycle. This measure improved the phosphate adsorption.

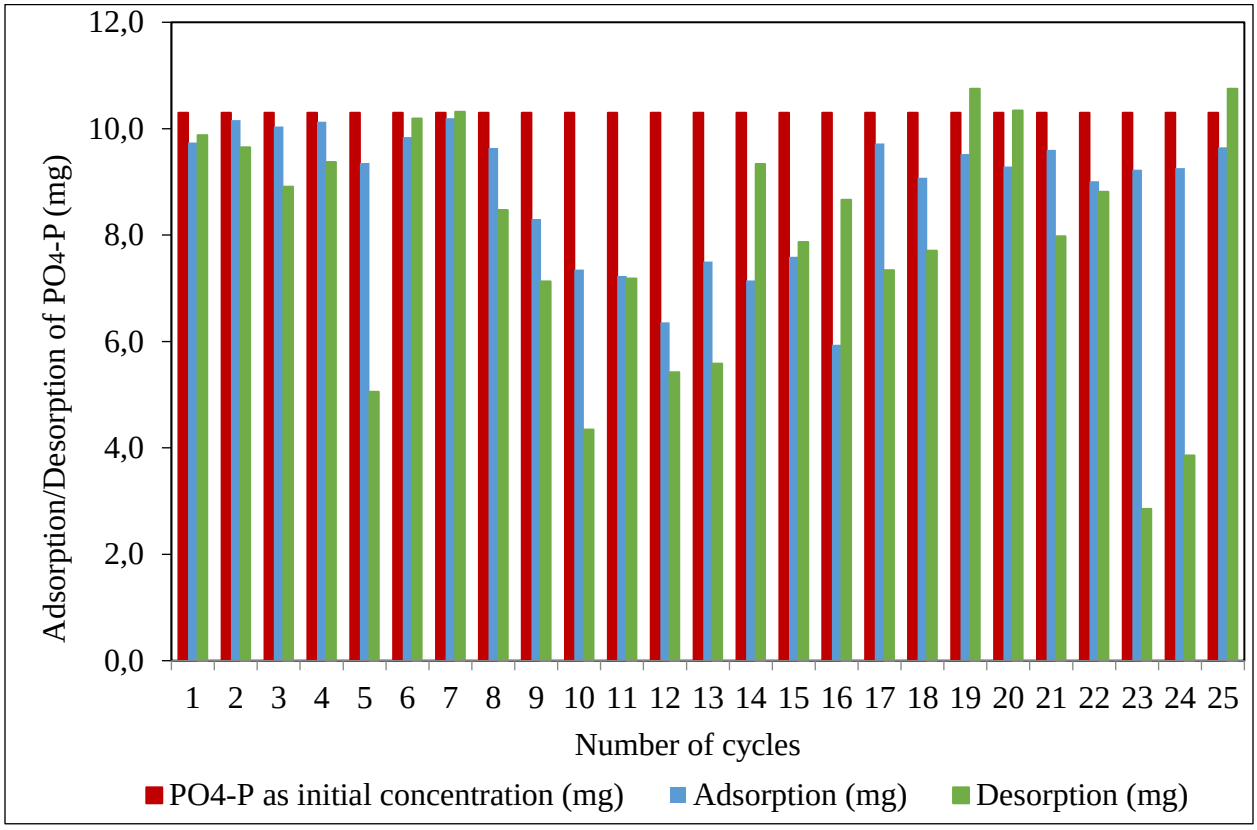

Figure 27. Adsorption/desorption of phosphate from UASB wastewater with 32 wt% ZnFeZr-LDH. Reaction conditions: 1 M NaOH desorption solution. Contact time= 20 min ads/des. Adsorption pH=7.0-8.0. Desorption pH=11.5-13.0. [LDH]=1 g/L. T=19-24 °C. $[PO_4\text{-}P]_{in}$= 10.3 mg per cycle.

Figure 28 shows that the adsorption performance was insufficient from cycle 8 to 16. It is important to note that the washing of the LDH-particles started from cycle 16 which enhanced the phosphate removal. Nonetheless, the desorption had significant fluctuations, a total of 85.8 %

of the dosed phosphate was adsorbed and 76.8 % was desorbed. Cycles 14, 16, 19, 20 and 25 had desorption efficiencies above 110 %, which could be attributed to non-desorbed phosphate adsorbed during previous cycles being released in these.

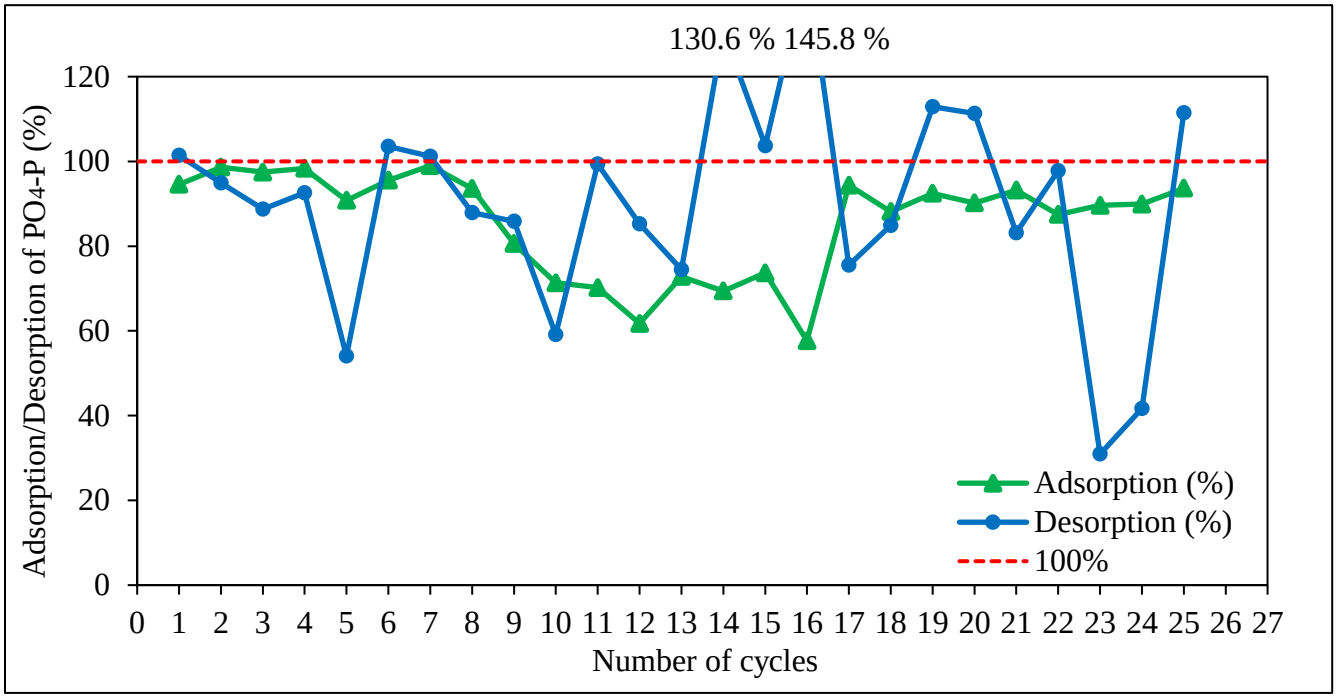

Figure 28. Adsorption/desorption efficiency of phosphate from UASB wastewater with 32 wt% ZnFeZr-LDH composite particles throughout 25 cycles.

Figure 29 illustrates the phosphate enrichment of the UASB reclaimed solution. The experimental data show that this type of wastewater does not allow enrichment more than 135 mgPO_4-P/L, shown by the nearly constant phosphate concentrations in the last desorption cycles.

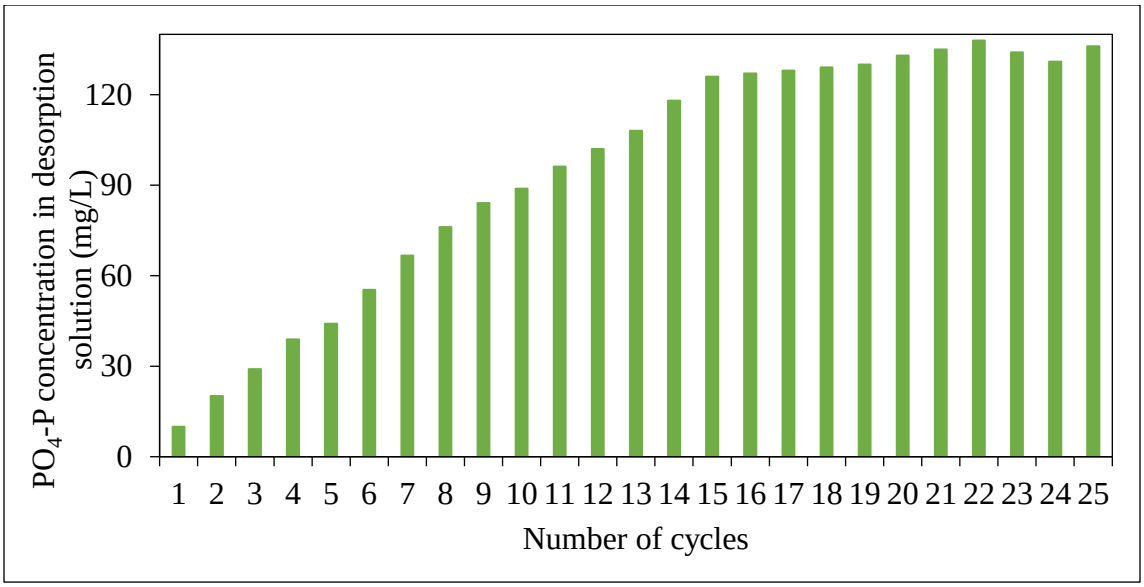

Figure 29. Enrichment of phosphate in UASB desorption solution after every desorption cycle.

It can be said that the more complex the RWW is, the more difficult it is to adsorb phosphate onto the LDH-particles, leading to a reduced phosphate enrichment of the reclaimed solution. From all performed adsorption/desorption cycle experiments, the LFKW 10 L experiment had the best adsorption total efficiency of 96.6 % and from this 85.4 % was desorbed. The DSLF experiment had the lowest adsorption total efficiency (75.4 %) and from this 53.4 % was desorbed.

4.2 Kinetics of phosphate removal during MAP precipitation at various molar ratios of Mg^{+2}:NH_4^+:PO_4^{-3}, using synthetic wastewater and the obtained enriched reclaimed solutions

As demonstrated in earlier experiments, pH has an important role on the struvite precipitation and on its kinetics. According to previous studies, the optimum pH range for struvite precipitation from synthetic WW is between 8.0 and 10.7, nevertheless pH higher than 9.0 leads to a decrease in the concentration of ammonium. As a result, keeping the pH around 8.5 is considered as ideal (Bouropoulos and Koutsoukos, 2000, Kofina and Koutsoukos, 2005, Ezquerro, 2010, Desmidt *et al*, 2013, Ariyanto *et al*, 2014 and Egle *et al*, 2015).

Regarding the struvite precipitation from real WW, many studies suggest that the optimum pH is between pH 8.0 and 9.0, whereas beyond pH 9.0 the ammonium in the system decreases (Perera *et al*, 2007, Ewert *et al*, 2014 and Huang *et al*, 2014).

Based on the above conclusions, the phosphate removal kinetics tests during struvite precipitation from all solutions were performed at pH 8.5 except for the LFKW 60th cycle regenerate, which was performed at pH 9.0. As variation, only the molar ratios of Mg^{+2}:NH_4^+:PO_4^{-3} were changed in the kinetics measurements.

The phosphate removal kinetics during struvite precipitation is very fast and usually follows first order kinetic model (Le Corre *et al*, 2007 and Ariyanto *et al*, 2014). The calculation of the order in the kinetic model was not subject of study in this master thesis.

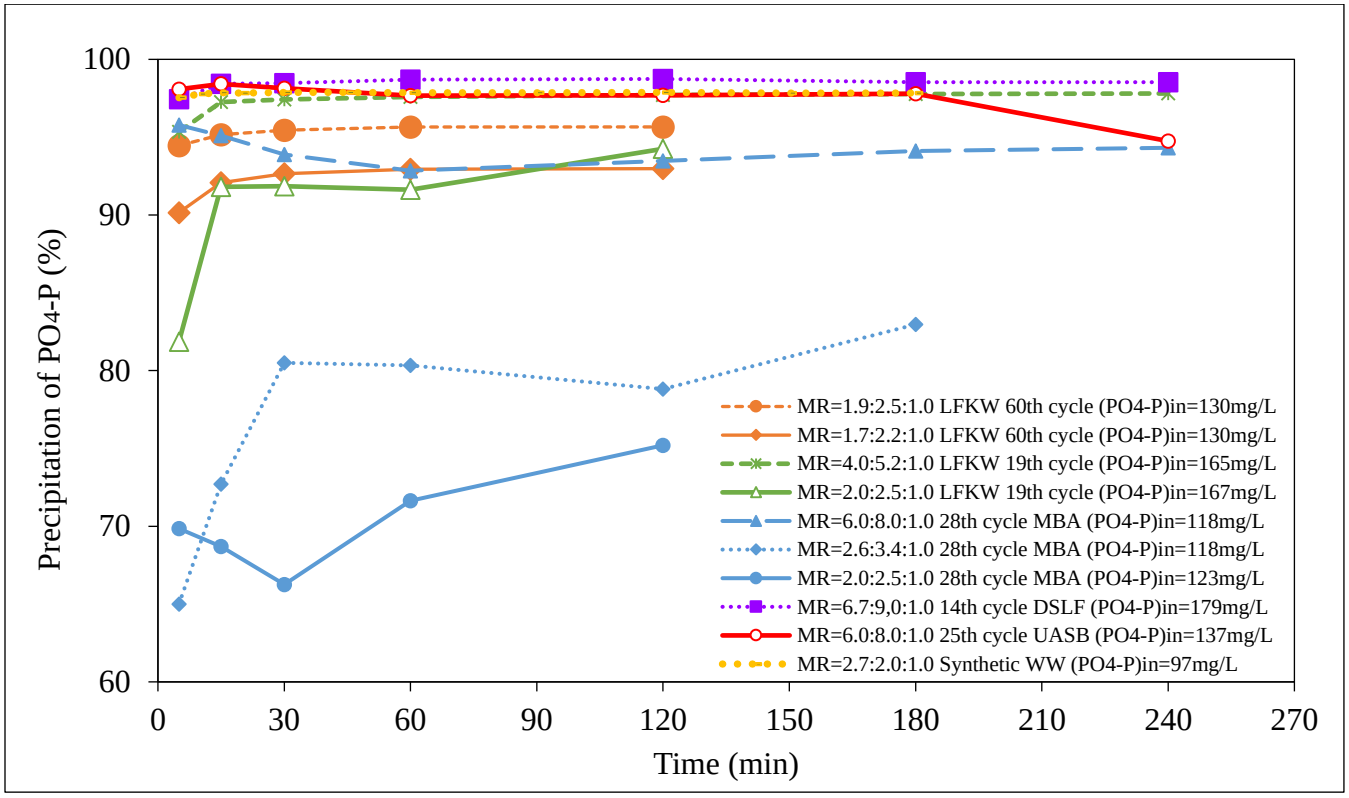

Figure 30. Phosphate removal kinetics during struvite precipitation from synthetic WW and the different enriched reclaimed solutions. Reaction conditions: pH=8.5 for all solutions, except for the 60th cycle reclaimed solution (pH=9.0). T°=23.0-25.0 °C. Remark: MR = Molar ratio Mg^{+2}:NH_4^+:PO_4^{-3}.

Figure 30 shows the phosphate uptake kinetics during struvite precipitation from the different enriched reclaimed solutions and the synthetic WW. The variation of the results obtained at pH 8.5 and 9.0 demonstrate the role of the pH in the struvite precipitation kinetics.

The best phosphate uptake was in the order: Synthetic WW (pH=8.5) > LFKW 10 L experiment (pH=8.5) > LFKW 60th cycles (pH=9.0) > MBA (pH=8.5). This indicates that when working at pH 8.5 the phosphate precipitation is a bit higher than at pH 9.0. The struvite precipitation from the MBA matrix showed lower phosphate removal efficiency than the same with the LFKW 10 L matrix, despite of the same pH and molar ratio during the reaction. This is due to the fact that the MBA reclaimed solution had a higher concentration of sodium (14365 mg/L) and potassium (1137 mg/L) than the others. This can cause the formation of the respective Na and K salts with the HPO_4^{-2} ions, (dominant species at pH 8.5). As a consequence, less phosphate ions were available for the struvite precipitation, or alternatively Na and K were co-precipitated in the struvite structure. Moreover, the synthetic WW had the highest phosphate uptake because the solution consisted only of the NH_4^+, Mg^{+2} and PO_4^{-3} ions, meaning that no other ions were present to interfere with its formation.

As stated in Desmidt *et al*, 2013, from an economical point of view, the minimum concentration of PO_4-P that should be present in the WW for struvite precipitation is 50.0 mg/L (153.2 mg PO_4^{-3}/L). The concentrations used for the struvite adsorption kinetics were: 50; 260; 170; 131; 185 and 168 mg PO_4-P/L for the synthetic WW, LFKW 60 cycles, LFKW 10 L, MBA, DSLF and UASB reclaimed solutions, respectively.

Regarding the reclaimed solutions obtained from the SST effluent of the LFKW treatment plant at ISWA, with a molar ratio of 1.9:2.5:1.0 for the LFKW 60 cycles and 2.0:2.5:1.0 for the LFKW 10 L experiment, the better performance it was detected with the LFKW 60 cycles reclaimed solution. The LFKW 60th cycles reclaimed solution did not contain originally ammonium, whereas the other had a concentration of 18.6 mg/L which could be lost as ammonia during the pH regulation, causing a decrease of the MAP formation and thus, lower phosphate removal efficiency.

Additionally, a comparison between both sludge liquors, the DSLF and the UASB, reveals that, even though their molar ratios were different, the performance was similar. This can be attributed to the low calcium concentrations (2.13 and 18.2 mg/L, respectively) which were not sufficient for the formation of struvite-formation hindering calcium carbonate, despite of the high carbonate concentrations (1457 mg/L and 423 mg/L, respectively). According to Desmidt *et al*, 2013 a molar ratio of Ca^{+2}:PO_4^{-3}=1.25 affects the struvite formation when the concentration of PO_4-P is 100 mg/L in the influent, which in the case of these RWWs was 0.012 and 0.13 for PO_4-P concentrations of 179 and 137 mg/L, for DSLF and UASB, respectively, which were much lower than the Ca^{+2}:PO_4^{-3}=1.25, therefore no calcium phosphate precipitation was detected.

Taking into account all the struvite precipitation kinetics, it can be concluded that the molar ratio of Mg^{+2}:NH_4^{+}:PO_4^{-3} is an important factor for the struvite formation; a higher molar ratio leads to better phosphate removal, regardless of the matrix type used for its precipitation.

4.3 Maximize the struvite yield from synthetic wastewater and the obtained enriched reclaimed solutions at the optimum Mg^{+2}:NH_4^{+}:PO_4^{-3} molar ratio and pH value

After finding the optimum conditions regarding the molar ratios and pH (table 5), struvite precipitation was performed from synthetic WW and the enriched reclaimed solutions.

As it was stated above, the minimum concentration for struvite precipitation is 153.2 mg PO_4^{-3}/L and according to table 6, all matrices had values higher than this.

Table 6. Struvite yield obtained from synthetic WW and the different enriched reclaimed solutions.

Number	Matrix type	Molar ratio Mg^{+2}:NH_4^+:PO_4^{-3}	PO_4-P (mg/L)	PO_4^{-3} (mg/L)	NH_4^+ and Mg^{+2} (mg/L)	Total volume reclaimed solution (mL)	Struvite mass (mg)	Struvite per volume reclaimed solution (mg/mL)
1	Synthetic WW	2.7:2.0:1.0	97.0	297.3	150.0	320	181.7	0.568
2	60th cycle LFKW	1.9:2.5:1.0	130.0	398.4	195.0	100	90.0	0.900
3	60th cycle LFKW	1.7:2.2:1.0	130.0	398.4	169.0	100	86.2	0.861
4	28th cycle MBA	6.0:8.0:1.0	118.0	361.6	542.4	190	176.2	0.927
5	19th cycle LFKW 10 L	2.0:2.5:1.0	167.0	511.8	250.5	300	394.2	1.314
6	19th cycle LFKW 10 L	4.0:5.2:1.0	165.0	505.7	505.7	680	894.9	1.315
7	14th cycle DSLF	6.7:9.0:1.0	179.0	548.6	934.7	600	977.0*	1.628*
8	25th cycle UASB	6.0:8.0:1.0	137.0	419.8	629.8	600	209.6*	0.349*

*It can be called a recycled solid and not struvite because the ammonium was not consumed after the analysis of the enriched reclaimed solution after precipitation.

It is difficult to make a comparison between the obtained struvite masses (table 6) with the different matrix types due to the differences in the total volume, initial phosphate concentration and molar ratios of each precipitation. Nevertheless, if the specific struvite yield per unit volume is compared, one can conclude that the synthetic WW had the lowest value despite of the overstoichiometric molar ratio of 2.7:2.0:1.0. A comparison of struvite per volume between the two samples from the LFKW 60th cycle reclaimed solution shows that the higher the molar ratio, the higher the struvite mass per volume obtained. Concerning the LFKW 10 L experiment, regardless of the molar ratio, the struvite mass per volume remained constant. Nevertheless, if only the mass is compared, the higher the molar ratio, the higher the struvite mass, similar to the previous case.

The recycled solid mass gained from the DSLF was the highest among the entire batch of experiments. That was expected because it follows the trend mentioned in the previous paragraph; it had the highest molar ratio, which helped in the solid precipitation process.

Figure 31. Struvite and recycled solids obtained from synthetic WW and the different enriched reclaimed solutions. Numbers correspond to the order in table 10.

Figure 31 shows the different struvite and recycled solids that were obtained from each precipitation. As it can be seen, the colors are in compliance with the literature (from white to yellow/brown (Dhakal, 2008 and Bergmans, 2011). Number 1 is purely white because the solution only contained NH_4Cl, $MgCl_2 \cdot 6H_2O$ and H_3PO_4 and therefore no contaminants were present. Samples 2, 3, 5 and 6, had a similar yellowish color because the enriched reclaimed solutions were obtained under similar conditions from the LFKW wastewater (figure 32).

Figure 32. Colors of the different enriched reclaimed solutions.

The MBA, DSLF and UASB solutions had a darker yellow-orange color (figure 32), which defined the darker color of the precipitated struvite / recycled solids. This effect can be explained by the presence of other anions, cations, organics and TSS (especially in the DSLF and UASB

solutions) that affected the color and the purity of the struvite. It is important to mention that the obtained solid product is not necessarily pure struvite because other compounds could be formed simultaneously, e.g. $MgKPO_4 \cdot 6H_2O$, $NiNH_4PO_4 \cdot 6H_2O$, $NiKPO_4 \cdot 6H_2O$, $Fe_3(PO_4)_2$, due to the presence of cations such as K, Al, Ni, Na, Ca, Fe, among others (Wollmann and Möller, 2015).

The recycled solid per unit volume obtained from the UASB matrix was the lowest one and this could be attributed to the presence of suspended solids (103 mg/L) that could inhibit the struvite precipitation. According to Zhou *et al*, 2015 the positively charged metal ions (such Mg^{+2}) have more affinity for the carboxyl groups present in humic substances than the phosphate ion (as HPO_4^{-2} predominant specie at pH 8.5).

According to Hutnik *et al*, 2016 struvite composed of 58-63 % MAP, 37-42 % of calcium phosphate and metal hydroxides, fluorosilicates, fluorides, sulphates and others. However, analyzing the composition and shape of the crystals was not a subject of this master thesis. In order to perform these analyses, it was necessary to obtain more struvite, whereas the masses generated in this study were less than 1.0 g (Table 10).

4.4 Comparison of the PO_4-P, main metals and anions concentrations of the RWWs, the enriched reclaimed solutions before and after struvite precipitation

The enriched reclaimed solutions were analyzed after the struvite precipitation to quantify the phosphate concentration in the supernatant liquids. Figure 33 shows the phosphate precipitated in all the enriched reclaimed solutions and from the synthetic WW when the struvite precipitation was performed. The uptake efficiencies of the samples measured were above 90 %. The highest performance corresponds to the DSLF, which can be explained by it having the highest molar ratio. The case of LFKW 60^{th} cycle regenerate, which showed the lowest performance, had the lowest molar ratio.

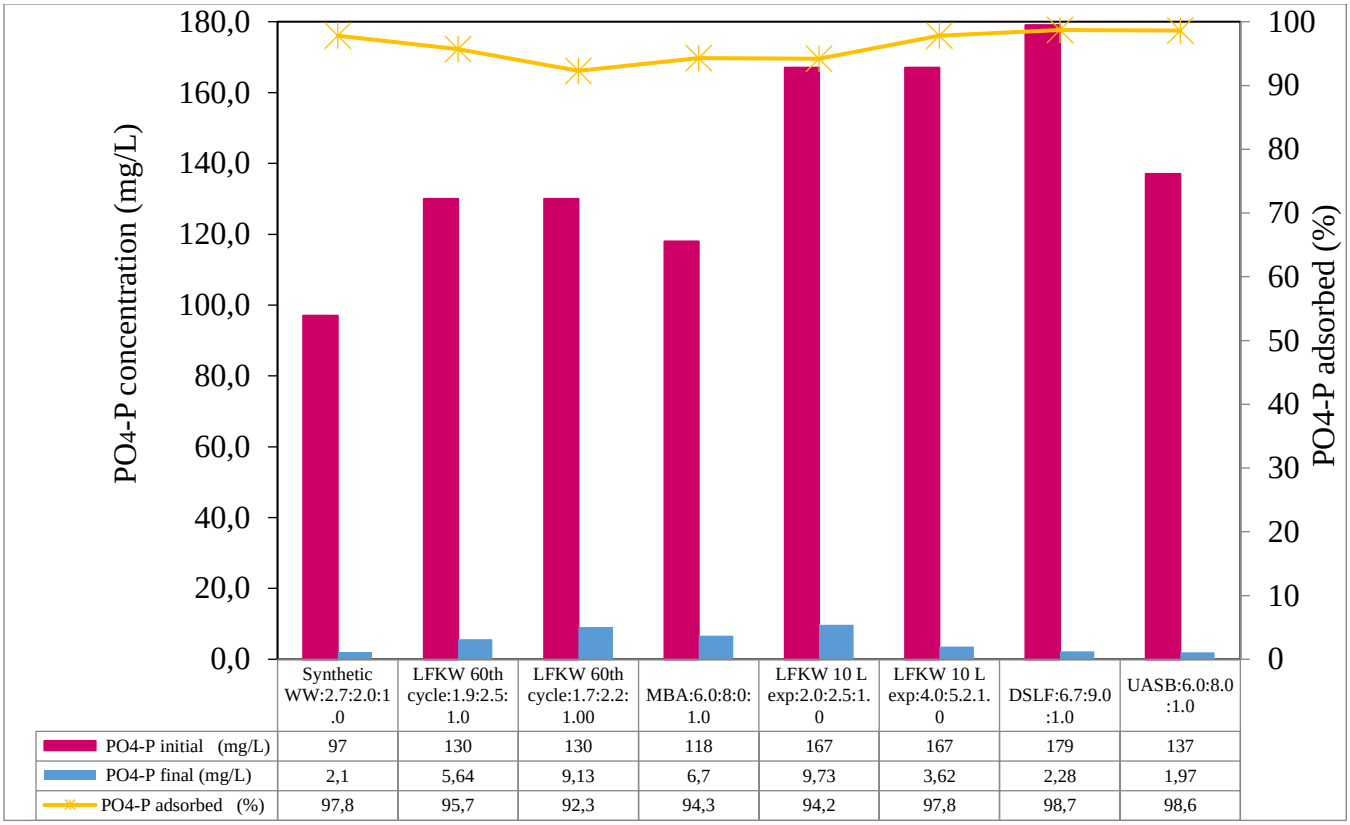

	Synthetic WW:2.7:2.0:1.0	LFKW 60th cycle:1.9:2.5:1.0	LFKW 60th cycle:1.7:2.2:1.00	MBA:6.0:8:0:1.0	LFKW 10 L exp:2.0:2.5:1.0	LFKW 10 L exp:4.0:5.2.1.0	DSLF:6.7:9.0:1.0	UASB:6.0:8.0:1.0
PO4-P initial (mg/L)	97	130	130	118	167	167	179	137
PO4-P final (mg/L)	2,1	5,64	9,13	6,7	9,73	3,62	2,28	1,97
PO4-P adsorbed (%)	97,8	95,7	92,3	94,3	94,2	97,8	98,7	98,6

Figure 33. Dissolved PO_4-P concentration before and after the struvite and recycled solid precipitation.

Table 7 shows the theoretical and the actual experimental molar ratios and the concentrations of magnesium, ammonium and phosphate after the struvite precipitation. As mentioned before, the phosphate precipitated almost completely in all enriched reclaimed solution. Counter intuitively, the ammonium and magnesium concentrations did not decrease as expected; this resulted in the molar ratio needing to be recalculated. The experimental molar ratios were lower than the theoretical ones and this could be attributed to the fact that metals such as Na, K, Zn and Al could be co-precipitated with the PO_4^{-3}. This could be concluded from the considerable reduction of their concentrations (see table 8) in the reclaimed solutions after the precipitation. These metals can inhibit the struvite precipitation by blocking the active sites, leading to a competition for orthophosphate ions to produce the respective salts with the phosphate. Moreover, table 8 shows that there was an excess of Cl^- ions (due to the pH regulation with HCl_{conc}), which, as well as the carbonate, could also contribute to the co-precipitation of the respective salts with the cations mentioned before.

Table 7. Theoretical and experimental data of the struvite precipitation from the different enriched reclaimed solutions.

Nr	Enriched reclaimed solution	Theoretical				Experimental			
		Molar ratio of Mg^{+2}:NH_4^+:PO_4^{-3}	Mg^{+2} (mol/L) Initial	NH_4^+ (mol/L) Initial	PO_4^{-3} (mol/L) Initial	Molar ratio of Mg^{+2}:NH_4^+:PO_4^{-3}	NH_4^+ (mol/L) ppted	Mg^{+2} (mol/L) ppted	PO_4^{-3} (mol/L) ppted
1	LFKW 60 cycles	1.7:2.2:1.0	0.0070	0.0094	0.0042	0.77:0.97:1.0	0.00380	0.0038	0.0039
2	MBA	6.0:8.0:1.0	0.023	0.030	0.0038	1.53:1.53:1.0	0.0055	0.0055	0.0036
3	LFKW 10 L	4.0:5.2:1.0	0.021	0.028	0.0053	2.8:3.6:1.0	0.015	0.019	0.0053
4	DSLF	6.7:9.0:1.0	0.039	0.052	0.0058	1.1:0.0:1.0	0.0062	0.0	0.0057
5	UASB	6.0:8.0:1.0	0.026	0.035	0.0044	0.57:0.0:1.0	0.0025	0.0	0.0044

Table 8. Chemical composition of the different RWWs and the enriched reclaimed solutions before and after the struvite and recycled solid precipitation.

Raw wastewater (mg/L)													
Nr	Matrix type	PO_4-P	P_{tot}	TSS	CO_3^{-2}	NH_4^+	Cl^-	Na	K	Ca	Mg	Zn	Al
1	LFKW - SST effluent+H_3PO_4 (unfiltered) ISWA	9.7	9.9	<1	39	0.05	149	135	18	84	13	0.053	-
2	MBA	4.7	5.6	<1	442	0,10	5400	2656	2174	148	223	0.032	0.047
3	DSLF	49.8	50.0	110	1060	1401.4	150	162	280	53.9	36	0.114	0.476
4	UASB	10.3	16.7	260	84	97.9	330	225	35.4	110	19.6	0.253	0.5
Reclaimed solution before struvite and recycled solid precipitation (mg/L)													
1	LFKW 60 cycles	260	260	-	571	-	75	8904	19.8	0.433	0.035	4.11	5.61
2	LFKW 10 L	167	170	-	5	18.6	170	7275	23.5	0.433	0.252	263	5.63
3	MBA	118	131	-	0	17.7	2300	14365	1137	0.261	0.324	336	3.44
4	DSLF	179	185	-	1457	934.7	150	5401	213	2.13	2.38	0.272	0.247
5	UASB	137	168	-	423	86.5	280	5510	40.2	18.2	7.74	63	3.06
Reclaimed solution after struvite and recycled solid precipitation (mg/L)													
1	LFKW 60 cycles	5.64	5.6	-	157	100.3	7260	4569	11.3	1.45	96	0.235	0.809
2	LFKW 10 L	9.73	17.2	-	113.2	167.1	8890	7065	22.4	1.030	153	0.7	0.171
3	MBA	2.96	4.1	-	401	442.3	19000	13200	1050	2.35	411	6.0	0.183
4	DSLF	2.28	2.4	102	1388	988.7	5730	4411	196	2.12	787	1.70	0.081
5	UASB	1.97	27.7	103	286	653.0	9100	4941	37.4	12.8	570	15.2	0.501

Table 8 shows the chemical composition of the different RWWs and the enriched reclaimed solutions before and after the struvite precipitation. As it was mentioned before, the ZnFeZr-

LDH composite material enriched efficiently the different RWWs and according to table 8, there was in fact a significant increase of PO_4-P for all the reclaimed solutions and almost a complete removal of the same after the precipitation reaction.

4.4.1 From raw wastewater to enriched reclaimed solution before struvite precipitation

A. LFKW 60th cycle and 10 L experiment

By characterizing the RWW from the SST effluent at LFKW, ISWA, it is possible to determine the different compounds that appear after the enrichment of the LFKW 60th cycle regenerate and 10 L experiment.

For instance, CO_3^{-2} increased from 39 to 571 mg/L in the LFKW 60th cycle regenerate, which could be attributed to the CO_2 present in the media transformed to CO_3^{-2} due to the high pH during the desorption cycles. In contrast, the CO_3^{-2} decreased from 39 to 5 mg/L in the 10 L experiment, which means that the carbonate was adsorbed on the LDH composite material and inhibited the phosphate uptake. The ammonium concentration in both reclaimed solutions remained low before and after the adsorption/desorption cycles because it was originally not present in the wastewater.

In the case of Cl^-, it was low in the LFKW 60th cycle and high in the LFKW 10 L experiment but this is strongly dependent on the season that the WW sample was collected. The performance of the adsorption/desorption cycles, as mentioned, is affected by the Cl^- concentration; during Winter, NaCl is used to melt snow and afterwards, the water runoff reaches the WWTP and increases the chloride concentration in the WW. The sodium concentration increased from 135 to 8904 mg/L for the 60th cycle regenerate and from 135 mg/L to 7275 mg/L for the 10 L experiment. Logical explanation for the increase of sodium is the use of NaOH as desorption medium which is transferred through the LDH composite material and released into the media.

The potassium concentration remained constant in both reclaimed solutions after the adsorption/desorption cycles. Both Ca and Mg had a decrease in their concentrations. In contrast, the Zn concentration increased in both reclaimed solutions after the enrichment, which can be

explained due to zinc release into the supernatant liquids at high pH from the LDH composite material.

B- MBA

The carbonate and the chloride concentrations decreased after the adsorption/desorption cycles, supporting the idea that there is competition with the phosphate for the active sites of the LDH composite material. The sodium concentration increased considerable, which could be due to the same reasons stated in section 4.4.1. Regarding the cations of K, Ca and Mg, their concentrations decreased, while the Zn and Al concentrations increased. As explained in the last section, the Zn was probably released from the LDH material.

C- DSLF and UASB

In both reclaimed solutions, it can be observed that the carbonate concentrations increased. The explanation for this phenomenon is the same as in section 4.4.1. On the other hand, there was a slight decrease in the ammonium concentrations, which was released as ammonia due to the high pH values during desorption cycles; supporting this fact was the odor detected during the measurements. The chloride concentrations stayed constant in both reclaimed solutions.

4.4.2 Enriched reclaimed solutions before and after MAP precipitation

Figure 33 and table 7, demonstrate the high PO_4-P uptake efficiencies (above 90 %) after the MAP precipitation.

A- LFKW 60th cycle regenerate

The carbonate and the cations (Na, K, Zn, Zr and Al) all decreased in concentration as follows, respectively: 571 to 157 mg/L, 8904 to 4569 mg/L, 19.8 to 11.3 mg/L, 4.11 to 0.235 mg/L and 5.61 to 0.809 mg/. It might have precipitated carbonates, hydroxides and phosphates with the mentioned cations, especially the aluminum.

The aluminum is amphoteric in the presence of OH^- anions, meaning that at pH < 4.0 it exists as $Al(OH)_6^{+3}$ and above 9.0 exists as $Al(OH)_4^-$, both complexes in a dissolved form but between pH 4.0 and 9.0 they precipitate as $Al(OH)_3$ (Brown *et al*, 2009). The struvite precipitation was performed at pH 9.0 and because of that there is a possibility that the precipitate also contained

aluminum hydroxide. The chloride concentration increased (from 170 to 8890 mg/L) after the precipitation because HCl_{conc} was used for the pH regulation and chloride salts of Mg^{+2} and NH_4^+ were added in case of their absence.

B- LFKW 10 L experiment

The carbonate concentration increased (5 to 113.5 mg/L), whereas the concentrations of Zn (263.0 to 0.7 mg/L) and Al (5.63 to 0.171 mg/L) decreased, probably due to the formation of carbonates, hydroxides ($Al(OH)_3$) and phosphates compounds as mentioned earlier. In the case of the cations Na, K and Ca, their concentrations remained constant. On the other hand, the ammonium and magnesium were not consumed as expected because their concentrations were still high after the precipitation.

C- MBA, DSLF and UASB

Regarding the MBA, the carbonate concentration increased from 0 to 400.1 mg/L. Meanwhile, from the 542.4 mg/L of ammonium that was added to the reclaimed solution for the ¨MAP¨ precipitation, only 100.1 mg/L were actually precipitated.

In the DSLF sample, the carbonate concentration remained constant, which means that the CO_3^{-2} did not affect the struvite precipitation. However, the ammonium was not consumed and therefore pure struvite was not formed, but rather a recycled solid.

Concerning the UASB sample, the carbonate concentration decreased from 423 to 286 mg/L, which probably co-precipitated with some of the metals whose concentrations also decreased: Na, K, Ca, Zn and Al. Moreover, the ammonium concentration was also not consumed, therefore pure struvite was not formed and the product was called recycled solid instead.

In the three reclaimed solutions, the Cl^- concentration increased as a result of the used of concentrated hydrochloric acid for the pH regulation.

In addition, in table 12, it can be observed that the reclaimed solution after the MAP precipitation had the following concentrations for calcium 2.12 and 12.8 mg/L for DSLF and UASB, respectively and for carbonate 1388 and 286 mg/L, for DSLF and UASB, respectively. The

concentration of carbonate in the DSLF did not change significantly but in the case of the UASB decreased by 32.8 %, which means that probably certain amount precipitated as calcium carbonate because the concentration of calcium decreased from 18.2 to 12.8 mg/L.

Chapter 5: Conclusions and recommendations

5.1 Conclusions

It was found out that the more complex the raw wastewater, the more difficult it was to adsorb phosphate onto ZnFeZr-LDH composite material and thus the enrichment of phosphate decreased. From the complete adsorption and desorption cycle experiments in the four different raw wastewaters, the LFKW 10 L experiment demonstrated the best total adsorption efficiency (96.6 %) and from this 85.4 % was desorbed, whereas the DSLF showed the lowest total adsorption efficiency (75.4 %) and from this 53.4 % was desorbed, despite of the fact that it had less TSS than the UASB wastewater. The presence of carbonate in the DSLF had a significant contribution to the low yield.

Furthermore, the DSLF reclaimed solution could not be enriched more than 180-190 mgPO_4-P/L because the phosphate concentration remained constant in the last desorption cycles. The same situation happened with the UASB solution, where from cycle 15 until 25 the enrichment remained constant (135 mg PO_4-P/L).

Regarding the phosphate removal kinetics during struvite precipitation in synthetic WW and in the different reclaimed solutions, working at pH 8.5 resulted in high phosphate uptake, regardless of the molar ratio of Mg^{+2}:NH_4^+:PO_4^{-3}. On the other hand the molar ratio of Mg^{+2}:NH_4^+:PO_4^{-3} was an important factor for the struvite precipitation, wherein at higher molar ratio higher phosphate removal occurred, regardless of the matrix type used for its precipitation.

Comparing the results obtained with different molar ratios, the best phosphate uptake was in the order: Synthetic WW (pH=8.5) > LFKW 10 L experiment (pH=8.5) > LFKW 60 cycle regenerate (pH=9.0) > MBA (pH=8.5). These results indicate that using pH 8.5 results in a better struvite precipitation than at pH 9.0. Moreover, the MBA struvite precipitation kinetics had the lowest performance compared to the synthetic WW and the LFKW 10 L reclaimed solution. This could be because the MBA reclaimed solution had a high concentration of sodium (14365 mg/L) and potassium (1137 mg/L), which could have caused the formation of the respective salts with the HPO_4^{-2} ions. Additionally, the synthetic WW had the highest phosphate removal efficiency

because it was prepared only with NH_4Cl, $MgCl_2 \cdot 6H_2O$ and H_3PO_4, therefore any other ions were not presented to interfere the struvite formation.

Concerning the struvite precipitation, it was seen that higher molar ratios lead to better phosphate uptake, regardless of the matrix type and the total volume used for its precipitation. Moreover, the color of the enriched reclaimed solutions influenced the color of the resulting struvite solid products, which was attributed to the presence of the contaminants.

The actual experimental Mg^{+2}:NH_4^+:PO_4^{-3} molar ratios were lower than the theoretical. In addition, the recycled solids obtained from the DSLF and the UASB reclaimed solutions were not pure struvite because the ammonium concentration in the liquid phase remained constant after the reaction, which means that ammonium did not co-precipitate.

5.2 Recommendations

Prior to the adsorption and desorption cycles with wastewaters such as MBA, DSLF and UASB, it is suggested to perform a complete analysis of the effects of the different experimental parameters, including contact time, adsorbent dosage and pH, in order to have a better understanding of the behavior of the ZnFeZr-LDH composite material in each RWW and to find the optimum parameters for the cycles performance.

It is recommended to perform struvite precipitation experiments under the same molar ratios of Mg^{+2}:NH_4^+:PO_4^{-3} in the different enriched reclaimed solutions and on synthetic WW in order to compare the results under the same conditions.

It will be interesting to carry out struvite precipitation from the enriched reclaimed solutions and synthetic WW by sampling every minute during the reaction in order to obtain the fitting kinetics model. In addition, it is proposed to study the effect of TSS on the struvite precipitation kinetics.

Finally, it is suggested to analyze microscopically each struvite product in order to identify its morphology (shape and structure), as well as utilizing XRD analysis to obtain the complete composition of the solid, e.g. the presence of MAP, calcium phosphate and other compounds.

Chapter 6: Bibliography

1. Ariyanto, E.; Sen, T.K. & Ang, H. M. (2014). The influence of various physico-chemical process parameters on kinetics and growth mechanism of struvite crystallization. Advanced Power Technology 25, 682-694. DOI:10.1016/j.apt.2013.10.014.

2. Ashekuzzaman, S.M. & Jiang, J. Q. (2014). Study on the sorption–desorption–regeneration performance of Ca-, Mg and CaMg-based layered double hydroxides for removing phosphate from water. Chemical Engineering Journal 246, 97-105. DOI:10.1016/j.cej.2014.02.061.

3. Bergmans, B. (2011). Struvite recovery from digested sludge. Master Thesis. Sanitary Engineering Section, Department of Water Management. Faculty of Civil Engineering and Geosciences. Delft University of Technology, Delft. Web site: http://www.citg.tudelft.nl/fileadmin/Faculteit/CiTG/Over_de_faculteit/Afdelingen/Afdeling_watermanagement/Secties/gezondheidstechniek/onderzoek/Theme12/doc/MSc_thesis_Bart_Bergmans.pdf Date of consultancy: November 18th, 2015.

4. Bird, A. (2015). Evaluation of the feasibility of struvite precipitation from domestic wastewater as an alternative phosphorus fertilizer resource. Master project. University of San Francisco. Web site: http://repository.usfca.edu/cgi/viewcontent.cgi?article=1145&context=capstone Date of consultancy: January 12th, 2016.

5. Bouropoulos, N. & Koutsoukos, P.G. (2000). Spontaneous precipitation of struvite from aqueous solutions. Journal of Crystal Growth 213, 381-388. PII:S0022-0248(00)00351–1.

6. Brown, T. L.; LeMay, E.; Bursten, B. & Murphy, C. J. (2009). Chemistry: The central science. Edition 11th. Pearson Prentice Hall. Pp: 748.

7. Capdevielle, A.; Sýkorová, E.; Biscans, B.; Béline, F. & Daumer, M. L. (2013). Optimization of struvite precipitation in synthetic biologically treated swine wastewater-Determination of the optimal process parameters. Journal of Hazardous Materials 244-245, 357-369. DOI:10.1016/j.jhazmat.2012.11.054.

8. Cai, P.; Zheng, H.; Wang, C.; Ma, H.; H, J.; Pu, Y. & Liang, P. (2012). Competitive adsorption characteristics of fluoride and phosphate on calcined Mg-Ale-CO_3 layered double hydroxides. Journal of Hazardous Materials 213-214, 100-108. DOI:10.1016/j.jhazmat.2012.01.069.

9. Cheng, X.; Huang, X.; Wang, X.; Zhao, B.; Chen, A. & Sun, D. (2009). Phosphate adsorption from sewage sludge filtrate using zinc-aluminum layered double hydroxides. Journal of Hazardous Materials 169, 958-964. DOI:10.1016/j.jhazmat.2009.04.052.

10. Cheng, X.; Huang, X.; Wang, X. & Sun, D. (2010). Influence of calcination on the adsorptive removal of phosphate by Zn-Al layered double hydroxides from excess sludge liquor. Journal of Hazardous Materials. 177, 516-523. DOI:10.1016/j.jhazmat.2009.12.063.

11. Chitraka,R.; Tekuza, S.; Sonoda, A.; Sakane, K.; Ooi, K. & Hirotsu, T. (2007). Synthesis and phosphate uptake behavior of Zr4+ incorporated MgAl-layered double hydroxides. Journal of Colloid and Interface science 313, 53-63. DOI:10.1016/j.jcis.2007.04.004.

12. Cooper, J.; Lombardi, R.; Boardman, D. & Carliell-Marquet, C. (2011). The future distribution and production of global phosphate rock reserves. Resources, Conservation and Recycling 57, 78-86. DOI:10.1016/j.resconrec.2011.09.009.

13. Cordell, D.; Drangert, J.O. & White, S. (2009). The story of phosphorus: Global food security and food for through. Global Environmental Change 19, 292-305. DOI:10.1016/j.gloenvcha.2008.10.009.

14. Cordell, D. & White, S. (2011). Peak Phophorus: Claryfying the Key Issues of a Vigorous Debate about Long-Term Phosphorus Security: A Review. Sustainability. 3, 2027-2049. DOI: 10.3390/su3102027.

15. Das, J.; Patra, J.; Baliarsingh, N. & Parida, K.M. (2006). Adsorption of phosphate by layered double hydroxides in aqueous solutions. Applied Clay Science. 32, 252-260. DOI:10.1016/j.clay.2006.02.005.

16. De Ridder, M.; De Jong, S.; Polchar, J. & Lingemann, S. (2012). Risks and Opportunities in the Global Phosphate Rock Market. Web site:http://www.phosphorusplatform.eu/images/download/HCSS_17_12_12_Phosphate.pdf Date of consultancy: June 2nd, 2015.

17. Desmidt, E.; Ghyselbrecht, K.; Monballiu, A.; Rabaey, K.; Verstraete, W. & Messchaert, B. D. (2013). Factors influencing urease driven struvite precipitation. Separation and Purification Technology 110, 150-157. DOI:10.1016/j.seppur.2013.03.010.

18. Desmidt, E.; Pinoy, L.; Ghyselbrecht, K.; Van der Bruggen, B.; Rabaey, K.; Zhang, Y.; Verstraete, W. & Meesschaert, B. (2015). Global Phosphorus Scarcity and Full-Scale P-Recovery Techniques: A Review. Critical Reviews in Environmental Science and Technology, 45:336–384. DOI:10.1080/10643389.2013.866531.

19. Dhakal, S. (2008). A laboratory study of struvite precipitation for phosphorus removal from concentrated animal feeding operation wastewater. Master Thesis. University of Missouri-Rolla. Web site: http://scholarsmine.mst.edu/cgi/viewcontent.cgi?article=7723&context=masters_theses Date of consultancy: December 15th, 2015.

20. Doyle, J. & Parsons, S. (2002). Struvite formation, control and recovery. Water Research 36, 3925-3940. PII: S 0043-1354(02)00126-4.

21. Drenkova-Tuhtan, A.; Mandel, K.; Paulus, A.; Meyer, C.; Hutter, F.; Gellermann, C.; Sextl, G.; Franzreb, M. & Steinmetz, H. (2013). Phosphate recovery from wastewater using engineered superparamagnetic particles modified with layered double hydroxide ion exchangers. Water Research 47, 5670-5677. DOI:10.1016/j.watres.2013.06.039.

22. Drenkova-Tuhtan, A.; Schneider, M.; Mandel, K.; Meyer, C.; Gellermann, C.; Sextl, G. & Steinmetz, H. (2016). Influence of cation building blocks of metal hydroxide precipitates on their adsorption and desorption capacity for phosphate in wastewater-A screening study. Colloids and Surfaces A: Physicochemical and Eng. Aspects 488, 145-153. DOI:10.1016/j.colsurfa.2015.10.017.

23. DWA Working Group CEC 1.1. (2013). Recovery of valuable materials from waste water and sewage sludge. Web site: http://www.deutsche-phosphor-plattform.de/content/dam/iwks/DeuPP/Phosphor%20Sonderdruck-KEK-1-1.pdf Date of consultancy: June 4th, 2015. DOI:10.3242/kae2013.10.001.

24. Egle L.; Rechberger, H. & Zessner, M. (2015). Overview and description of technologies for recovering phosphosrus from municipal wastewater. Resources, Conservation and Recycling 105, 325-346. DOI:10.1016/j.resconrec.2015.09.016.

25. Ewert, O.; Hermanussen, C.; Kabbe, C.; Mele, C.; Niewersch, H.; Paillard, E.; Wagenbach A. & Stemann J. (2014). P-REX: Sustainable sewage sludge management fostering phosphorus recovery and energy efficiency. Web site: http://www.p-rex.eu/fileadmin/P-REX-Reserach/Downloads/P-REX_D_5_online.pdf Date of consultancy: June 4th, 2015.

26. Ezquerro, A. (2010). Struvite precipitation and biological dissolution. Degree Project. KTH-Water, Sewage and Waste technology. Department of Land and Water Resources Engineering. Royal Institute of Technology (KTH). Stockholm, Sweden. Web site: http://rymd.lwr.kth.se/Publikationer/PDF_Files/LWR_EX_10_22.pdf Date of consultancy: November 21st, 2015.

27. Ferguson, J.F. & McCarty, P.L. (1971). Effects of carbonate and magnesium on calcium phosphate precipitation. Environ. Sci. Technol 5, 534-540. DOI:10.1021/es60053a005.

28. Goh, K.H.; Lim, T.T. & Dong, Z. (2008). Application of layered double hydroxides for removal of oxyanions: A review. Water Research 42, 1343-1368. DOI:10.1016/j.watres.2007.10.043.

29. Harrison, M.L.; Johns, M.R.; White, E.T. & Mehra, C.M. (2011). Growth rate kinetics for struvite crystallization. Chemical Engineerging Transactions. Volume 25, 309-314. DOI:10.3303/CET1125052.

30. Huang, H.; Xiao, D.; Zhang, Q. & Ding, L. (2014). Removal of ammonia from landfill leachate by struvite precipitation with the use of low-cost phosphate and magnesium sources. Journal of Environmental Management 145 (2014) 191e198. DOI:10.1016/j.jenvman.2014.06.021.

31. Hutnik, N.; Kozik, A.; Mazienczuk, A.; Piotrowski. & Matynia, A. (2016). Recovery of struvite deom phosphorus mineral fertilizer industry wastewater in continuous jet pump crystallizer. Internaional Journal of Chemical and Applications, Vol 7, N° 1. Web site: http://www.ijcea.org/vol7/538-P0015.pdf Date of consultancy: May 2nd, 2016.

32. Jeffery, G.H.; Bassett, J.; Mendham, J. & Denney, R.C. (1989). Textbook of Quantitative Chemical Analysis. 5th Edition. Longman Scientific & Technical. Page: 186.

33. Jiménez-Gutiérrez, Yamileth-Milena. (2015). Determination of the process variables for adsorption and desorption of phosphate from wastewater by selective ion exchange on magnetic particles. Student Research Project. Institute for Sanitary Engineering, Water Quality and Solid Waste Management. University of Stuttgart, Germany.

34. Kalmykova, Y.; Palme, U.; Karlfeldt Fedje, K. & Yu, S. (2015). Total Material Requirement Assessment of Phosphorus Sources from Phosphate ore and urban sinks: Sewage Sludge and MSW incineration fly ash. Int. J. Environ. Res., 9 (2): 561-566. ISSN: 1735-6865.

35. Kataki, S.; West, H.; Clarke, M. & Baruah. D.C. (2016). Phosphorus recovery as struvite: Recent concerns for use of seed, alternative Mg source, nitrogen conservation and fertilizer potential. Resources, Conservation and Recycling 107, 142-156. DOI:10.1016/j.resconrec.2015.12.009.

36. Kofina, A. N. & Koutsoukos, P.G. (2005). Spontaneous precipitation of struvite from synthetic wastewater solutions. Growth and Design, Vol 5, N° 2, 489-496. DOI:10.1021/cg049803e.

37. Koilraj, P. & Kannan, S. (2010). Phosphate uptake behavior of ZnAlZr ternary layered double hydroxides through surface precipitation. Journal of Colloid and Interface Science 341, 289-297. DOI:10.1016/j.jcis.2009.09.059.

38. Kozik, A.; Hutnik, N.; Piotrowski, K. & Matynia, A. (2014). Continuous reaction crystallization of struvite from diluted aqueous solution of phosphate (V) ions in the presence of magnesium ions excess. Chemical Engineering Research and Design. 92, 481-490. DOI:10.1016/j.cherd.2013.08.032.

39. LAGA (Bund/Länder-Arbeitsgemeinschaft Abfall). (2010). Evaluation of Options for the Sustainable Use of Secondary Phosphorus Reserves. Ministerium Für Unwelt, Klima und Energiewirtschaft. Web-site: http://www.laga-online.de Date of consultancy: June 4th, 2015.

40. Le Corre, K.; Valsami-Jones, E.; Hobbs, P. & Parsons, S. (2005). Impact of calcium on struvite cristal size, shape and purity. Journal of Crystal Growth 283, 514-522. DOI:10.1016/j.jcrysgro.2005.06.012.

41. Le Corre, K. S.; Valsami-Jones, E.; Hobss, P. & Parsons, S. A. (2007). Kinetics of struvite precipitation: Effect of the magnesium dose on induction times and precipitations rates. Environmental Technology 28, 1317-1324. Web site: https://dspace.lib.cranfield.ac.uk/bitstream/1826/8717/1/Kinetics_of_Struvite_Precipitation-2007.pdf Date of consultancy: December 16th , 2015.

42. Martin, B. (2010). Removal and Recovery of Phosphorus from Municipal Wastewater using a Ferric Nanoparticle Adsorbent. PhD Thesis. School of Applied Science, Department of Sustainable Systems, Center for Water Science. Cranfield University. Web site: http://core.ac.uk/download/pdf/140404.pdf Date of consultancy: November 4th, 2014.

43. Mandel, K.; Drenkova-Tuhtan, A.; Hutter, F.; Gellermann, C.; Steinmetz, H. & Sextl, G. (2013). Layered double hydroxide ion exchangers on superparamagnetic microparticles for recovery of phosphate from waste water. J. Mater. Chem, 2013, 1, 1840-1848. DOI:10.1039/c2ta00571a.

44. Mehta, C. M. & Batstone, D.J. (2013). Nucleation and growth kinetics of struvite crystallization. Water Research 47, 2890-2900. DOI:10.1016/j.watres.2013.03.007.

45. Meyer, C. (2014). Lecture: Water Softening. Summer Semester. University of Stuttgart.

46. Nelson, N.O.; Mikkelsen, R.L. & Hesterberg, D.L. (2007). Struvite precipitation in anaerobic swine lagoon liquid: effect of pH and Mg:P ratio and determination of rate constant. Bioresource Technology 89, 229–236. DOI:10.1016/S0960-8524(03)00076-2.

47. Nieminen, J. (2010). Phosphorus Recovery and Recycling From Municipal Wastewater Sludge. Master Thesis. Aaltpo University. Web site: http://www.sswm.info/sites/default/files/reference_attachments/NIEMINEN%202010%2

0Phosphorus%20Recovery%20and%20Recycling%20from%20Municipal%20Wastewater%20Sludge.pdf Date of consultancy: April 14th, 2016.

48. Ostara Nutrient Recovery Technologies Inc. (2016). Web site: http://ostara.com/ Date of consultancy: April 15th, 2016.

49. Panasiuk, O. (2010). Phosphorus Removal and Recovery from Wastewater using Magnetite. Master of Science Thesis. Royal Institute of Technology. Stockholm, Sweden. Web site: http://www.diva-portal.org/smash/get/diva2:473397/FULLTEXT01.pdf Date of consultancy: November 4th, 2014.

50. Parsons, S. & Smith, J. (2008). Phosphorus Removal and Recovery from Municipal Wastewaters. Elements, Vol. 4, pp 109-112. DOI:10.2113/GSELEMENTS.4.2.109.

51. Pastor, L.; Mangin, D.; Barat, R. & Seco, A. (2008). A pilot-scale study of struvite precipitation in a stirred tank reactor: Conditions influencing the process. Bioresource Technology 99, 6285–6291. DOI:10.1016/j.biortech.2007.12.003.

52. Perera, P. W.; Han, Z. Y.; Chen, Y. X. & Wu, W. X. (2007). Recovery of nitrogen and phosphorus from swine waste biogas digester effluent. Biomedical and environmental sciences 20, 343-350. Web site: http://www.besjournal.com/Articles/Archive/2007/No5/200906/P020090604701889032056862007205149 5.pdf Date of consultancy: December 16th, 2015.

53. Ping, Q.; Li, Y.; Wu, X.; Yang, L. & Wang, L. (2016). Characterization of morphology abd component of struvite pellets crystallized from sludge dewatering liquor: Effects of total suspended solid and phosphate concentrations. Journal of Hazardous Materials 30, 261-269. DOI: http:10.1016/j.jhazmat.2016.02.047.

54. Quintana, M.; Sánchez, E.; Comenarejo,M.F.; Barrera, J.; García, G. & Borja, R. (2005). Kinetics of phosphorus removal and struvite formation by the utilization of by-product of

magnesium production. Chemical Engineering 111, 45-52. DOI:10.1016/j.cej.2005.05.005.

55. Rahman, M.; Salleh, M.; Rashid, U.; Ahsan, M.; Hossain, M. & Ra, C. (2014). Production of slow release crystal fertilizer from wastewaters through struvite precipitation-A review. Arabian Journal of Chemistry 7, 139-155. DOI:10.1016/j.arabjc.2013.10.007.

56. Rittmann, B.E.; Mayer, B.; Westerhoff, P. & Edwards, M. (2011). Capturing the lost of phosphorus. Chemosphere 84 (2011) 846-853. DOI:10.1016/j.chemosphere.2011.02.001.

57. Song, Y.; Yuan, P.; Zheng, B.; Peng, J.; Yuan, F. & G, Y. (2007). Nutrients removal and recovery by crystallization of magnesium ammonium phosphate from synthetic swine wastewater. Chemosphere 69, 319-324. DOI:10.1016/j.chemosphere.2007.06.001.

58. Stolzenburg, P.; Capdevielle, A.; Teychené, S. & Biscans, B. (2015). Struvite precipitation with MgO as a precursor: Application to wastewater treatment. Chemical Engineering Science 133, 9-15. DOI:10.1016/j.ces.2015.03.008.

59. Türker, M. & Çelen, I. (2010). Chemical equilibrium model of struvite precipitation from anaerobic digester effluents. Turkish J. Eng. Env. Sci 34, 39-48. Web site: http://journals.tubitak.gov.tr/engineering/issues/muh-11-35-1/muh-35-1-4-1008-15.pdf Date of consultancy: December 15th, 2015.

60. Van Kauwenbergh, S. (2010). World Phosphate Rock Reserves and Resources. IFDC. Web site: http://pdf.usaid.gov/pdf_docs/PNADW835.pdf Date of consultancy: June 2nd, 2015.

61. Yan, L.G.; Yang, K.; Shan, R.R.; Wei, J.; Yu, S.J. Yu, H.Q. & Du, B. (2015). Kinetic, isotherm and thermodynamic investigations of phosphate adsorption onto core-shell

Fe_3O_4@LDHs composites with easy magnetic separation assistance. Journal of Colloid and Interface Science 448, 508-516. DOI:10.1016/j.jcis.2015.02.048.

62. Yang, K.; Yan, L-G.; Yang, Y-M.; Yu, S.J.; Shan,R.R.; Yu, H-Q. Zhu, B.C. & Du. B. (2014). Adsorptive removal of phosphate by Mg-Al and Zn-Al layered double hydroxides: Kinetics, isotherms and mechanism. Separation and Purification Technology 124, 36-42. http://dx.doi.org/10.1016/j.seppur.2013.12.042

63. Yuan, Z.; Pratt, S. & Batstone, D. (2012). Phospohorus recovery from wastewater through microbial processes. Current opinion in Biotechnology, 23: 878-883. DOI:10.1016/j.copbio.2012.08.001.

64. Wollmann, I. & Möller, K. (2015). Assessment of Alternative Phosphorus Fertilizers for Organic Farming: Sewage Precipitation Products. Web site: https://www.fibl.org/fileadmin/documents/shop/1665-sewage-precipitation-products.pdf Date of Consultancy: November 20th, 2015.

65. Wvgv (Wirtschafts- und Verlagsgesellschaft Gas und Wasser). (2015). Profile of the German Water Sector 2015. Web site: https://www.dvgw.de/fileadmin/dvgw/wasser/organisation/branchenbild_engl_2015_langfassung.pdf Date of consultancy: January 6th, 2016.

66. Zhou, Z.; Hu, D.; Ren, W.; Zhao, Y.; Jiang, L.M. & Wang, L. (2015). Effect of humic substances on phosphorus removal by struvite precipitation. Chemosphere 141, 94-99. DOI:10.1016/j.chemosphere.2015.06.089.

Appendix with the experimental data

Appendix A1. Experiment: Adsorption/Desorption cycles by using the composite particle with 15 or 32 wt % ZnFeZr-LDH under 1 M NaOH desorption solution.

Table A1-1. Experimental data obtained in the phosphate adsorption/desorption cycle by using the raw wastewater from the SST from ISWA with the 15 wt% ZnFeZr-LDH composite material, V=10.0 L and 1 g/L LDH.

	0 min (WW+particles)		20 min (in reactor)		3 M H2SO4	Conductivity	PO4-P WW	PO4-P 20 min
Cycle	pH	T(°C)	pH	T(°C)	(ml/10L)	(uS/cm)	(mg/L)	(mg/L)
1	7,35	16,5	7,32	16,3	0,500	1226	9,34	1,105
2	7,17	18,9	7,41	19,0	75,0	6680	9,40	0,050
3	7,38	18,6	7,46	18,8	71,2	6460	9,43	0,050
4	7,32	18,7	7,46	18,7	75,7	6890	9,42	0,843
5	7,05	20,1	7,41	20,3	68,5	6530	9,44	0,054
6	7,22	21,4	7,44	21,4	59,9	6370	10,10	0,05
7	7,25	17,0	7,52	17,3	42,53	4700	10,70	0,095
8	7,10	18,5	7,34	18,7	37,24	4250	10,80	0,058
9	7,34	18,4	7,46	18,5	40,0	4950	10,40	2,47
10	7,38	25,0	7,46	25,0	42,5	5000	10,70	0,38
11	7,41	25,0	7,46	25,0	40,5	4470	10,60	0,24
12	7,09	25,0	7,20	25,0	34,3	3950	10,60	0,132
13	7,36	25,0	7,41	25,0	33,6	4000	10,40	0,191
14	11,95	25,0	7,20	25,0	4,068	3240	10,30	0,089
15	11,87	25,0	7,79	25,0	3,18	2920	10,30	0,181
16	11,97	25,0	7,27	25,0	11,88	3270	10,10	0,133
17	11,9	25,0	7,55	25,0	3,00	2770	10,40	0,135
18	11,83	25,0	7,81	25,0	3,00	2800	10,30	0,21
19	11,75	25,0	7,40	25,0	2,76	2610	11,00	0,114

	0 min (desorption+particles)	20 min (in reactor)			Conductivity	Desorption solution	Sample quantity	PO4-P
Cycle	pH	T(°C)	pH	T(°C)	(uS/cm)	(ml)	(mL)	20min (mg/L) (with enrichement)
1	13,09	17,1	13,69	17,2	163600	10000	50	8,55
2	13,32	18,1	13,66	1,0	152300	9950	50	16,70
3	13,02	19,5	13,63	19,6	139600	9900	15	25,20
4	12,28	18,4	13,63	18,9	133800	9885	15	29,50
5	12,43	19,9	13,56	19,8	121300	9870	15	38,30
6	13,07	19,4	13,25	19,4	120400	9855	15	49,90
7	13,40	19,8	13,56	19,7	113500	9840	15	62,70
8	13,43	17,6	13,60	17,7	107900	9825	15	68,10
9	12,59	18,6	13,56	18,7	96700	9810	15	71,30
10	12,32	19,6	13,50	19,6	91700	9795	15	81,30
11	12,03	21,5	13,44	21,4	85100	9780	15	90,20
12	12,34	19,0	13,44	25,0	79300	9765	15	98,00
13	12,05	20,6	13,41	20,7	72900	9750	15	110,00
14	13,18	21,4	13,36	21,4	68100	9735	15	119,00
15	13,14	21,7	13,33	21,8	64100	9720	15	127,00
16	13,09	21,7	13,3	21,9	59900	9705	10	138,00
17	13,1	21,7	13,29	21,8	56000	9695	10	147,00
18	13,11	19,8	13,34	19,8	53000	9685	10	156,00
19	13,19	19,9	13,32	19,9	49800	9675	10	169,00

Table A1-2. Experimental data obtained in the phosphate adsorption/desorption cycle by using the raw wastewater MBA with the 32 wt% ZnFeZr-LDH composite material and V=1.0 L.

	Comments	0 min (WW+particles)		20 min (in reactor)		3 M H2SO4	Conductivity	PO4-P WW	PO4-P 20 min
Cycle		pH	T(°C)	pH	T(°C)	(ml/L)	(uS/cm)	(mg/L)	(mg/L)
1	1,0 g/L Particles with 32 % LDH 0,320 g/L LDHs Vdes=950 mL	8,035	22,4	8,01	22,5	no pH regulation	20000	4,69	2,620
2		7,745	22,5	7,616	22,7	1,50	20900	4,69	1,060
3		7,643	22,7	7,617	22,8	1,40	21000	4,69	3,000
4		7,662	22,8	7,628	22,9	1,50	21000	4,69	1,840
5		7,864	22,7	7,763	22,8	0,90	20900	4,69	2,170
6	2,0 g/L Particles with 32 % LDH 0,640 g/L LDHs Vdes=920 mL	7,745	23,7	7,655	23,9	1,10	20500	4,69	0,648
7		7,895	24,1	7,885	24,2	2,30	21300	4,69	0,613
8		7,778	24,2	7,748	24,4	1,60	21200	4,69	0,569
9		7,743	24,4	7,720	24,5	2,10	21200	4,69	0,657
10		7,648	23,3	7,559	23,4	1,90	21200	4,69	1,11
11	2,5 g/L Particles with 32 % LDH 0,800 g/L LDHs Vdes=880 mL	7,854	22,4	7,794	22,5	1,80	21000	4,69	0,706
12		7,880	22,7	7,847	22,8	2,30	21400	4,69	0,441
13		7,831	22,8	7,748	22,9	2,60	21400	4,69	0,756
14		7,744	23,0	4,690	23,1	1,90	21200	4,69	0,465
15		7,628	23,0	7,536	23,2	2,10	21200	4,69	0,817
16		9,440	22,3	7,550	22,6	0,92	20200	4,69	0,628
17		9,340	22,3	7,550	22,7	0,69	20000	4,69	0,467
18		9,270	22,6	7,550	22,9	0,91	20000	4,69	0,452
19		9,250	22,5	7,540	22,8	0,75	19900	4,69	0,416
20	3,1 g/L Particles with 32 % LDH 1,0 g/L LDHs Vdes=820 mL	9,230	21,6	7,520	23,1	0,95	19840	4,69	0,331
21		9,410	21,9	7,550	22,3	1,09	20300	4,69	0,28
22		9,390	21,9	7,530	21,9	0,99	20300	4,69	0,319
23		9,340	21,0	7,550	21,2	0,79	20200	4,69	0,506
24		9,310	21,5	7,540	22,0	0,89	20200	4,69	0,354
25		9,240	21,3	7,520	21,7	0,79	20200	4,69	0,59
26		9,240	21,7	7,490	22,1	0,78	20100	4,69	0,927
27		9,270	22,4	7,540	22,8	0,86	20200	4,69	0,528
28		9,130	23,1	7,440	23,4	0,80	20100	4,69	0,414

	0 min (desorption+particles)	20 min (in reactor)			Conductivity	Desorption solution	Sample quantity	PO4-P
Cycle	pH	T(°C)	pH	T(°C)	(uS/cm)	(ml)	(mL)	20 min (mg/L)
1	12,914	22,3	13,127	22,8	176400	1000	20	1,81
2	12,636	22,4	13,111	23,1	172100	982	10	5,07
3	12,949	22,9	13,115	23,0	168800	971	10	6,66
4	12,950	22,7	13,087	23,4	165000	962	10	9,10
5	12,506	22,3	13,117	22,9	166000	953	10	11,60
6	12,471	24,1	13,049	24,2	no	940	5	15,70
7	12,685	24,2	13,008	24,7	no	936	5	19,80
8	12,308	24,1	12,992	24,8	159000	931	5	24,10
9	12,350	23,9	12,969	25,0	156200	920	5	28,20
10	12,277	23,4	13,016	23,9	153300	910	5	32,00
11	11,744	20,0	13,182	19,9	150100	908	5	36,50
12	12,259	22,1	13,083	22,3	146000	900	5	40,50
13	12,325	22,5	12,031	23,2	141900	890	5	43,90
14	12,240	22,4	13,001	23,6	138500	887	5	50,00
15	11,885	23,1	12,944	23,7	135500	882	5	54,70
16	12,980	22,6	13,050	22,8	128500	875	5	60,00
17	12,920	23,1	13,010	23,3	125800	870	5	65,20
18	12,860	23,2	12,970	23,3	123600	865	5	69,80
19	12,960	22,0	13,090	22,3	121900	860	5	74,70
20	12,930	22,1	13,020	22,2	118600	855	5	78,90
21	13,010	22,3	13,080	22,4	115600	850	5	83,80
22	12,870	22,6	12,970	22,8	112600	845	5	89,60
23	12,960	21,9	13,050	22,1	109800	840	5	94,50
24	12,950	22,0	13,010	22,7	107100	835	5	100,00
25	12,930	22,4	12,980	22,6	104600	830	5	106,00
26	12,890	22,9	12,990	23,1	101500	825	5	111,00
27	12,870	23,4	12,960	23,6	98900	820	5	117,00
28	12,850	23,8	12,990	23,9	96400	815	5	123,00

Table A1-3. Experimental data obtained in the phosphate adsorption/desorption cycle by using the raw wastewater DSLF with the 32 wt% ZnFeZr-LDH composite material and V=1.0 L.

	Comments	pH at the beginning	0 min (WW+particles)		20 min (in reactor)		pH regulation	Conductivity	PO4-P WW	PO4-P 20 min
Cycle	3,75 g/L Particles		pH	T(°C)	pH	T(°C)	(ml/L)	(uS/cm)	(mg/L)	(mg/L)
1	with 32 % LDH		7,534	13,7	7,50	13,6	NaOH 1 M 0,8 ml	8190	49,80	23,400
2	1,20 g/L LDHs	pH: 8,940; 16°C	7,616	16,1	7,183	16,4	6,9 ml H2SO4 3M, 3 ml NaOH 1M	12170	49,80	15,000
3	pH=7,5-9,0	pH: 9,147; 15,9°C	7,629	16,7	7,620	16,8	6 ml H2SO4 3M	11720	49,80	36,700
4			8,966	16,4	9,078	16,9	No pH regulation	8960	49,80	19,800
5	6,25 g/L Particles	pH: 9,435; 17,4°C	7,654	19,3	7,598	19,3	5,4 mL H2SO4 3M	11030	49,80	12,600
6	with 32 % LDH		9,503	18,9	9,497	19,5	No pH regulation	9360	49,80	17,600
7	2,0 g/L LDHs		9,486	19,6	9,463	19,9	No pH regulation	9220	49,80	10,900
8	pH=7,5-9,0		8,300	22,6	8,331	22,5	No pH regulation	7890	49,80	4,640
9	Particles were washed		8,209	17,4	8,372	18,5	No pH regulation	7480	49,80	7,080
10	6,25 g/L Particles	pH: 8,138; 24,9°C	5,158	24,5	5,057	24,4	5,1ml H2SO4 9,17M, 1,2 ml H2SO4 3M	10600	49,80	0,487
11	with 32 % LDH	pH: 7,983; 23,4°C	4,975	24,1	5,022	24,1	4,7 ml H2SO4 9,17M	9660	49,80	1,510
12	2,0 g/L LDHs	pH: 8,160; 23,2°C	4,998	24,1	5,080	23,9	4,5 ml H2SO4 9,17M	9380	49,80	3,950
13	pH=5,0	pH: 7,770; 23,8°C	4,964	24,5	4,994	24,3	4,5 ml H2SO4 9,17M	9380	49,80	13,400
14	Particles were washed	pH: 8,370; 22,9°C	4,966	24,1	5,009	24,0	4,4 ml H2SO4 9,17M	9120	49,80	14,200
15		pH: 7,647; 22,8°C	5,048	24,0	5,086	23,8	4,3 ml H2SO4 9,17M	9160	49,80	28,100
16		pH: 8,478; 23,1°C	5,009	24,3	5,096	24,2	4,95 ml H2SO4 9,17M	9740	49,80	2,830
17	6,25 g/L Particles	pH: 8,193; 22,4°C	5,061	24,1	5,114	24,0	4,8 ml H2SO4 9,17M	9530	49,80	2,660
18	with 32 % LDH	pH: 8,613; 22,5°C	5,080	24,7	4,957	24,5	4,7 ml H2SO4 9,17M	9160	49,80	2,910
19	2,0 g/L LDHs	pH: 8,103; 22,9°C	5,029	24,4	5,123	24,4	4,7 ml H2SO4 9,17M	9650	49,80	5,800
20	pH=5,0 Particles were	pH: 8,213; 21,4°C	5,032	24,4	5,074	24,4	4,6 ml H2SO4 9,17M	9100	49,80	6,900
21	washed and a new	pH: 8,297; 22,4°C	4,932	24,3	5,138	24,3	4,8 ml H2SO4 9,17M	9430	49,80	9,540
22	desorption solution	pH: 8,278; 22,5°C	5,006	24,4	4,963	24,3	4,6 ml H2SO4 9,17M	9500	49,80	8,680
23	was used from cycle	pH: 8,165; 19,5°C	4,968	20,2	4,983	20,5	4,3 ml H2SO4 9,17M	9330	49,80	8,650
24	15 th	pH: 8,070; 20,3°C	4,970	20,70	5,045	21,9	4,35 ml H2SO4 9,17M	9260	49,80	13,600
25		pH: 8,148; 22,3°C	5,000	24,7	5,118	24,6	4,3 ml H2SO4 9,17M	8770	49,80	15,500
26		pH: 7,890; 23,3°C	4,945	24,7	5,055	24,8	4,2 ml H2SO4 9,17M	8880	49,80	16,300
27		pH: 8,255; 23,5°C	4,810	24,3	5,174	24,5	4,0 ml H2SO4 9,17M	8990	49,80	27,900

	0 min (desorption+particles)		20 min (in reactor)		Conductivity	Desorption solution	Sample quantity	PO4-P
Cycle	pH	T(°C)	pH	T(°C)	(uS/cm)	(ml)	(mL)	20min (mg/L)
1	12,838	19,5	13,056	23,3	166500	1000	10	25,70
2	12,393	18,3	13,118	20,1	154400	1013	10	58,60
3	12,019	16,1	13,226	16,6	144000	963	10	66,10
4	12,065	16,1	13,214	16,9	133300	1028	10	90,50
5	12,167	18,3	13,114	18,4	113800	996	5	116,00
6	12,138	18,9	13,049	19,3	99400	982	5	135,00
7	12,224	19,7	12,980	20,0	84900	1034	5	157,00
8	12,543	20,7	12,829	21,0	69900	1001	5	169,00
9	12,003	18,8	12,858	19,5	53900	999	5	169,00
10	11,610	22,8	12,495	23,3	40100	1059	5	174,00
11	12,008	23,3	13,135	24,0	28800	993	5	186,00
12	11,710	22,0	11,886	22,5	19900	989	5	197,00
13	10,589	22,3	10,928	22,7	16970	945	5	195,00
14	10,328	17,1	10,227	17,8	16240	989	5	180,00
15	12,831	26,6	12,81	28,6	150000	998	5	49,90
16	12,044	22,5	12,968	25,1	129600	979	5	77,80
17	12,123	21,2	13,061	22,3	113400	1002	5	101,00
18	11,907	22,9	12,940	23,7	98500	1012	5	123,00
19	12,095	21,5	12,877	24,0	88200	1002	5	132,00
20	12,004	22,1	12,866	23,1	75400	999	5	154,00
21	12,219	22,3	12,756	23,9	63100	1041	5	165,00
22	11,969	17,1	12,881	17,5	50300	1030	5	176,00
23	12,100	20,0	12,661	21,1	42300	1046	5	183,00
24	12,316	21,4	12,452	22,1	34300	990	5	189,00
25	11,742	22,5	12,078	23,2	26100	971	5	192,00
26	11,559	23,1	10,878	24,3	22800	1040	5	185,00
27	10,450	21,4	10,376	22,2	22000	1040	5	190,00

Table A1-4. Experimental data obtained in the phosphate adsorption/desorption cycle by using the raw wastewater UASB with the 32 wt% ZnFeZr-LDH composite material and V=1.0 L.

	0 min (WW+particles)		20 min (in reactor)		pH regulation	Conductivity	PO4-P WW	PO4-P 20 min	PO4-P adsorpt 20min
Cycle	pH	T(°C)	pH	T(°C)	(ml/L)	(uS/cm)	(mg/L)	(mg/L)	(mg/L)
1	6,653	20,7	6,960	23,2	Nothing	2140	10,30	0,559	9,741
2	7,265	23,7	7,473	23,4	3,95 ml H2SO4 9,17M, 1 ml NaOH 1M	8011	10,30	0,139	10,161
3	7,275	23,5	7,485	23,1	2,9 ml H2SO4 9,17M, 1,3 ml NaOH 1M	6700	10,30	0,260	10,040
4	5,096	233,7	5,093	23,4	3,65 ml H2SO4 9,17M	7420	10,30	0,171	10,129
5	4,985	19,0	4,880	19,3	2,80 ml H2SO4 9,17M	6240	10,30	0,947	9,353
6	5,097	19,2	5,043	19,3	1,65 ml H2SO4 9,17M	4300	10,30	0,457	9,843
7	5,095	19,6	5,110	19,9	1,42 ml H2SO4 9,17M	4110	10,30	0,104	10,196
8	7,010	20,1	7,142	20,3	0,92 ml H2SO4 9,17M	3730	10,30	0,663	9,637
9	7,650	18,5	7,448	18,4	1,4 ml H2SO4 9,17M	4470	10,30	2,000	8,300
10	7,682	20,2	7,539	20,5	1,6 ml H2SO4 9,17M	4600	10,30	2,950	7,350
11	7,607	20,9	7,679	21,0	1,25 ml H2SO4 9,17M	4330	10,30	3,070	7,230
12	7,547	24,3	7,551	24,2	1,325 ml H2SO4 9,17M	4550	10,30	3,940	6,360
13	7,553	23,1	7,623	23,2	1,1 ml H2SO4 9,17M	4130	10,30	2,800	7,500
14	7,706	23,9	7,791	23,4	9,75 ml H2SO4 9,17M	3900	10,30	3,150	7,150
15	7,523	21,4	7,477	21,7	1,1 ml H2SO4 9,17M	4050	10,30	2,710	7,590
16	7,601	19,5	7,595	19,7	1,775 ml H2SO4 9,17M	5110	10,30	4,360	5,940
17	7,940	20,6	7,771	21,1	0,038 ml H2SO4 9,17M	2220	10,30	0,580	9,720
18	7,727	18,3	7,540	17,9	0,025 ml H2SO4 9,17M	2230	10,30	1,220	9,080
19	7,325	20,9	7,570	22,0	0,038 ml H2SO4 9,17M	2180	10,30	0,779	9,521
20	7,850	19,7	7,558	19,1	0,125 ml H2SO4 9,17M	2260	10,30	1,010	9,290
21	7,566	21,1	7,658	21,3	0,025 ml H2SO4 9,17M	2180	10,30	0,700	9,600
22	7,677	19,3	7,719	19,6	Nothing	2180	10,30	1,290	9,010
23	7,529	21,5	7,606	22,0	0,025 ml H2SO4 9,17M	2170	10,30	1,070	9,230
24	7,574	23,1	7,735	23,1	0,025 ml H2SO4 9,17M	2170	10,30	1,040	9,260
25	7,790	20,5	7,641	21,3	0,050 ml H2SO4 9,17M	2170	10,30	0,653	9,647

	0 min (desorption+particles)		20 min (in reactor)		Conductivity	Desorption solution	Sample quantity	PO4-P
Cycle	pH	T(°C)	pH	T(°C)	(uS/cm)	(ml)	(mL)	20min (mg/L)
1	12,553	19,5	13,176	20,7	168400	1000	20	9,88
2	11,845	19,7	13,144	20,6	155700	944	20	20,10
3	12,152	19,8	13,103	20,9	142100	1001	20	29,00
4	12,630	19,1	13,056	20,8	129300	947	5	38,90
5	13,099	19,1	13,162	19,3	124200	972	5	44,10
6	13,030	19,7	13,110	20,0	119500	910	5	55,30
7	12,982	20,4	13,054	20,6	115100	905	5	66,70
8	13,090	18,0	13,148	18,3	112900	901	5	76,10
9	11,815	18,7	13,094	19,1	103900	891	5	84,10
10	12,221	19,7	13,029	19,7	93500	905	5	88,90
11	11,365	20,0	12,99	20,8	90800	984	5	96,20
12	12,313	21,2	12,996	21,1	85800	935	5	102,00
13	11,812	20,2	12,966	21,4	81000	931	5	108,00
14	11,570	21,5	12,915	21,9	76400	934	5	118,00
15	12,990	21,2	12,924	21,4	70800	984	5	126,00
16	12,192	19,7	12,961	20,00	64900	911	5	127,00
17	12,032	21,1	12,872	21,7	60300	990	5	128,00
18	11,434	19,2	12,973	19,7	56300	968	5	129,00
19	11,995	18,1	12,994	19,1	53600	950	5	130,00
20	11,818	21,2	12,925	20,1	50600	961	5	133,00
21	12,172	19,6	12,890	20,3	46700	944	5	135,00
22	11,417	19,9	12,858	20,5	44000	967	5	138,00
23	11,550	21,9	12,783	22,3	41200	974	5	134,00
24	11,552	22,7	12,700	23,7	38100	957	5	131,00
25	11,975	22,3	12,701	22,6	35900	964	5	136,00

Appendix A2. Experiment: Struvite kinetic at diverse molar ratios of Mg^{+2}:NH_4^+:PO_4^{-3} on synthetic wastewater and on the obtained enriched reclaimed solutions

Table A2-1. Experimental data obtained in the struvite kinetic with synthetic WW with molar ratio 0.34:0.34:1.0 of Mg^{+2}:NH_4^+:PO_4^{-3}, V=600 mL.

Contact time	pH	Temperature (°C)	pH regulation	Volume take it (mL)	Conductivity (uS/cm)	Cn PO4-P (mg/l)	PO4-P adsorp (mg/L)
5 min	8.593	24,9	2,1m NaOH 1M 0,9 mL HCl 0,1 M	20	1329	32,5	16,2
10 min	8.600	25,0	0,5 mL HCl 0,1 M	20	1352	32,7	16,0
15 min	8.574	25,0	0,4 mL HCl 0,1 M	20	1338	35,5	13,2
20 min	8.597	25,0	Nothing	20	1360	35,9	12,8
30 min	8.612	25,1	Nothing	20	1351	37,0	11,7
45 min	8.544	25,1	0,8 mL NaOH 0,1 M 0,04 mL NaOH 1 M	20	1369	39,7	9,0
1 h	8.507	25,2	0,150 mL NaOH 1 M	30	1315	29,8	18,9
1,5 h	8.543	25,2	0,18 mL NaOH 1 M	30	1281	22,7	26,0
2 h	8.531	25,3	Nothing	30	1275	21,9	26,8

Table A2-2. Experimental data obtained in the struvite kinetic with synthetic WW with molar ratio 0.5:0.5:1.0 Mg^{+2}:NH_4^+:PO_4^{-3}, V=600 mL.

Contact time	pH	Temperature (°C)	pH regulation	Volume take it (mL)	Conductivity (uS/cm)	Cn PO4-P (mg/l)	PO4-P adsorp (mg/L)
5 min	9,032	23,2	2,8mL NaOH 1M 3,0 mL NaOH 1 M	20	2570	2,39	94,61
10 min	9,027	23,2	Nothing	20	2540	2,17	94,83
15 min	9,012	23,3	Nothing	20	2540	2,09	94,91
20 min	9,014	23,3	Nothing	20	2530	2,11	94,89
30 min	9,027	23,4	0,030 mL NaOH 1 M	20	2530	2,07	94,93
45 min	9,024	23,5	Nothing	30	2520	2,06	94,94
1 h	9,020	23,6	Nothing	30	2530	2,08	94,92
1,5 h	9,012	23,6	Nothing	30	2540	2,08	94,92
2 h	9,018	23,6	0,020 mL NaOH 1 M	30	2530	2,06	94,94
2,5 h	9,014	23,7	0,010 mL NaOH 1 M	30	2530	2,1	94,90
3 h	9,014	23,9	0,010 mL NaOH 1 M	30	2520	2,1	94,90

Table A2-3. Experimental data obtained in the struvite kinetic with the 60th cycle regenerated RWW with molar ratio 0.5:0.5:1.0 of Mg^{+2}:NH_4^+:PO_4^{-3}, V=200 mL.

Contact time	pH	Temperature (°C)	pH regulation	Volume take it (mL)	Conductivity (uS/cm)	Cn PO4-P (mg/l)	PO4-P adsorp (mg/L)
5 min	9,116	24,8	1,9 mL NaOH 1 M	20	21600	7,20	122,80
15 min	9,116	24,8	Nothing	20	21700	6,29	123,71
30 min	9,113	24,7	Nothing	20	21500	5,93	124,07
1 h	9,107	24,6	Nothing	20	21600	5,65	124,35
2 h	9,090	24,7	Nothing	20	21700	5,64	124,36

Table A2-4. Experimental data obtained in the struvite kinetic with the 60th cycle regenerated RWW with molar ratio 0.42:0.42:1,0 of Mg^{+2}:NH_4^+:PO_4^-3, V=200 mL.

Contact time	pH	Temperature (°C)	pH regulation	Volume take it (mL)	Conductivity (uS/cm)	Cn PO4-P (mg/l)	PO4-P adsorp (mg/L)
5 min	9,106	23,9	1,7 mL NaOH 1 M	20	21400	12,80	117,20
15 min	9,097	24,0	Nothing	20	21400	10,3	119,7
30 min	9,085	24,1	Nothing	20	21400	9,55	120,45
1 h	9,078	24,3	Nothing	20	21400	9,19	120,81
2 h	9,065	24,4	Nothing	20	21400	9,13	120,87

Table A2-5. Experimental data obtained in the struvite kinetic with the 10 L experiment with molar ratio 0.5:0.5:1.0 of Mg^{+2}:NH_4^+:PO_4^{-3}, V=100 mL.

Contact time	pH	Temperature (°C)	pH regulation	Volume take it (mL)	Conductivity (uS/cm)	Cn PO4-P (mg/l)	PO4-P adsorp (mg/L)
5 min	8,505	24,8	1,1 mL NaOH 0,1 M	20	27300	30,30	136,70
15 min	8,515	24,6	1,8 mL NaOH 0,1 M	20	26600	13,7	153,3
30 min	8,507	24,5	0,1 L NaOH 0,1 M	20	26300	13,6	153,4
1 h	8,531	24,6	0,1mL NaOH 0,1 M	20	26300	14,0	153,0
2 h	8,504	24,9	Nothing	25	26300	9,6	157,4

Table A2-6. Experimental data obtained in the struvite kinetic with the 10.0 L experiment with molar ratio 1.0:1.0:1.0 of Mg^{+2}:NH_4^+:PO_4^{-3}, V=900 mL.

Contact time	pH	Temperature (°C)	pH regulation	Volume take it (mL)	Conductivity (uS/cm)	Cn PO4-P (mg/l)	PO4-P adsorp (mg/L)
Blind sample after neutraization	9,184	24,6	17,01 mL HCl conc	10		121	44,00
5 min	8,505	24,7	3,85 mL NaOH 1 M	20	29100	7,69	157,31
15 min	8,504	24,7	0,3 mL NaOH 1 M	20	28900	4,51	160,49
30 min	8,502	24,6	-	20	28800	4,25	160,75
1 h	8,507	24,6	0,1 mL NaOH 1 M	40	28900	3,98	161,02
2 h	8,505	24,9	0,1 mL NaOH 1 M	40	29000	3,77	161,23
3 h	8,529	25,1	0,2 mL NaOH 1 M	40	28900	3,66	161,34
4 h	8,532	25,3	Nothing	40	28900	3,62	161,38

Table A2-7. Experimental data obtained in the struvite kinetic with the MBA with molar ratio 0.5:0.5:1.0 of NH_4^+:Mg^{+2}:PO_4^{-3}, V=100 mL.

Contact time	pH	Temperature (°C)	pH regulation	Volume take it (mL)	Conductivity (uS/cm)	Cn PO4-P (mg/l)	PO4-P adsorp (mg/L)
5 min	8,554	27,3	0,35 mL HCl 1 M	20	51900	37,10	85,90
15 min	8,541	26,7	Nothing	20	52100	38,5	84,5
30 min	8,519	26,1	0,1 mL HCl 1 M	20	52600	41,5	81,5
1 h	8,538	25,4	Nothing	20	52100	34,9	88,1
2 h	8,552	25,3	0,4 mL NaOH 0,1 M	25	51400	30,5	92,5

Table A2-8. Experimental data obtained in the struvite kinetic with the MBA with molar ratio 0.65:0.65:1.0 of Mg^{+2}:NH_4^+:PO_4^{-3}, V=100 mL.

Contact time	pH	Temperature (°C)	pH regulation	Volume take it (mL)	Conductivity (uS/cm)	Cn PO4-P (mg/l)	PO4-P adsorp (mg/L)
Blind sample after neutralization	13,09	21,4	6,49 mL Hclconc	10	52300	88,4	29,6
5 min	8,561	24,3	0,2 mL HCl 1 M	10	43400	41,30	76,70
15 min	8,570	24,3	Nothing	10	45200	32,2	85,8
30 min	8,497	24,5	0,05 mL HCl 1 M	10	48100	23,00	95,00
1 h	8,505	25,7	Nothing	20	52300	23,2	94,8
2 h	8,538	24,4	Nothing	20	52000	25,0	93,0
3 h	8,572	25,4	0,025 mL HCl 1 M	25	51800	20,1	97,9

Table A2-9. Experimental data obtained in the struvite kinetic with the MBA with molar ratio 1.5:1.5:1.0 of Mg^{+2}:NH_4^+:PO_4^{-3}, V=300 mL.

Contact time	pH	Temperature (°C)	pH regulation	Volume take it (mL)	Conductivity (uS/cm)	Cn PO4-P (mg/l)	PO4-P adsorp (mg/L)
Blind sample after neutralization	9,17	24,9	19,48 mL HCl conc	5	52100	88,6	29,4
5 min	8,516	24,5	0,225 mL HCl 1 M	10	43400	4,98	113,02
15 min	8,522	24,4	0,3 mL NaOH	10	45200	5,78	112,22
30 min	8m510	24,3	Nothing	10	48100	7,22	110,78
1 h	8,508	24,3	Nothing	20	52300	8,44	109,56
2 h	8,507	24,7	Nothing	20	52000	7,7	110,30
3 h	8,551	25,1	0,1 mL NaOH 1 M	25	51800	6,94	111,06
4 h	8,560	25,4	Nothing	25	51800	6,70	111,30

Table A2-10. Experimental data obtained in the struvite kinetic with the DSLF with molar ratio 1.7:1.7:1.0 of Mg^{+2}:NH_4^+:PO_4^{-3}, V=110 mL.

Contact time	pH	Temperature (°C)	pH regulation	Volume take it (mL)	Conductivity (uS/cm)	Cn PO4-P (mg/l)	PO4-P adsorp (mg/L)
Blind sample after neutralization	9,199	22,0	0,98 mL HCl conc	10	19440	180	-1
5 min	8,558	22,6	3,14 mL HCl conc	10	22300	4,59	174,41
15 min	8,581	22,9	-	10	20300	2,81	176,19
30 min	8,534	23,2	0,2 mL HCl 1M	10	17150	2,72	176,28
1 h	8,556	24,1	0,1 mL HCl 1M	20	25500	2,35	176,65
2 h	8,574	24,5	0,4 mL HCl 1M	20	25700	2,26	176,74
3 h	8,561	24,9	0,4 mL HCl 1M	20	25800	2,62	176,38
4 h	8,587	24,9	0,3 mL HCl 1 M	21	25900	2,61	176,39

Table A2-11. Experimental data obtained in the struvite kinetic with the DSLF with molar ratio 1.5:1.5:1.0 of Mg^{+2}:NH_4^+:PO_4^{-3}, V=110 mL.

Contact time	pH	Temperature (°C)	pH regulation	Volume take it (mL)	Conductivity (uS/cm)	Cn PO4-P (mg/l)	PO4-P adsorp (mg/L)
Blind sample after neutralization	9,145	24,3	2,77 mL HCl conc	10	20700	114	23
5 min	8,578	22,6	0,4 mL NaOH 1 M	10	11930	2,61	134,39
15 min	8,581	22,9	-	10	7610	2,16	134,84
30 min	8,534	23,2	-	10	5790	2,53	134,47
1 h	8,556	24,1	0,1 mL HCl 1M/0,05 mL NaOH 1 M	20	26700	3,19	133,81
2 h	8,574	24,5	0,1 mL HCl 1M	20	26700	3,15	133,85
3 h	8,561	24,9	0,2 mL HCl 1M/0,05 mL NaOH 1M	20	26600	3,02	133,98
4 h	8,537	24,7	0,1 mL HCl 1M/0,05 mL NaOH 1M	21	25400	7,19	129,81

Appendix A3. Physicochemical characteristics of the different raw wastewaters, enriched reclaimeds solutions before and after of the struvite precipitation.

Table A3-1. Experimental data obtained in the raw wastewaters.

Nr	Matrix WW	pH	T(°C)	Conductivity (uS/cm)	PO4-P (mg/L)	Ptot (mg/L)	Total suspended solids (mg/L)	COD (mg/L)	TC (mg/L)	TOC (mg/L)	TIC (mg/L)	TKN (mg/L)	NH4+-N (mg/L)	NO3-N (mg/L)	NO2-N (mg/L)	SO4 2- (mg/L)	SO4-S (mg/L)	Cl- (mg/L)	
1	SST effluent+H3PO4 (unfiltered) ISWA	7,2	24,2	1086	**9,7**	**9,9**	<1	18	45	6	39	11	0,04	9,2	0,08	76	25	149	
2	MBA Process water-Deponie Kahlenberg	8,1	23,3	20800	**4,7**	**5,6**	<1	279	548	106	442	11	0,08	170	12,3	100	33	5400	
3	Digested sludge liquor effluent Offenburg	7,6	19,7	8600	**49,8**	**50**	110	388	1190	130	1060	1150	1090	1,2	<0,27	18	6	150	
4	Upflow anaerobic blanket reactor, centrifuged and filtered fold	6,9	18	2230	**10,3**	**16,7**	260	927	387	303	84	112	76,2	<1	<0,2	52	17	330	
5	Pilot scale SST ISWA	6,9	12,6	1177	**9,6**	**9,9**	5	22	53	7	46	<5	0,06	8,9	<0,2	94	31	240	
Nr	Matrix WW	Na (mg/L)	K (mg/L)	Ca (mg/L)	Mg (mg/L)	Si (mg/L)	Fe (mg/L)	Zn (mg/L)	Zr (mg/L)	Al (mg/L)	Cd (mg/L)	Cr (mg/L)	Cu (mg/L)	Ni (mg/L)	Pb (mg/L)	Mo (mg/L)	Se (mg/L)	Br- (mg/L)	F- (mg/L)
1	SST effluent+H3PO4 (unfiltered) ISWA	135	18	84	13	2,3	0,08	0,053	-	-	-	-	-	-	-	-	-	<0,4	<0,4
2	MBA Process water-Deponie Kahlenberg	2656	2174	148	223	23,8	0,194	0,032	0,031	0,047	<0,001	0,051	0,048	0,048	0,075	0,012	0,011	-	-
3	Digested sludge liquor effluent Offenburg	162	280	53,9	36	21,2	2,55	0,114	0,021	0,476	0,001	0,005	0,035	0,228	0,011	0,600	0,030	-	-
4	Upflow anaerobic blanket reactor, centrifuged and filtered fold	225	35,4	110	19,6	5,7	1,11	0,253	0,041	0,5	<0,001	0,007	0,023	0,011	0,001	0,003	0,007	-	-
5	Pilot scale SST ISWA	-	-	-	-	-	-	-	-	-	-	-	-	-	-	-	-	-	-

Table A3-2. Experimental data obtained in the enriched reclaimed solutions before struvite precipitation.

Nr	Regenerate	pH	T(°C)	Conductivity (uS/cm)	PO4-P (mg/L)	Ptot (mg/L)	PO4-P after HCl regulation(mg/L)	COD (mg/L)	TC (mg/L)	TOC (mg/L)	TIC (mg/L)	TKN (mg/L)	NH4+-N (mg/L)	NO3-N (mg/L)	NO2-N (mg/L)	SO4 2- (mg/L)	SO4-S (mg/L)	Cl- (mg/L)	
1	Regenerate after 60 cycles	12,7	25,8	71400	**260**	**260**	-	-	627	56	571	-	-	5,9	<0,040	298	99	75	
2	Regenerated MBA after 28 th cycles	12,9	23,9	96000	**118**	**131**	88,9	489	580	580	0	29,4	13,8	79,5	<0,200	400	134	2300	
3	Regenerate 10 L experiment (SST ISWA) after 19 cycles	12,8	20,0	50000	**169**	**170**	121	87	136	131	5	20,9	14,50	6,2	<0,800	1100	367	170	
4	Regenerate DSLF (digested sludge liquor filtered) after 14 cycles	10	17,9	16740	**179**	**185**	180	545	1710	253	1457	895	727	<1	<0,200	1850	618	150	
5	Regenerate UASB (upflow anaerobic slufge blanket) after 25 cycles	12,7	22,6	35900	**137**	**168**	114	2220	1170	747	423	250	67,3	<1	<0,200	770	257	280	
Nr	Regenerate	Na (mg/L)	K (mg/L)	Ca (mg/L)	Mg (mg/L)	Si (mg/L)	Fe (mg/L)	Zn (mg/L)	Zr (mg/L)	Al (mg/L)	Cd (mg/L)	Cr (mg/L)	Cu (mg/L)	Ni (mg/L)	Pb (mg/L)	Mo (mg/L)	Se (mg/L)	Br- (mg/L)	F- (mg/L)
1	Regenerate after 60 cycles	8904	19,8	0,433	0,035	17,4	0,091	4,11	0,120	5,61	0,001	0,009	0,048	<0,001	0,001	0,119	0,008	2,9	1,9
2	Regenerated MBA after 28 th cycles	14365	1137	0,261	0,324	106,0	1,67	336,0	0,826	3,44	<0,001	0,062	0,026	0,048	0,010	0,030	<0,005	-	-
3	Regenerate 10 L experiment (SST ISWA) after 19 cycles	7275	23,5	0,433	0,252	46,3	1,21	263,0	0,181	5,63	0,001	0,008	0,630	0,013	0,007	0,017	<0,005	-	-
4	Regenerate DSLF (digested sludge liquor filtered) after 14 cycles	5401	213	2,13	2,38	50,4	8,52	5,7	0,272	0,247	<0,001	0,011	0,16	0,042	0,002	0,001	0,010	-	-
5	Regenerate UASB (upflow anaerobic slufge blanket) after 25 cycles	5510	40,2	18,2	7,74	17,4	10,8	63	0,002	3,06	0,001	0,027	0,117	0,037	0,002	0,01	0,015	-	-

Table A3-3. Experimental data obtained in the enriched reclaimed solutions after struvite precipitation.

Nr	Regenerate	pH	T(°C)	Conductivity (uS/cm)	PO4-P (mg/L)	Ptot (mg/L)	Total suspended solids (mg/L)	COD (mg/L)	TC (mg/L)	TOC (mg/L)	TIC (mg/L)	TKN (mg/L)	NH4+-N (mg/L)	NO3-N (mg/L)	NO2-N (mg/L)	SO4 2- (mg/L)	SO4-S (mg/L)	Cl- (mg/L)	
1	Regenerate after 60 cycles	9,4	21,3	21700	**5,64**	**5,6**	-	-	183	26	157	-	78	3,1	<0,10	15	5	7260	
2	Regenerate MBA Kahlenberg after 28 cycles	8,6	23,5	53100	**2,96**	**4,1**	-	559	526	125	401	373	344	63	<0,2	300	100	19000	
3	Regenerate 10 L experiment (SST ISWA) after 19 cycles	8,9	17,6	27100	**9,73**	**17,2**	-	210	151	37,8	113,2	161	130,00	<1	<0,2	1240	413,3	8890	
4	Regenerate DSLF (digested sludge liquor filtered) after 14 cycles	8,6	22,6	25700	**2,28**	**2,4**	102	477	1600	212	1388	790	769	<2	<0,2	1970	658	5730	
5	Regenerate UASB (upflow anaerobic slufge blanket) after 25 cycles	8,6	20,5	27500	**1,97**	**27,7**	103	1780	1020	734	286	593	508	<3	<0,2	583	195	9100	

Nr	Regenerate	Na (mg/L)	K (mg/L)	Ca (mg/L)	Mg (mg/L)	Si (mg/L)	Fe (mg/L)	Zn (mg/L)	Zr (mg/L)	Al (mg/L)	Cd (mg/L)	Cr (mg/L)	Cu (mg/L)	Ni (mg/L)	Pb (mg/L)	Mo (mg/L)	Se (mg/L)	Br- (mg/L)	F- (mg/L)
1	Regenerate after 60 cycles	4569	11,3	1,45	96	12,3	0,11	0,235	0,019	0,809	0,0002	0,005	0,04	0,027	0,007	0,069	0,003	<0,5	<1
2	Regenerate MBA Kahlenberg after 28 cycles	13200	1050	2,35	411	47,6	0,158	6,0	<0,002	0,183	0,001	0,048	0,08	0,034	0,003	0,037	0,016	-	-
3	Regenerate 10 L experiment (SST ISWA) after 19 cycles	7065	22,4	1030	153	16,7	0,108	0,7	<0,002	0,171	<0,001	0,008	0,436	0,008	0,002	0,017	0,010	-	-
4	Regenerate DSLF (digested sludge liquor filtered) after 14 cycles	4411	196	2,12	787	11,8	1,52	1,7	2,05	0,081	0,001	0,004	0,16	0,04	0,002	0,014	0,036	-	-
5	Regenerate UASB (upflow anaerobic slufge blanket) after 25 cycles	4941	37,4	12,8	570	<0,1	1,23	15,2	0,994	0,501	0,001	0,008	0,155	0,098	0,005	0,009	0,028	-	-